# Characteristics of Supersonic Jets with Shifted Cross-Wire

By

K. P. V. Paparao

DEPARTMENT OF AEROSPACE ENGINEERING

Indian Institute of Technology Kanpur

MAY. 2004

Characteristics of Supersonic Jets with Shifted Cross-Wire

A Thesis Submitted
in Partial Fulfillment of the Requirements
for the Degree of

Master of Technology

by

K. P. V. Paparao

to the

Department of Aerospace Engineering
Indian Institute of Technology, Kanpur

May, 2004

A148450

Certificate

This is to certify that the work contained in the thesis entitled " *Characteristics of Supersonic Jets with Shifted Cross-Wire* ", by *K. P. V. Paparao*, has been carried out under my supervision and that this work has not been submitted elsewhere for a degree.

May, 2004

(Dr. E. Rathakrishnan)
Department of Aerospace Engineering,
Indian Institute of Technology,
Kanpur.

Dedicated

to

My Beloved Parents

Acknowledgements

Abstract

This thesis presents the results of an experimental investigation carried out to study the effectiveness of a passive control in the form of cross-wire located downstream of supresonic nozzle for promoting the jet mixing. This kind of control has a specific advantage namely the precious nozzle exit area is not blocked leading to thrust loss. Jets from Mach 1.83, 1.86 and 1.94 De Laval nozzles of rectangular cross section were studied. With cross-wire at an axial distances of 0.5D, 1D, 1.5D and 2D from the nozzle exit were investigated for correctly expanded, underexpanded and overexpanded conditions. The results show that the shifted cross-wire serves as an effective control. Wire at 1D location is found to be optimum, resulting in maximum mixing promotion compared to other locations. With control the entire jet activity downstream of the wire taking place at a much reduced Pitot pressure level compared to uncontrolled jets. Further, downstream of the wire the shock cells become weaker compared to the uncontrolled ones. The flow visualization results reveal that the optimum control location of wire namely, 1D is that in the vicinity of first Mach disc location or shock crossing point. As high as 30.76% of core reduction was obtained for Mach 1.86 jet at NPR 7.

A_e Nozzle exit area

AR Aspect ratio (Ratio of major axix to minor axis)

C-W Cross-wire

CPD Centreline Pressure Decay

D Equivalent Diameter

M Mach number

$\dot{m}$ Mass flow rate

NPR Nozzle pressure ratio

P_a Atmospheric pressure

P_b Back pressure

P_0 Stagnation chamber pressure

P_t Pitot pressure

R Gas constant

T_e Nozzle exit temparature

T_0 Staganation temparature

V_e Exit velocity of the jet

X Co-ordinate perpendicular to exit plane

Y Transverse co-ordinate parallel to plane of symmetry

Z Spanwise co-ordinate perpendicular to plane of symmetry

γ Ratio of specific heats

ρ_e Nozzle exit density of the fluid

ρ_0 Total density

List of Figures

Contents

Chapter 1

Introduction to Jet and Its Control

Jet is a free shear flow driven by momentum introduced at the exit of, usually, a nozzle or an orifice which exhibits a characteristic, that the ratio of width to axial distance is constant. The jet may also be defined as a fluid flow on either side of the tangential separation surfaces. Free jets can be defined as a pressure driven unrestricted flow of a fluid into a quiescent ambience. Since a fluid boundary can't sustain a pressure difference across it, the jet boundary is a free shear layer, in which static pressure is constant throughout. The boundary layer at the exit of the nozzle develops as a free shear layer, mixing with the ambient fluid thereby entraining the ambient fluid into the jet stream. Thus, mass flow at any cross-section of the jet progressively increases along the downstream direction. Hence, to conserve momentum the centerline velocity decreases with downstream distance. The vast quanta of knowledge presently available and the continuous research currently being carried out stand testimony to the importance associated with the jet flows. This is owing to their extensive nature of applicability, from household appliances to hi-tech rockets. High speed jets find application in numerous engineering fields; aircraft, rockets, missile, propulsive systems of aircraft, thrust augmenting ejectors, powder metallurgy, metal cutting, and food processing and so on. In terms of academic interest, studies on jets have provided insight to the understanding of the jet dynamics of free shear layers and vortical structures.

1.1 Classification of jets

Basically jets can be classified into two categories namely incompressible and compressible jets. The jets with Mach number less than 0.3 up to which the compressible effects are negligible are called incompressible jets and these are subsonic jets. Compressible jets can be again subdivided into subsonic jets and supersonic jets. Supersonic jets are the jets with Mach number more than one, these can be further classified into overexpanded, underexpanded and correctly expanded jets.

1.1.1 Subsonic jets

These are jets with Mach numbers in between 0.3 to 0.8, and showing the following properties.

- The exit velocity is preserved up to some axial distance along the centreline from the exit of the nozzle known as potential core.

- The core extends about 6 times the nozzle exit diameter.

- The characteristic decay dominates from about 6D to 12D.

- In reality the velocity becomes insignificant after about 30D.

- Jet develops with an included angle of about 10 degrees.

- Subsonic jets are always correctly expanded.

A schematic diagram of a typical subsonic jet and the flow zones in it are shown in Fig. 1.1

1.1.2 Overexpanded jets

If the pressure in the ambient medium is larger than that at the exit of the nozzle, the jet is said to be an overexpanded jet. In this oblique shock waves are formed at the edge of the nozzle exit. These oblique shocks will be reflected as wedge shaped expansion waves on the boundary of the jet. Fig. 1.2 shows a sketch of such a jet. If the pressure difference between exit pressure and back pressure is small, a periodic shock cell structure will exist in the jet and the wave length of these periodic structures will increase with Mach number.

When the flow is overexpanded the exhaust gas pressure, P_e, is higher than the supersonic isentropic exit pressure but lower than the ambient pressure, P_a. This causes an oblique shock (A) to form at the exit plane of the nozzle. To reach ambient pressure, the exhaust gas undergoes compression as it moves away from the nozzle exit and passes through the oblique shock wave standing at the exit plane.

Flow that has passed through the shock waves will be turned towards the center line (2). At the same time, the oblique shock wave, directed towards the centerline of the nozzle, can not penetrate the center plane since the center plane acts like a streamline. This causes the oblique shock wave to be reflected outwards (B) from the center plane. The gas flow goes through this reflected shocks and is further compressed but the flow is now turned parallel (3) to the center line. This causes the pressure of the exhaust gases to increase above the ambient pressure. Deflected shock wave now hits the free boundary called a contact discontinuity (or the boundary where outer edge of the gas flow meets the free stream air). Pressure is same across the boundary and so is the direction of the flow. Since the jet flow is at a higher pressure than ambient pressure, the pressure must reduce. Thus, at the reflected shock wave-contact discontinuity intersection and expansion waves of the Prandtl-Mayer (P-M) type are set up (C) to reduce the pressure to P_a. These expansion waves turn the flow away from the center line (4). The P-M expansion waves in turn reflect from the center plane towards the contact discontinuity (D). The gas flow passing through the reflected P-M waves is now turned back parallel to the center line but undergoes a further reduction of pressure. The reflected P-M waves now meet the contact discontinuity and reflect from the contact discontinuity towards the centerline as P-M waves (E). This allows the gas flow to pass through the P-M compression waves and increase its pressure to ambient pressure, but passes through the compression waves turns the flow back towards the centerline (6). The P-M compression waves now reflect from the centerline as compression waves (F) further increasing the pressure above ambient, but turn the flow parallel to the nozzle center line (7). The flow process is now back to when the flow had just passed through the reflected shock wave (B), i.e., the flow pressure is above the ambient pressure and the flow is parallel to the centerline (3). This process of expansion and compression wave formation continue until the pressure of the jet field is same as the ambient pressure and the flow is parallel to the centerline of the nozzle. These expansion and compression waves which interact with each other, leads to the diamond patterns termed as shock cells. Ideally this process would continue without end; but a turbulent shear layer created by the large velocity difference across the contact discontinuity will dissipate

the wave patterns [20].

1.1.3 Underexpanded jets

If the pressure in the ambient medium is lower than that at the exit of the nozzle, the jet is said to be underexpanded jet.If the back pressure is less than the nozzle exit pressure, wedge shaped expansion waves occur at the edge of the nozzle, these waves cross one another and are reflected from the opposite boundaries of the jet as compression waves. The compression waves again cross one another and are reflected on the boundaries of the jet as expansion waves. Fig. 1.3 shows a sketch of such a jet.

1.1.4 Correctly expanded jets

If the nozzle exit pressure is equal to the back pressure then the jet is said to be correctly expanded. This jet is also wave dominated as imperfectly expanded jets, unlike what we think that there wont be any waves. The reason for this is that as the jet is issuing from the confined area to an infinite area, jet tries to expands through expansion waves and after that gets compressed through compression waves, which results into a periodic wave structure.

1.2 Need for jet control

The diverse nature of applicability of jets demands that they be made suitable for their application by controlling them. Here control may be defined as the ability to modify the flow characteristics in such a way as to achieve engineering efficiency, the technological ease, economy, adherence to standards etc.

1.3 Jet control

1.3.1 Flow control

Flow control is aimed at modifying the flow development to suit the specific needs. This is done by manipulating the evolution and developing components comprising the flow. Jet flows are an important part of various mixing devices and propulsion systems, wherein enhanced rate of mixing or thrust augmentation is desirable. In combustion systems, both large and small scale mixing enhancement is sought since

large scale mixing determines the rapidity of the mixing process and small scale or micro scale level mixing ensures effective molecular level mixing for efficient combustion. In combustion chambers with space constraint, the entire mixing process has to be completed with in a short distance. In this context, it is worth mentioning that jet entrainment enhancement helps in oil well fire fighting where sand is entrained and carried by jet to extinguish fire in oil wells.

1.3.2 Jet noise and its control

Even though the jet noise popularly refers to the noise produced by jet powered aircraft, strictly it covers only those source associated with the jet flow from the exhaust nozzle.

Noise is inevitable wherever there is relative motion between solids and/or fluids in an ambient medium capable of transmitting sound, i.e. media which possess elasticity and inertia. Thus noise is inseparable from jet flows and cannot be eliminated. So, jet noise studies primarily aim at reducing the noise emitted from the jets to the maximum extent possible. Since the total acoustic power emitted by a jet is directly proportional to the 8th power of characteristic velocity of the exhaust gases incase of subsonic and 3rd power of characteristic velocity incase of high speed jet, more so in the case of imperfectly expanded jets. While on one hand the aerospace industry endeavours to increase the speed of passenger aircraft, the environmental standards enforcement agencies of several nations have made regulations so stringent that, meeting both demands has been a challenging task for the engineering community. Hence, jet acoustic studies are chiefly motivated by the need to reduce the noise and aims at understanding the noise source in jets and noise reduction methods which work without much penalty, like for example loss of thrust.

1.4   Types of control

All types of jet controls can be broadly classified into active and passive controls. In active control, an auxiliary power source (like micro jets) is used to control the jet characteristics. The method is termed as passive control wherein the controlling energy is drawn directly from the flow to be controlled. Both active and passive controls mainly aim at modifying the flow and noise characteristics.

1.4.1 Passive controls of jets

Among the two main types of jet control, passive controls are mostly desired not only because no external power source is required, but since in some cases the engineer is left with no other option. Passive control methods use geometrical modifications which alter the flow structure. Some commonly used passive control methods are shown in Fig. 1.4. These methods mostly aim at disturbing the boundary layer at nozzle exit to achieve the desired flow behaviour. Particularly, the grooves or tabs at the exit trip the boundary layer developing inside the nozzle. This drastically influences the shear layer growth, and flow behavior, thus providing the lot of scope for passive control.

The present aim of shifted control is prompted by the important feature namely, it will avoid the thrust loss completely. In other forms of the passive control in literature, all of them were based on modification of nozzle exit geometry, in the form of grooves, cutouts, tabs, cross-wire and so on. One of the serious short comings associated with exit geometry modifications is that, they result in considerable loss of thrust, which is higly undesirable in propulsion point of view.

1.5 Applications of controlled jets

Jet control widely finds application in the following fields.

1.5.1 Supersonic combustion

An important application of supersonic mixing enhancement is in scramjet combustion. While the axial thrust consideration based on the momentum of the injected fuel makes parallel fuel injection desirable, high-speed parallel or near parallel shear flows spread very slowly. This results in a long combustor length to complete the fuel-air mixing. However, because of the drag and weight consideration at high speed a relatively short combustor length is required. Thus, the inherently low mixing rate associated with supersonic shear layers must be increased with use of suitable mixing enhancement techniques.

1.5.2 Ejectors

Ejectors are fluid dynamic pumps without moving parts. They use the shearing force from the primary jet to entrain the secondary shrouded flow into a mixing duct. It

is important to enhance the mixing between the two streams because the ejector performance depends strongly on the degree of mixing. Supersonic ejectors have the potential to be used as thrust augmentation devices and/or noise suppression devices for aircraft application. Supersonic ejector-diffuser systems are encountered also in certain pressure recovery devices. One such application is in a chemical laser, for which the pressure recovery equipment is a main limitation on the physical size of the laser system. By increasing the supersonic mixing, one may obtain further reduction in size.

1.5.3 Noise suppression

Another important application of supersonic mixing control is in noise suppression. Controlled jets reduce the temperature gradient and also shock associated noise.

1.5.4 Metal deposition

The area of metal deposition and metal coating using liquid dynamic compression may also benefit from supersonic mixing studies. To produce fine powders of reactive metals such as aluminum, magnesium and titanium with uniform size, a supersonic coaxial jet of inert gas can be discharged over a laminar center jet containing the molten metal. The atomization of metal occurs in two phases shear flow where the high shear and rapid cooling from supersonic expansion result in fine crystal structure and low level metal oxidation.

1.5.5 Thrust vector control

Thrust vector control of aircraft is commonly obtained with the use of either fluid dynamic means such as secondary asymmetric injection of gas or, liquid, or mechanical means such as physically moving the nozzle exhaust bell and tabs.

1.5.6 Base heat reduction in case of launch vehicles

The base pressure field in the case of rockets and missile plays a vital role from drag point of view and also due to the fact that the high temperature plumes issuing from the nozzle will get attracted towards the base region when the base pressure is at low sub-atmospheric level. The heated base might affect the electronic devices which are housed inside the rocket shell. Therefore, care must be taken to ensure that the base

pressure is kept at remarkably high level so that base heating can be minimized or prevented.

1.6 Analysis of jets

The following tools are used to analyze the jet flow fields

1.6.1 Centreline pressure decay (CPD)

It is the plot of local Pitot pressure ratio (P_t/P_0) Vs axial distance along the jet axis, it gives the clear picture of the jet flow field. Fig. 1.5 shows the typical CPD curve for a supersonic jet of Mach 1.86 at NPR 5 of present study. It is used to find out the flow analyzing parameters such as a core length, number of shock cells and other details such as location of Mach discs and/or refelction point of intercepting shocks very easily. The climbing nature of the curve indicates that the flow is subsonic and accelerating. The down trend of the curve shows that the flow is passing through the compression waves and finally it crosses the Mach disc/reflection point at the minimum pressure ratio location, flow in this region is supersonic. After the flow crossing the periodic nature of shock pattern it reaches a subsonic zone which is indicated by drooping line (without waves). The slope of the curve after core length (the length upto which the wave dominated flow exits) indicates directly the mixing enhancement rate of the jet.

1.6.2 Isobaric curves

These curves represent the extent of the mass entrainment by comparing the isobaric curves of free jet and controlled jet.

1.6.3 Flow visualization

Visualization of fluid flows proved to be an excellent tool for describing and calculating the flow properties in many problems of practical interest, in both subsonic and supersonic flow regimes. Researchers in this field have developed many techniques to visualize the motion of air. Smoke streams can be introduced into the flow to indicate not only its direction but also whether it is smooth or disturbed flow. Small tufts of wool even fine stands of hen-feathers or cat's whiskers can also be utilized to show direction oscillations in a down field. In the flow of water, aluminum powder sprinkled

at the liquid surface will indicate local motions which can be photographed. Flow in water can also be studied by streams of hydrogen bubbles released by electrolysis from thin charged wires arranged across it. If attention is focused on the layer of air near a surface, chemical films can be applied on which the air will create patterns by evaporation, showing the direction and steadiness of the flow. In supersonic flows, the air density changes are sufficiently large to allow the air to be photographed directly using optical systems sensitive to density changes.

The general principle for flow visualization is to render the 'fluid particles' visible either by observing the motion of suitable selected foreign materials added to the flowing fluid. Optical properties (such as refractive index) due to the variation of the properties of the flowing fluid itself. A third class of visualization technique is based on a combination of the above two principles. Each of these group techniques is generally used for incompressible, compressible and low density gas flows respectively. Some of popularly used visulisation techniques to study flow problems of practical interest are the following [16].

- *Smoke flow visualization* is one of the popular techniques used in low speed flow fields with velocities upto 30 *m/s*. Smoke visualization is used to study problems like; boundary layer, air pollution problems, design of exhaust system of locomotives, cars, ships, topographical influence of disposal of stack grasses etc.

- *Tufts* are used to visualize flow fields in the speed range from 40–150 m/s. This technique is usually employed to study boundary layer flow, flow separation, stall spread, and so on.

- *Chemical coating* is used to visualize flow with medium speed in the range 40 to 150 m/s. Boundary layer flow, transition of the flow from laminar to turbulent and so on are usually described by this visualization technique.

- *Interferometry* is a technique to visualize high speed flows in the ranges of transonic and supersonic Mach numbers. This gives a qualitative estimate of flow density in the field.

- *Schlieren* is used to study high speed flows in the transonic and supersonic Mach number ranges. This again gives only a qualitative estimate of the density gradient of the field. This is used to visualize faint shock waves, expansion waves etc.

- *Shadowgraph* is yet another flow visulaization technique meant for high speed flow with transonic and supersonic Mach numbers. This is employed for fields with strong shock waves.

■ *The direct shadow/shadowgraph technique*

This is admirably suited to the demonstration of compressibility phenomena, particularly to visualization of shock waves and wakes. The method consists of a light source on one side of the tunnel and a screen on the other side. The visualization of the flow around a two-dimensional body in a wind tunnel, however , a more satisfactory arrangement is obtained by a collimating the light from the source into a parallel beam before it passes through the working section, by using a lens or mirror. The mechanism of the direct shadow is as follows. In the disturbed field the rays are deflected, and if the refractive index gradient $\frac{\partial n}{\partial x}$ is constant, i.e. $\frac{\partial^2 n}{\partial x^2} = 0$. The deflected rays remain parallel. However, if $\frac{\partial^2 n}{\partial x^2}$ is positive the rays will diverge and if it is negative the rays will converge. Fig. 1.6 shows the general nature of the variations of the density and its first and second derivatives through a shock wave. Thus at the front of the shock wave $\frac{\partial^2 n}{\partial x^2}$ is positive and the rays diverge, giving a region of decreased illumination at the screen, at the rear of the shock wave the rays converge and increase the illumination.

1.7   Aim of present investigation

The present investigation primarily aims at evaluating the efficiency of a shifted cross wire as the passive control technique to modify the mixing characteristics of correctly and incorrectly expanded supersonic rectangular jets. Thrust loss due to the presence of cross-wire has been calculated. The effect of cross wire location on jet decay characteristics is also investigated.
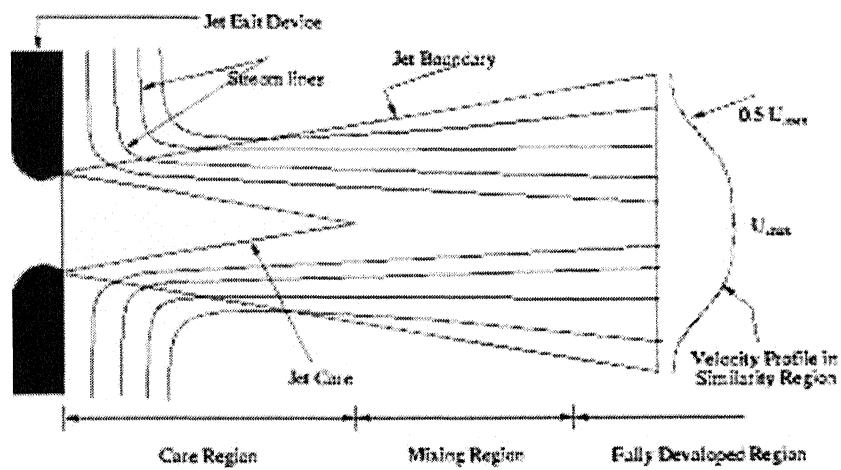
Figure 1.1 Schematic of subsonic jet flow and zones within jet
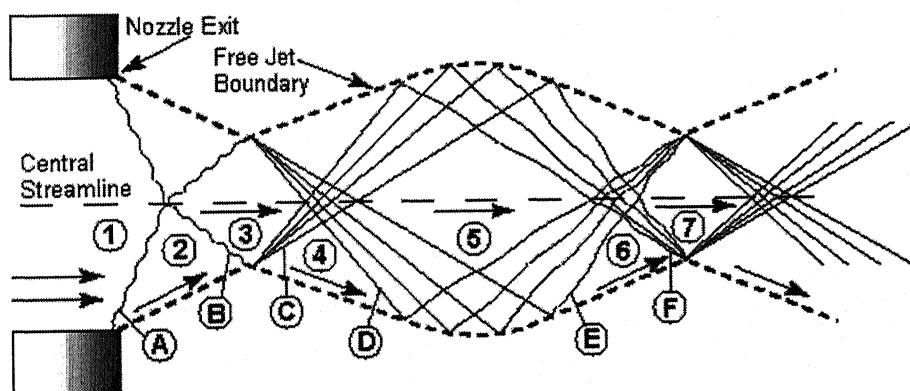
Figure 1.2 Schematic of overexpanded jet[20]

11
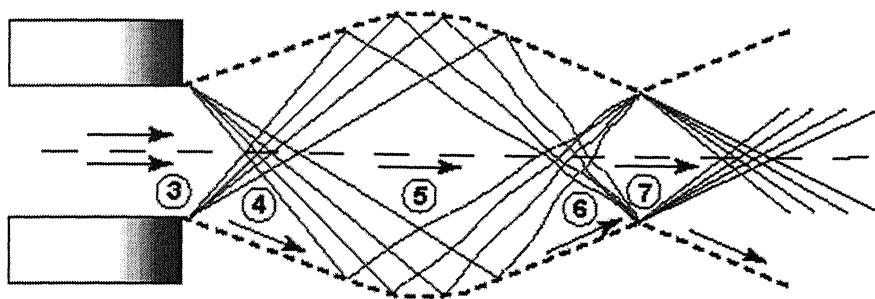
Figure 1.3 Schematic of underexpanded jet[20]

Tabs at Nozzle Exit

Grooved Nozzles

Notches at Exit

Multiple Jets
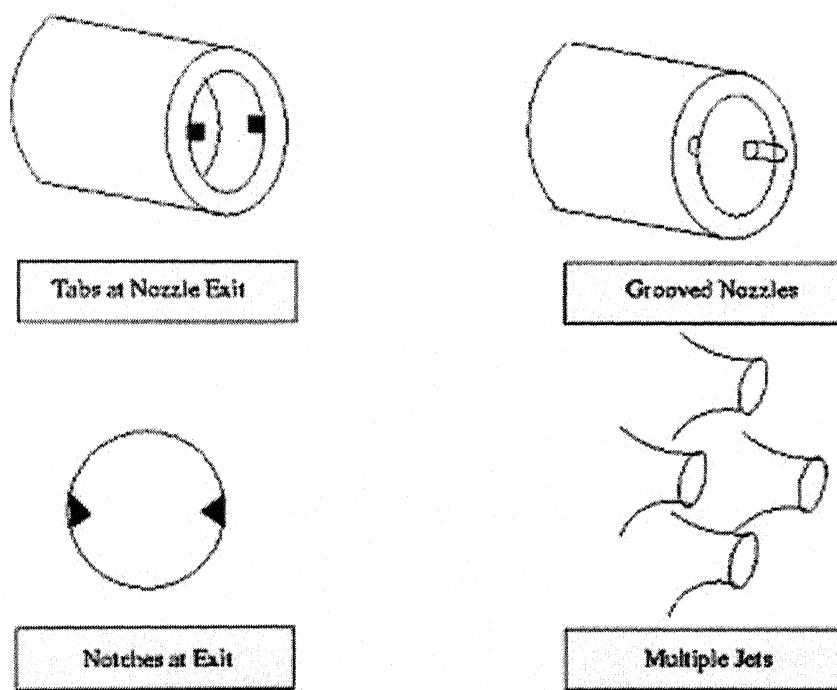
Figure 1.4 Few passive controls
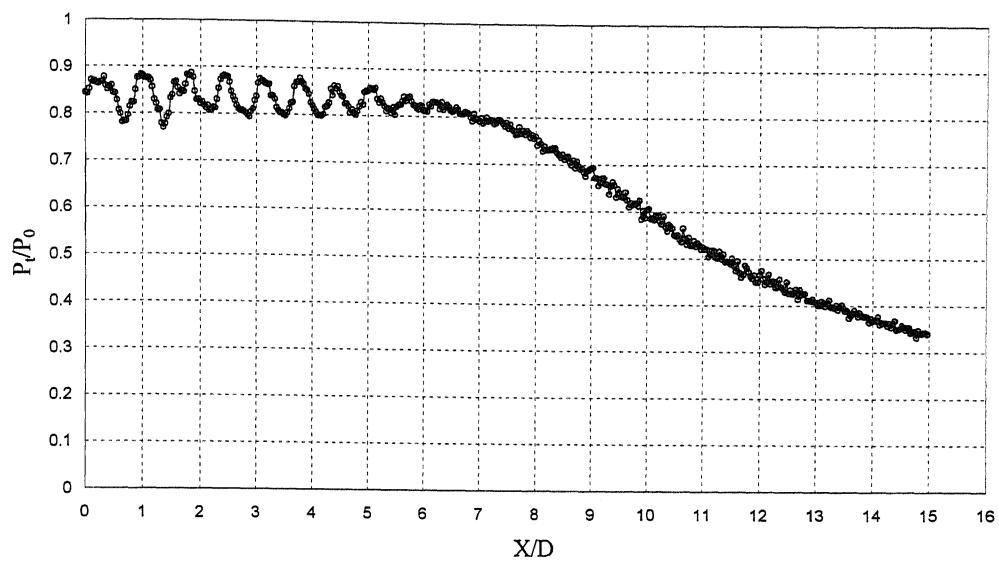
Figure 1.5 Centerline pressure decay of Mach 1.86 jet at NPR 5
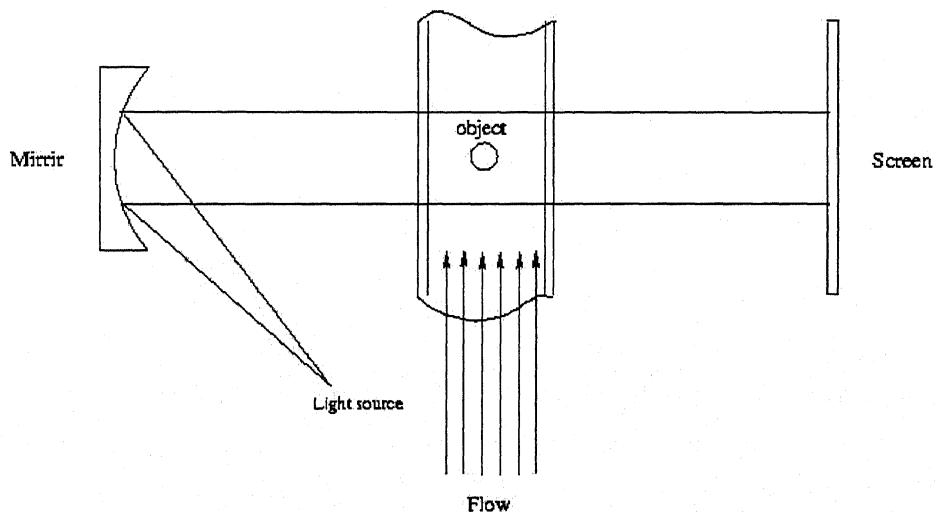
Figure 1.6 Schematic of shadowgraph arrangement

Chapter 2

Literature Review

Free jet can be defined as a pressure driven unrestricted flow of a fluid into a quiescent ambience, since a fluid boundary can't sustain pressure difference across it, the jet boundary is a free shear layer in which static pressure is constant throughout. The boundary layer at the exit of a nozzle develops as a free shear layer, mixing with the ambient fluid there by entraining the ambient fluid into the jet stream. Thus, the mass flow at the any cross-section of the jet progressively increases along the down stream direction. Many text books[1-3] have been dedicated to jet flows, fully or in part, starting from the monograph of Abramovich in 1936. The ultimate goal of the jet researchers has been the control of mixing enhancement, noise supression, etc.

2.1 Flow control with non circular jets

Non-circular jets were identified as an effective technique of passive flow control that allows significant improvement of performance in various practical systems at relatively low expenditure[4], because non-circular jets rely solely on changes in the geometry of the nozzle. The flow pattern associated with non-circular jets involves mechanism of vortex evolution and interaction, flow instabilities and fine scale augmentation. Elliptic and rectangular jets were investigated extensively because of their increased entrainment and enhanced mixing properties[5]. Improved mixing helps in achieving thrust augmentation, heat transfer promotion, augmentation of combustion efficiency, etc. While coherent structures are beneficial in enhancing large scale mixing, they prevent fine scale mixing particularly during the initial vortex development process [6]. Among the several passive control techniques used, non-circular geometries were recognized to be very effective in producing both small and large

scale mixing. Results showed that the presence of sharp corners in these geometries significantly increases the small scale turbulence intensity at the corners relative to the flat segment of the nozzle[7, 8, and 9].

Zaman compared the spread rate of asymmetric jets with that of their counter part symmetric ones. It is shown that spreading of most asymmetric jets is not much different from that of a round jet. In fact, a jet from an orifice with small aspect ratio (AR) exhibits virtually no increase in spreading [10]. A noticeable increase commences only when AR is larger than 10. Increase of aspect ratio is relatively inefficient mechanism for increasing jet spreading. The biggest increase in jet spreading is observed with the tabs. This is true in subsonic as well as in supersonic regime, inspite of the fact that screech is eliminated by the tabs. The characteristic spreading of the tabbed jets is explained by the induced motion of the tab generated streamwise vortex pairs. The primary concept of mixing enhancement using asymmetric jet is to stretch the perimeter of shear layer exposed to the ambient so that more entrainment takes place.

2.2 Effect of tabs on jet flows

The discrepancies that have been observed in the spread of nominally axisymmetric jets, depend on various factors. These factors include the nozzle boundary layer thickness, turbulence level and convergence. It was found that none of these factors had a significant effect on the jet development. By contrast, the insertion of small rectangular tabs into the jet flow on the nozzle perimeter was found to have a very profound effect on the jet development . E.J.S.Bradbury et al [11], found that just two tabs produce gross distortion in the jet development resulting in the jet almost splitting in two with high velocity regions, on either side of the diameter of adjoining the tabs. It has been found that the existence of flow structure which have some coherence around the entire circumference of the jet are the major source of jet noise and it seems that the inserting tabs is to prevent the occurrence of these structures. As far as boundary layer is concerned, it was found that the jet centreline velocity was not observably affected by the turbulent nozzle boundary layer thickness when the displacement thickness was less than 0.01 of the jet diameter. The potential core region was shortened by about half a diameter. The jet nozzle turbulence is unlikely to have much effect until it reaches an intensity of about 20%. The tabs with square sides (1/16D as width) in two numbers showed an apparent potential core length

reduction about 2D, followed by a rapid decay of the centre line mean velocity. There seemed to be two possible mechanisms by which gross distortion on this scale could occur namely, (1) By the stirring action of trailing vortex motion shed from the tabs. (2) By the simple deflection of the flow over the tab such as that might occur in a potential flow jet with circumferential variations in flow angle.

The vortex generators, in the form of small tabs protruding normally into the flow at the nozzle exit, produce distortion of the jet essentially same at subsonic and underexpanded supersonic conditions [12]. Thus the underlying mechanism is independent of compressibility effects. A tab with a height as small as 2% of the jet diameter but larger than the efflux boundary layer thickness is found to produce significant effect. The tabs however weaken the shock structure drastically in the supersonic regime which is accompanied by an elimination of the screech noise. But the basic effect must originate from changes in the vorticity distribution caused by the tabs.

From the above discussions, it is evident that tabs are identified as a passive control mechanism with potential, to enhance jet mixing and attenuate jet noise. As the primary structures or ring vortices roll up and move downstream they grow in size due to the entrainment of ambient fluid. The resulting jet decay is proportional to the velocity gradient across the shock layer and is a strong function of the distance downstream of the jet exit.

2.3   Effect of tab geometry on jet flows

For under expanded flows, the width of tab has a more profound effect on jet decay for the same blockage area ratio. It was determined that the end shape of the tab has an insignificant effect on the distortion produced as long as the blockage area to flow was kept constant [13]. Sreejith and Rathakrishnan [14] proved that the argument made by Zaman at al, is not true and the tabs can extend up to the radius of nozzle exit.

2.4   Dynamics of streamwise vortex pair

Each tab produces a pair of counter rotating streamwise vortices. The sense of rotation of the pair is such that, between the two vortices surrounding fluid is ingested into the core of the jet. The inward motion however, is restricted as the two pairs

approach each other, and shortly downstream, they rearrange to form two out flow pairs. The latter pairs eject jet core fluid while vortex induced motion propels them laterally away from the jet axis. This is what causes the rapid axis switching as well as the large lateral spreading of the jet as illustrated in Fig. 2.1 The mechanism of how a tab produces such a vortex pair has been discussed by Zaman et al [12]. The primary source of a vorticity is a pressure hill (pressure rise) formed upstream of the tab as a result of the fact that the approach flow is slowed down. The gradient of lateral pressure distribution, together with the presence of the wall, generates a pair of stream wise vortex.

2.5   Cross-wire as passive control

Recently Sreejith and Rathakrishnan [14] demonstrated that the tab geometry can extend upto the centre of the nozzle i.e. the tabs can run across the diameter. Thus, essentially a limit for tabs termed as *Rathakrishnan limit*. Also, they showed that, as reported by many in literature, there is no need for a favorable pressure gradient for a tab to be effective. In fact, the core length reduction was maximum at correctly expanded condition for some case of jets. They showed that the centreline pressure decay of jets from clean nozzle is much different from those nozzle with cross-wire, the jet decay enhanced significantly by cross wire. Thus, the streamwise vortices introduced by the cross wire is very effective in promoting jet mixing. Cross wire was found to be effective for correct, under and overexpanded jets. For some combination of parameters were found to get reduced by 50%.

From the review it is evident that end geometry modification as well as geometrical projections in the form of tabs and cross wire can serve as effective controls of jets but all these controls will result in significant thrust loss since the nozzle exit area is partially blocked, also a flow is made uncleaned by the pertrubution introduced by these controls. Therefore, it will be highly beneficial if the control is located downstream of the nozzle exit is deviced to achieve the control of the jet exhibiting characteristics similar to those with exit geometry modifications in this direction a cross-wire termed as shifted cross-wire is employed for jet control in present investigation.
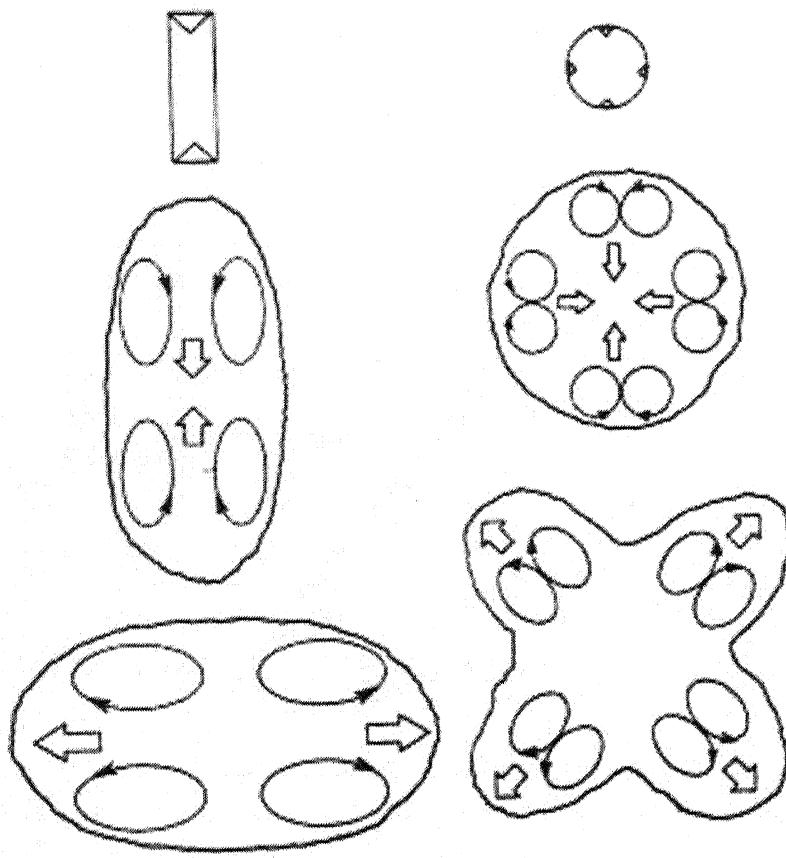
Figure 2.1 Vortex formations in tabbed jets

Chapter 3

Experimental Setup and Procedure

This chapter gives an overview of the test facility, experimental arrangements, describes the measurements carried out, the experimental arrangements, and various tools developed for the present study.

3.1   The test facility

The experiments were conducted in the free jet facility at high speed aerodynamic laboratory, Indian Institute of Technology Kanpur, India. The layout of the lab is shown in the Fig. 3.1. The test facility consists of (1) compressor, (2) storage tanks and (3) Jet test facility.

A two stage reciprocating compressor, capable of delivering 360 cfm of air at a pressure 500 psig is being used in this laboratory. The compressor used in present investigation is driven by a 150 hp 3 phase induction motor. A cooling water circuit, driven by an independent pump, cools the compressed air through an inter- cooler. The compressed air is then passed through a pre filter consisting of porous stone candles, to remove solid contaminants, like rust particles and oil droplets. An activated carbon filter is used for finer filtering. The compressed air is dried in a dual-tower semi-automatic silica gel dryer. While one tower is in use, a portion of the dried air is heated and used to reactivate the other. A diaphragm type back pressure valve operated by pressure relief pilot permits the dryer to operate at 500 psig, while the pressure in the storage tanks builds up from atmospheric to storage pressure. The compressed air is stored in three tanks, having total capacity of 3000 ft^3 at 300 psig.

The air enters the settling chamber through the tunnel section with a gate valve followed by a pressure regulating valve and a mixing length of 3" diameter. The

settling chamber is connected to the mixing length by a wide angle diffuser. The flow is further conditioned inside the settling chamber by closely meshed grids meant for minimizing turbulence. The settling chamber is a constant area circular section of 300 mm inside diameter and 600 mm length. The test models are fixed at the end of the settling chamber by a slot holder arrangement, which is a short pipe like protrusion with embedded O- ring to prevent leakage. Model to be studied is placed over the O-ring, over which an annular retaining sleeve with internal threads is screwed tightly. Fig. 3.2 shows a view of the free jet test facility at highspeed aerodynamics lab IIT Kanpur, India.

3.2 Instrumentation for pressure measurement

The Pitot pressure sensed by the probe was measured using a PSI model 9010, 16-channel pressure transducer (interfaced with a Pentium 4 computer loaded with VI based software for data acquisition). The model 9010 transducer is capable of measuring pressures upto 300 psig which is approximately 20 atm.

The system 9010 intelligent pressure scanner is a pressure measuring device intended for use in test and production environments. It consists of 16 channels and is working in differential mode. It has an asynchronous RS 422/485 host communication interface. It also has a standard RS-232 diagnostic interface that may also be used as host interface. The optomux style command set is used to send commands and receives response form all ports. It may be configured to communicate in the multidrop network communication always at selected baud rate using the optomux protocol. The multidrop communication always operates with no parity, 8 bit data bits and 1 stop bit. The default baud rate is 9600. Changes to baud rate can be made using special procedure via the DIP switch used to select the node address during initialization at power up. During this special baud rate selection procedure, the number of averages used during the data acquisition is also selected.

The application software developed using the Lab VIEW (shown in Fig. 3.3) links the host computer to the pressure scanner via RS 232 communication. The application software performs all the required functions like initialize, reset, rezero calibration and read pressure. The detailed description of this application software is described in Appendix A.

3.3 Models studied and measurements made

The experimental models tested in the present investigation are with design Mach 1.6, 1.8 and 2.0 of De Laval nozzles made of brass. However on calibration the nozzles were found to deliver flow of Mach 1.83, 1.86 and 1.94. The exit area of all the nozzles is same and is 750 mm^2, the cross-wire used 1 mm diameter stainless steel wire. The same wire diameter was used for all the nozzles. Fig. 3.5 shows the schematic of Mach 1.8 nozzle with cross-wire at 1D axial distance from the nozzle exit, of present investigation.

The flow measurements include Pitot pressure survey along the (geometric) centre-line of the jet for Mach numbers 1.6, 1.8 and 2.0 at correctly and incorrectly expanded flow conditions. For spread and entrainment analysis, Pitot pressure was measured at points on rectangular grids in the X-Y and X-Z planes from nozzle exit. These data also yielded the cross-sectional iso-baric contours.

The Pitot pressure probe is mounted on a three-dimensional traverse for the Pitot pressure surveys conducted over the entire flow field. The traverse has six degrees of freedom, which also includes a probe-yawing mechanism. The traverse has spatial resolution of 0.1 mm in all the three-dimensions. The Pitot probe used had an inner diameter of 0.4 mm and an outer diameter of 0.6 mm.

3.4 Pressure measurement and experimental procedure

The stagnation pressure in the settling chamber during the experimental runs was monitored on a computer screen through the VI based application software. The temperature in the settling chamber was measured by a sensitive thermometer. The ambient pressure was measured by a mercury barometer.

For preliminary studies on jet flow field, Pitot probe was used for the measurement of the total pressure in the flow field. The probe was balanced by yawing about its axis and was calibrated for pitch. In case of sonic and supersonic jets, due to the fluctuating nature of the flow field and also due to the fact that the core region of the supersonic jets is wave dominated (where a five hole or three hole probe can not be used), only a single hole Pitot probe designed in accordance with recommendations suggested by Nagai was used. Fig. 3.4 shows the schematic of the Pitot tube used in the present investigation.

The waves in the jet core again visualized by shadowgraph technique by viewing the flow normal to the cross-wire and along the cross-wire. In addition to this the flow field in the plane normal to the jet axis was visualized by placing a transparent plate coated with carbon oil paste. This surface flow visualization was carried out at different downstream locations. The resulting surface pattern formed due to the jet impingement on the plates was photgraphed and from these surface pattern the activites of the vortices prevailing in the jet field were inferred.

The Mach numbers at the nozzle exit were obtained from the measured Pitot pressure using the following normal shock relation.

$$\frac{P_t}{P_0} = \left(\left(1 + \frac{2\gamma}{\gamma+1}\left(M^2 - 1\right)\right)^{\frac{-1}{\gamma-1}}\right)\left(\frac{(\gamma+1)\,M^2}{(\gamma-1)\,M^2 + 2}\right)^{\frac{\gamma}{\gamma-1}}$$

Here, γ is assumed to be equal to 1.4, P_t is the absolute total pressure given by

$$P_t = P_{tgauge} + P_a$$

The data obtained by the above discussed procedure is accurate enough in subsonic flow region, but for the supersonic flow regions the data obtained is useful for qualitative comparison purpose only. The results presented are mostly of a comparative nature and hence, the inference made out of the results may be considered reasonably relevant to realistic and practical situations.

3.5 Precautions observed

In addition to the measures taken to minimize errors, like linearity checks, rezero calibrations, etc., the following precautions were also observed during the experiments:

- The horizontal alignment of the settling chamber was ensured.

- Care was exercised in the alignment of the models, to ensure proper positioning of the measurement planes.

- The nearest wall is 150 diameters hence wall effects are negligible.

- The pressure lines and the settling chamber ports were ensured to be leak- free.

- During the experiment the stagnation pressure reading was constantly monitored.

3.6 Data accuracy

The possible sources of error of the present investigation are due to

- The linear movement of traverse along X, Y and Z directions.

- The settling chamber stagnation pressure measurement.

- The error in the measurement of total pressure in the jet field.

- The possible inaccuracies in nozzle dimensions.

The room temperature was almost constant with maximum variation of $a \pm 0.50$ during one experimental run. The nearest wall from the apparatus was as far as 3.5 m so that wall effects could be neglected. The stagnation pressure was maintained with an accuracy of $a \pm 0.1\%$
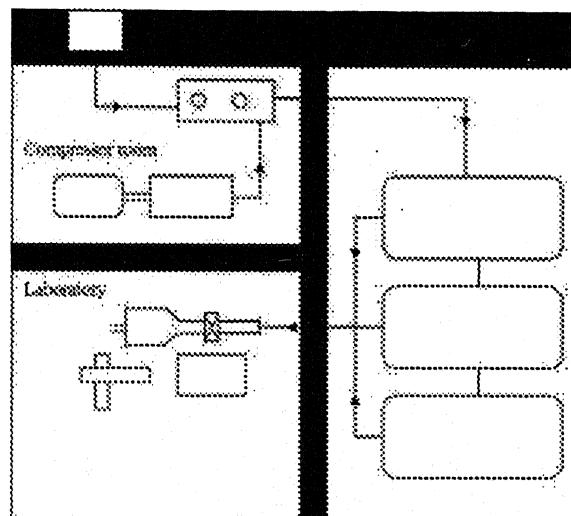
Figure 3.1: A view of the laboratory layout
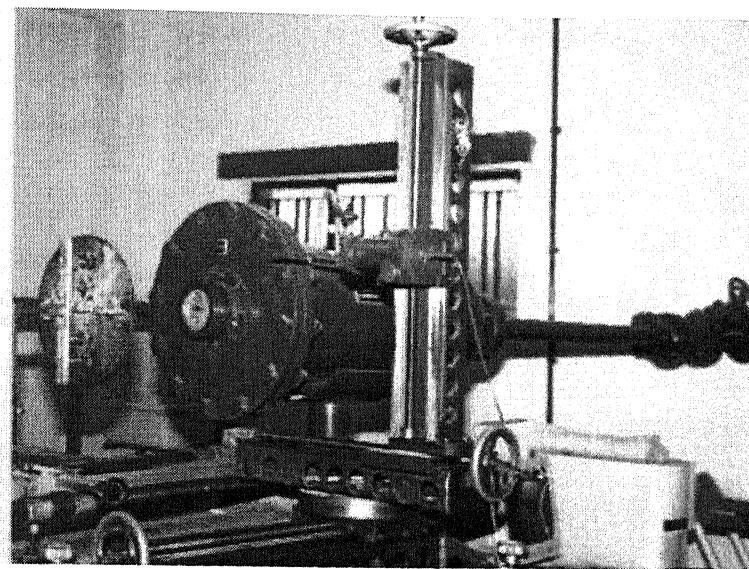
Figure 3.2 Schematic of jet test facility at IIT K
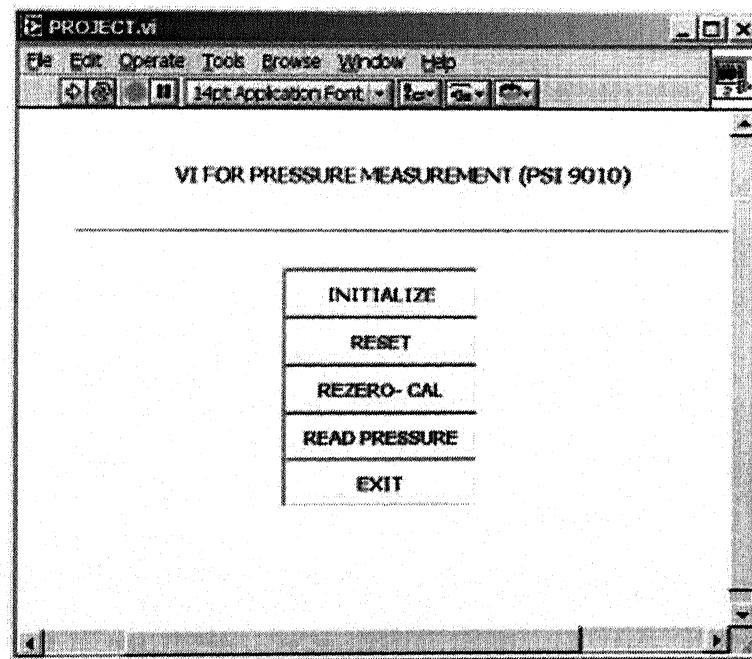
Figure 3.3 VI main program front panel
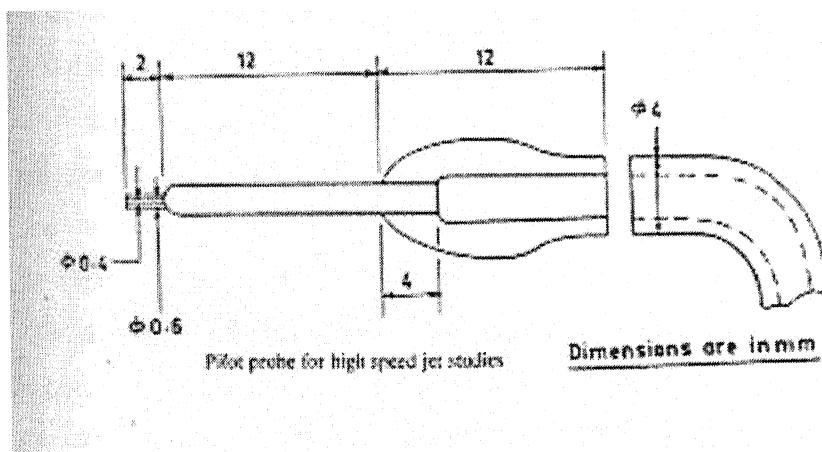
Figure 3.4 Pitot pressure probe

Figure 3.5 Schematic of nozzle with cross-wire

Chapter 4

Results and Discussion

The aim of the present investigation is to understand the effectiveness of shifted cross-wire as a passive control on the aerodynamic characteristics of supersonic jets. The effect of cross-wire location on the jet flow characteristics is also investigated. The Mach numbers of present study are 1.83, 1.86 and 1.94. These Mach numbers were specially chosen to study the effect of shifted cross-wire on jets which are screech prone (M 1.6, 1.8) and jets without screech (M 2). Another aspect of interest on jet control is the control effectiveness in the presence of adverse pressure gradient. To achieve this goal, the nozzle pressure ratios were considered in such a manner that, the jets generated were of the type underexpanded, correctly expanded and overexpanded. The nozzle pressure ratios (NPR) tested were 3, 5 and 7. The cross-wire locations studied were 0D, 0.5D, 1D, 1.5D and 2D. Even though it is well established that, cross-wire is an effective jet control [14], even in the presence of adverse pressure gradient. There is a serious setback with this type of control. That is, the control results in the blockage of the precious area at the nozzle exit, which strongly governs the thrust generated. Also in the literature so far, the very fundamental aspect namely, presence of any solid surface in a supersonic stream will result in the generation of shock/expansion waves has not been accounted for in the thrust loss consideration. In the present case of cross-wire, it is a slender cylinder kept normal to the flow hence, there will be a detached shock envelope all over the length of the wire. Therefore, if the thrust loss based on the projected geometrical area of the cross-wire is calculated, it will be highly erroneous. For proper estimation of the thrust loss, the nozzle exit area influenced by the shock envelop because of the wire should be estimated. Therefore, in present study the effective blockage area is estimated with wire at the nozzle exit (see appendix B), and utilized in the thrust loss determination.

26

4.1 Nozzles without control

Centreline pressure decay results for Mach 1.83 jet at NPR 3, 5 and 7 are given in Figs. 4.1a–c. From these plots it is seen that the shock cells in the core become stronger with increase of NPR. Also, the core length is about 1D for NPR 3, 6.1D for NPR 5 and 7D for NPR 7. The centreline pressure decay for Mach 1.86 jet at NPR 3, 5 and 7 are given in Figs. 4.2a–c. For NPR 3 the core length is around 4.5D, for NPR 5 it is 6.3D, for NPR 7 it is around 13D. Compared to Mach 1.83 jet the shock cells for Mach 1.86 jet are relatively weaker at NPR 3. This is because at NPR 3 the overexpansion level for Mach 1.86 jet is higher than that for Mach 1.83 jet. But at NPR 5 shock cells for Mach 1.94 jet are much stronger than those for Mach 1.83 and 1.86 jet. It should be noted that correct expansion NPRs for Mach 1.83, 1.86 and 1.94 are 6.02, 6.30 and 7.13 respectively. Therefore, NPR 3 and 5 are corresponding to an overrexpanded condition for Mach 1.83, 1.86 and 1.94. At NPR 7 the shock strength of shock cells of Mach 1.83 and 1.86 jets are stronger. The results of centreline pressure decay of Mach 1.96 jet are shown in Figs. 4.3a–c for NPR 3, 5 and 7. These results also exhibit that the core length as well as the shock cell strength in the core are dictated by the level of expansion at nozzle exit. From the above results of Mach 1.83, 1.86 and 1.94 jets, it is clear that the propagation of shock structure in the core region is governed by the jet Mach number and the level of expansion.

4.2 Nozzles with control

Centreline pressure decay of Mach 1.83, 1.86 and 1.94 jets controlled by a cross-wire positioned at 0D–2.0D insteps of 0.5D downstream of nozzle exit at different NPRs are given in Figs. 4.4–4.12 for different cases of the present investigation. As mentioned in the objective, aim of the present investigation is to study the effectiveness of a limiting tab in the form of cross-wire to control the mixing characteristics of supersonic jets. To asses the control effectiveness of cross-wire at different downstream locations in the presence of adverse and favorable pressure gradients, the results are analyzed systematically in the following sections.

4.2.1 Mach 1.83 jet

Centreline pressure decay results of Mach 1.83 jet with and without control at NPR 3 are shown in Figs. 4.4a and b. This is significantly an overexpanded jet. There are only mild shocks present in the core of uncontrolled jets, but when the wire is introduced the jet activity is reduced to a lower Pitot pressure level. Also, the shocks in the near field are getting weakened for wire at X/D = 0. But for wire at X/D = 0.5, downstream of the wire the jet becomes subsonic. Similar is the case with other wire locations. For this NPR at wire location X/D =1.5 results in best mixing performance. This is because for this case of highly overexpanded condition the jet looses its kinetic energy significantly in the initial shock cells and becomes subsonic beyond 1.5D. Therefore, the wire location is almost in the subsonic portion of the jet. The same is true for wire location X/D = 2. But for X/D = 2 the jet activities downstream of the wire is at Pitot pressure level which is appreciably above that for a X/D = 1.5.

Centreline pressure decay results for NPR 5 are given in Figs. 4.5a and b. This is also an overexpanded jet, but the level of overexpansion is much smaller than that of NPR 3. Therefore, it can be viewed that compared to NPR 3, the adverse pressure gradient prevailing is weaker. The results show that the strong shocks in the uncontrolled jet core are significantly diffused by the wire at X/D = 0, 0.5, 1.0, and 1.5. Also the core length reduction enjoyed for these locations are significant but for X/D = 2 the jet behaves distinctly different. For this NPR the optimized location was identified as X/D = 1 in corelength reduction and decay point of view.

Centreline pressure decay results for NPR 7 are shown in Figs. 4.6a and b. This is an underexpanded jet. For this case even though the jet activity after the control is taking place at much reduced Pitot pressure level, the shocks in the core are not influenced favorably by the control, except for wire at X/D = 1. For X/D = 1 location of the wire here again the control effectiveness seems to be the optimum.

4.2.2 Mach 1.86 jet

Centreline pressure decay at NPR 3 with cross-wire at X/D = 0, 0.5, 1.0, 1.5 and 2.0 are presented in Figs. 4.7a and b, centreline pressure decay for plain nozzle is also shown for comparison. This is the jet from a nozzle which is an overexpanded jet, i.e. with adverse pressure gradient. From these results, it is seen that the wire at the nozzle exit as well as downstream locations is effective in promoting jet mixing. Also, the shocks present in the core region of the uncontrolled jet are getting weaker or

even almost diffused when the wire is introduced. Another important feature seen is that, downstream of the wire the entire jet activity is taking place at a much reduced Pitot pressures compared to the uncontrolled jet. Further, among the wire locations wire at X/D = 1 proves to be the best location causing maximum mixing compared to the other locations. This is clearly seen from the centreline pressure decay shown in Fig. 4.7b.

The physical reason for this could be the following. The cross-wire is identically equivalent to a thin cylinder placed in supersonic stream. Therefore, there will be a detached shock envelop surrounding the wire. This detached shock due to the presence of wire will interact with the waves in the jet core. In addition to this the wire continuously sheds a pair of counter rotating streamwise vortices all along its length. These vortices once shed will trigger mixing at that location. Already vortices at the jet boundary would be propagating towards the centerline, promoting mixing along their path. Therefore, the combination of mixing initiated at the jet boundary, moving towards the centerline and the mixing initiated by the streamwise vortices shed by the wire would result in maximum mixing when the wire is placed at an optimum distance from the nozzle exit. For NPR 3 the optimum wire location is found to be X/D = 1. In addition to promoting aerodynamic mixing, weakening/diffusing the shocks in the jet core can be regarded as a great advantage from noise reduction point of view. It is well established that the lengths of third and fourth shock-cells and the strength of the shocks are the cause for establishing a feedback mechanism between Mach wave radiation frequency and the vortex shedding frequency at nozzle lip [19]. Therefore, one of the primary objectives of any jet control is to reduce these shock-cell strength and make them weak. This will ensure the destruction of the feedback loop and the associated screech tone in screech prone jets. Therefore the advantage seen from the results with wire at X/D = 1 for NPR 3 appears to be beneficial from both aerodynamic and aero/jet acoustic points of view. A probable reason for the specific advantage may be better understood if the waves in the shock-cells are visualized for a controlled jets. Visualization results are discussed in the subsequent sections.

The centreline pressure decay results for controlled and uncontrolled jet at NPR 5 are given in Figs. 4.8a and b. For this NPR Mach 1.86 jet is moderately overexpanded. The behaviour of this jet is slightly different from that at NPR 3. The shocks in the core are not getting diffused for the controlled jets. However, downstream of the controlled jet the entire jet activities are at much lower Pitot pressure level compared to the uncontrolled one. For this case also wire at X/D = 1.3 results in maximum

mixing compared to the other cases. Here it is to be noted that, even though the wire was located at $X/D = 1$, due to the flow and slender nature of the wire, the wire gets deflected with maximum deflection at the nozzle axis. Therefore, the resultant position of the wire at $X/D = 1.3$ instead of 1. Similar is the case with other locations, as seen from Figs. 4.7a and b.

The results for NPR 7 are shown in Figs. 4.9a and b. The jet is moderately under-expanded. There are large number of shock-cells in the jet core and also the shocks are much stronger compared to the lower NPRs. When the wire is introduced, the jet activity is taking place at a much lower pressure ratio compared to the uncontrolled jet. Also, the shock cells undergo some reduction in strength which are away from the wire. This is the case for wire at 0D, 0.5D, 1.5D and 2D. But for wire at $X/D = 1$ the results are remarkable in the sense that the control is very effective in reducing the Pitot pressure level in the jet as well as weakening the shock cell strength.

4.2.3 Mach 1.94 jet

Centreline pressure decay for Mach 1.94 jet at NPR 3 are given in Figs. 4.10a and b. This is a highly overexpanded jet. The introduction of wire has a marginal influence in the jet field, except for $X/D = 1$ location for which the corelength reduction is significant compare to other cases.

For NPR 5 the results of centreline pressure decay are shown in Figs.4.11a and b. This is again an overexpanded jet. For this case the wire influences the jet field significantly and brings down the Pitot pressure level lower than the uncontrolled jet for all locations, except $X/D = 2$. Another important feature observed is that, wire at $X/D = 1$ location does not appear to be the optimum for this case.

Centreline pressure decay results for NPR 7 are shown in Figs.4.12a and b. This is a jet with approximately correct expansion. Behavior of controlled jet at this NPR is almost identical to that at NPR 5.

From the above results of centreline pressure decay of Mach 1.83, 1.86 and 1.94 jets with and without control, it is seen that in the field beyond the beginning of characteristic decay zone the jet control is effective, resulting in significant mixing. Also, the combination of Mach numbers and level of expansion plays a decisive role in dictating the control effectiveness of cross-wire at all its locations.

4.2.4 Core length

To quantify the effect of wire location on mixing enhancement, the jet core lengths are measured. Variations of core length with wire location, for Mach 1.83, 1.86 and 1.94 jets tested NPRs of 3, 5 and 7 are plotted in Figs. 4.13–4.15. It is seen that, wire at $X/D = 1.0$ results in maximum core length reduction at all NPRs and Mach numbers of the present investigation. For Mach 1.83 jet the reduction of core length is about 14.2 % is achieved with wire at $X/D = 1$ at NPR 7. The corresponding reduction of core length for the same NPR for Mach 1.86 jet is 30.76% and for Mach 1.94 it is about 25% at NPR 7.

4.3 Optical visualization results

To gain an insight into the physics of mixing process associated with shifted cross-wire, the flow field was visualized with shadowgraph technique to study the waves in the jet field and by surface impingement technique to study the vortex activities.

In the shadowgraph visualization the jet flow field was visualized for both controlled and uncontrolled nozzles, normal to the major axis (larger side of the rectangle) and normal to the minor axis (shorter side of the rectangle) planes.

4.3.1 Mach 1.83 jet

The visualized wave pattern in the major and minor axis plane for Mach 1.83 jet at NPR 3 are given in Figs. 4.16a and b. At NPR 3 the jet is highly overexpanded, therefore there is a set of oblique shocks at the exit of nozzle for the plain nozzle. When the wire is kept at $X/D = 0$ the interaction of the waves at the nozzle lip and detached shock from the wire, establishes a Mach disc just downstream of the wire, after that there are no waves seen in the downstream. For the wire at $X/D = 0.5$ the detached shock around the wire and a single disc after the wire are clearly seen for wire at $X/D = 1$. The detached shock at the wire has become weaker and also the Mach disc downstream of the wire for $X/D = 1.5$, the wave pattern is similar to those at $X/D = 1$. But for wire at $X/D = 2$, the detached shock at the wire is very weak and could not able to form a Mach disc downstream of it. This is because by the time the flow reaches the wire it looses a significant amount of kinetic energy in overcoming the interaction of the waves.

Results for NPR 5 are shown in Figs.4.17a and b. The waves in the uncontrolled

jets have become stronger compared to NPR 3. For wire at X/D = 0.5, unlike NPR 3 case, there is no Mach disc downstream of the wire, only an interaction point is seen. Similar is the case with wire at X/D = 1. But for wire at X/D = 1.5 the interacting waves downstream of the wire are very weak compared to the previous locations of wire, for wire at X/D = 2 the waves downstream of the wire become much weaker than those for X/D = 1.

Results for NPR 7 are shown in Figs. 4.18a and b. This is an underexpanded jet, therefore the flow expands outside the nozzle and waves occupy larger area compared to NPR 5. For wire at X/D = 0 the interaction between the waves intensified because of the additional waves generated by wire. Similar is the case for X/D = 0.5. But for wire locations X/D = 1, 1.5 and 2.0, after the wire the waves in the field appear much weaker both in the major and minor axis planes.

4.3.2   Mach 1.86 jet

The visualized waves in the major and minor axis plane for Mach 1.86 jet at NPR 3 are given in Figs. 4.19a and b. From these results the oblique shock waves at the nozzle lips and the shock cells in the jet flow field are clearly seen in both the planes. But when the cross-wire is placed at nozzle exit (see Fig. 4.19a) there are additional waves generated because of the detached shock due to the presence of wire. These waves interact with other waves in the downstream. These interactions lead to a faster spread as seen in the picture along the minor axis plane for wire at X/D = 0.5 (Fig. 4.19a). In the major axis plane the detached shock envelop infront of the wire and the distinct Mach disc downstream of the wire are clearly seen. The waves downstream of the Mach disc are very weak compared to the uncontrolled jet whereas in the minor axis plane the waves from the detached shock envelop around the wire and their interaction with the waves in the shock cells are clearly seen.

For wire at X/D = 1.0, once again it is seen that there is a detached shock envelop around the cross-wire and Mach disc downstream of the wire in major axis plane. In minor axis plane it is seen that, after the wire only one shock cell is prominent and downstream of it the shocks almost got diffused (Fig. 4.19b). For wire at X/D = 1.5 the detached shock envelop around the wire appears to be weaker than those for wire at upstream location. Similar is the case with cross-wire at X/D = 2.0.

Visualization results for the jets with and without control for NPR 5 are shown in Figs. 4.20a and b. In the uncontrolled jet the oblique shock waves fromed at the nozzle exit and the wave pattern in the jet field are clearly seen. It is seen that the

waves become stronger with increase of NPR. When the wire is introduced at X/D = 0 the interaction of the prevailing shocks and those because of the wire is clearly seen in both the planes. Also, the shock interaction point in the controlled jet has become more prominent than the uncontrolled one. For wire at X/D = 0.5 it is seen that the interacting waves occupy less extent compared to X/D = 0. Similar is the case for wire at X/D = 1, 1.5 and 2.0.

The results for NPR 7 are given in Figs. 4.21a and b. This is an underexpanded jet. Therefore, there are expansion fans positioned at the exit for the plain nozzle. Shocks from wire at X/D = 0 interfear with the expansion fan and the downstream field, causing the generation of additional waves in the jet field. For wire at downstream locations of X/D = 0 it is clearly seen that the waves upto the wire are unaffected. But downstream of the wire the flow field is dominated by the interaction of the prevailing waves and those due to the presence of wire.

4.3.3   Mach 1.94 jet

At NPR 3, this jet is highly overexpanded. Visualization pictures for this jet at different NPRs are shown in Figs. 4.22a and b. Wire at X/D = 0 results in the establishment of a Mach disk downstream of a wire. For X/D = 0.5 location the detached shock at the wire and Mach disc downstream of the wire are seen, but the extent of Mach disc is lower than that of X/D = 0. For wire at X/D = 1, the detached shock at wire has become weaker and also the Mach disc downstream of a wire is very weak . For wire at X/D = 1.5 and 2, the detached shock strength as well as the Mach disc downstream of a wire got reduced compared to X/D = 1.

Wave pattern of Mach 1.94 jet at NPR 5 are shown in Figs. 4.23a and b. For this NPR the jet is still an overexpanded, but compared to NPR 3 the waves are stronger in the field. With wire at X/D = 0 the waves interact severely and the shock-cells become shorter. For X/D = 0.5, it is interesting to note that the wire location is just downstream of the wave interaction point. Due to this the wave at the wire takes a shape influenced by the intersection point and the waves downstream of the intersection point. This influence affects the flow field downstream of the wire also. For wire at X/D = 1 the detached wave is loyal to the wire and the waves downstream of the wire appear to be weaker and same is the case with wire at X/D = 1.5 and 2.0.

For NPR 7 the first wave interaction point shifted downstream, exhibiting the effect due to the decrease of adverse pressure gradient. This NPR is nearing the correct NPR of 7.13 for Mach 1.94 jet. When the wire is introduced at X/D = 0 the

interaction of the waves become severe, as seen from the results for wire at $X/D = 0.5$. The interaction of the waves become weaker for $X/D = 1$. Here again the interacting waves downstream of wire are much weaker than those for $X/D = 0.5$. But for $X/D = 1.5$, the waves downstream of the wire appear stronger than those for $X/D = 1.0$, this implies that the positioning of the wire plays a dominant role in dictating the strength of shocks downstream of the wire. For $X/D = 2$ the waves downstream of the wire are weaker, but prevail over a large distance compared to $X/D = 1.5$.

From the above discussions, it is evident that the location of wire has a dominant role to play in controlling the mixing process. In general, it can be stated that, for the present combination of parameters, with location $X/D = 1$ appears to be best location for mixing promotion.

4.4 Surface visualization

To get an insight into the shear activity in the jet field, a flat plate coated with carbon powder mixed with oil, which can easily be removed by shearing action, was kept normal to the jet axis. On impingement, the vortices present in the field act on the coated material. If they are large scale structure they do not remove the coating efficiently compared to their small scale counter parts. Therefore, on the surface where there is considerable removal of material is the zone of small scale structure activity and locations where the coating is intact is the zone of large scale activity.

The nozzle used to generate jet is a rectangular one. There are four sharp corners at the exit, also two sides are langer than the other two sides. It is well known that the size of a vortex shed is proportional to the radius of curvature of the edge from which it is shed. Therefore, at the longer edge the vortex shed will have a larger size compared to the shorter edge. Also, the vortices near the corner will be small eddies which are interacting. All these details are seen on the visualized pattern shown in Figs. 4.25–4.33.

Figure 4.28 shows the flow pattern of Mach 1.86 jet without control with plate kept at $X/D = 1$. It is seen that at the four corners the shear activities are dominant. This is because of small eddies shed at the corners. Along the major and minor axis directions the material at the centre is intact, indicating that four pairs of counter rotating vortices generated from the corners propagate towards the core. As the jet moves downstream, these vortices are seen around the axis in the visualization. Along the major axis it is seen that the vortices because of counter rotating nature

are repelling away leaving the coating intact. For wire at X/D = 0.5 visualization at X/D = 1 shows that the mixing activities are much larger extent compared to the plain jet. Even at the extremities of the minor and major axes, the shear activities are predominant indicating that the streamwise vortices shed by the corners dominate the mixing process. At X/D = 2, once again the controlled jet experiences larger spread due to the mixing enhancement compared to the plain jet. For wire at X/D = 1, at an axial distance of 2D jet exhibits mixing much larger distance compared to clean jet as seen from the visualization.

Visualization pictures for X/D = 3 location for plain nozzle, and for wire at X/D = 0.5, 1, 1.5 are shown in Fig. 4.30. Here once again wire at X/D = 1 location appears to be efficient in mixing promotion compared to other locations.

Visualization picture for Mach 1.83 jet for NPR 3 are shown in Figs. 4.25–4.27. It is seen that the spread of the controlled jet has increased compared to the uncontrolled one. Field at X/D = 2 for wire at X/D = 0.5, 1 and 1.5 are compared in Fig. 4.27 it is interesting to note that, both X/D = 0.5 and 1 wire locations are showing much higher spread compared to uncontrolled ones. The results for wire at X/D = 3 shown in Fig. 4.75 reveals that, wire at X/D = 1 is optimum to enhance mixing.

The results for Mach 1.94 jet at X/D = 1 location is shown in Fig. 4.31. It is seen that the control is effective in promoting the mixing. Similar results for X/D = 2 with wire at X/D = 0.5, 1 and 1.5 are given in Fig. 4.32. It is seen that the streamwise vortices generated by wire at X/D = 1 is more efficient in promoting the mixing, compared to other locations of wire. Results for X/D = 3 are shown in Fig. 4.33. These results once again exhibit that wire at X/D = 1 and 1.5 are superior mixing promoters compared to the other locations.

4.5   Thrust loss

To account for thrust loss due to the presence of wire at the nozzle exit, Pitot pressure survey at the nozzle exit, with and without wire were made. Using the measured Pitot pressure and settling chamber pressure, the Mach numbers at the nozzle exit plane were computed using normal shock relations. For the nozzle without wire the Mach number was found to be fairly uniform. But when the wire is introduced the Mach number around the wire assumes a much lower value. This reduction of Mach number and the extent of this reduced Mach number zone are influenced by the nozzle exit Mach number and the level of expansion as seen from Figs. 4.34–4.36.

The mumentum thrust is given by

$$\text{Thrust} = \dot{m}V_j = (\rho_e A_e V_e)\ V_e$$

where $\dot{m}$ is the mass flow rate, V_e is the flow velocity at the nozzle exit, A_e is the nozzle exit area and ρ_e is the density at nozzle exit.

For the case without control it is fairly straight forward to use the average velocity and density in the thrust equation to obtain thrust. But for the nozzle with cross-wire the flow velocity and density around the wire are different as seen from the Mach number plots. Therefore, appropriate density and velocity are to be used at the nozzle exit. A typical procedure employed to estimate the thrust for with and without wire is given in appendix B.

The loss of thrust in percentage was obtained for all the tests of the present investigation using the relation as given below

$$\boxed{\%\ \text{Thrust loss} = \frac{T_{\text{without wire}} - T_{\text{with wire}}}{T_{\text{with wire}}} \times 100}$$

The estimated thrust losses are tabulated in Table 4.1. It is intresting to note that the thrust loss is very close to the blockage area of 4% which is same for all nozzles. A closer look at flow mechanism can clarify this observation in a supersonic stream. To maintain the mass conservation, a decrease in density must be compensated by increase of both area and velocity and vice versa [15]. In accordance with this theory, eventhough much larger area compared to the projected area of the wire adversely influences, the density increase caused by the flow retardation, compensated significantly at the loss of thrust. Therefore, the net mumentum thrust is slighly close to the geometrical blockage.
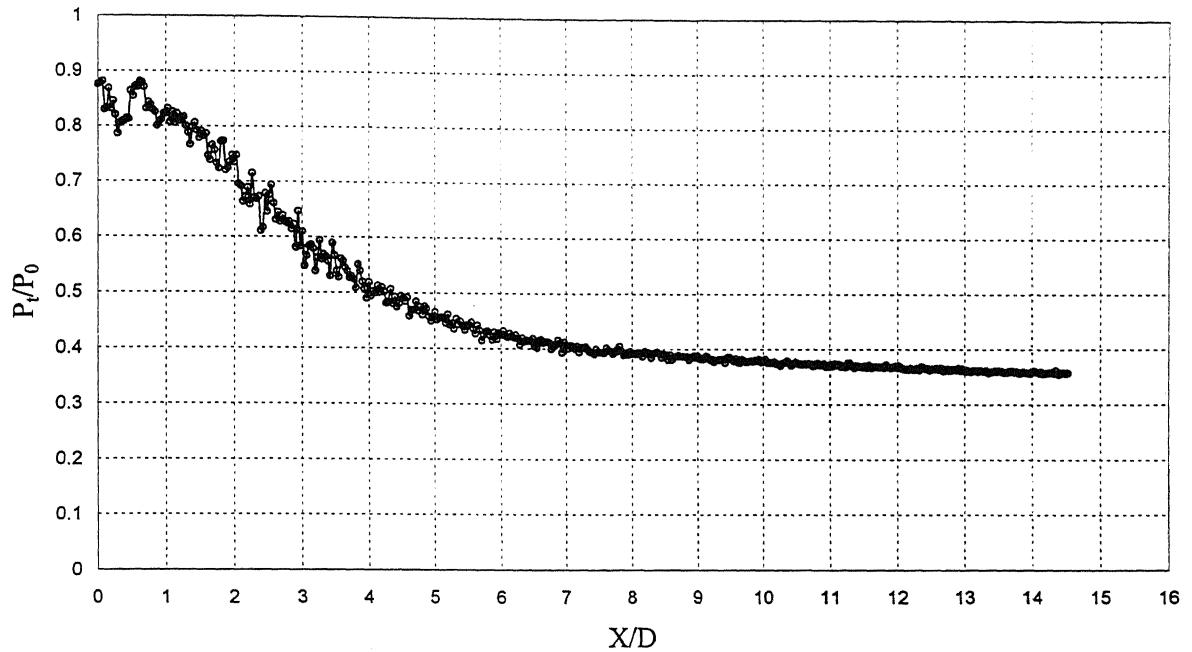
Figure 4.1a CPD of Mach 1.83 jet at NPR 3
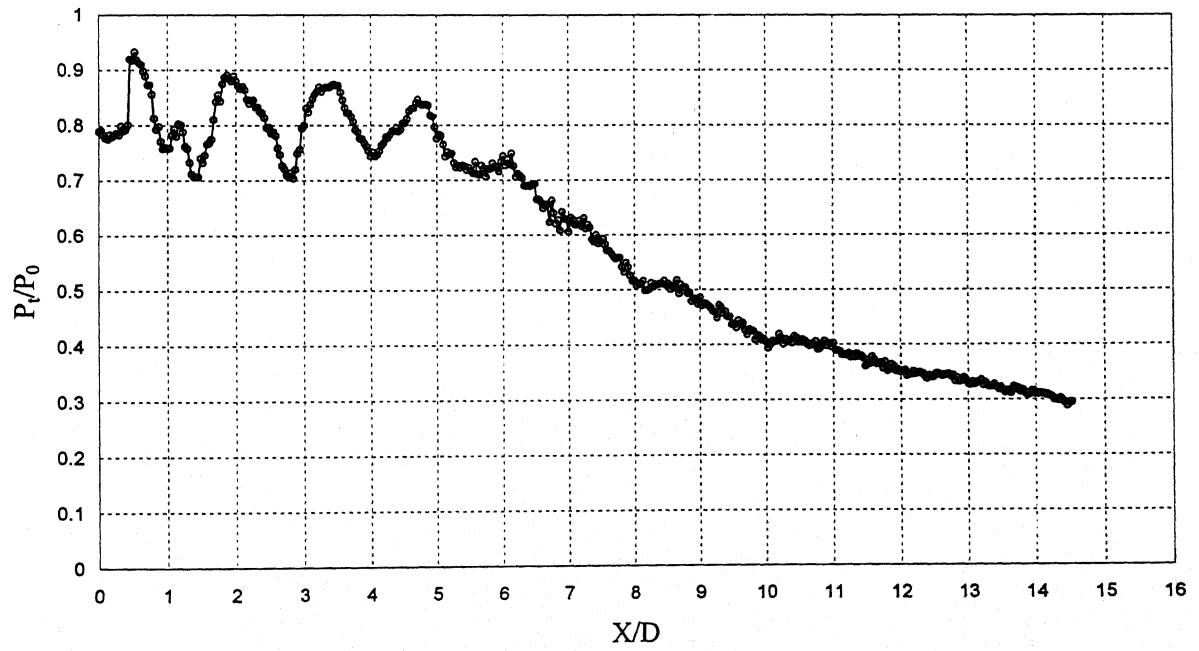
Figure 4.1b CPD of Mach 1.83 jet at NPR 5

37
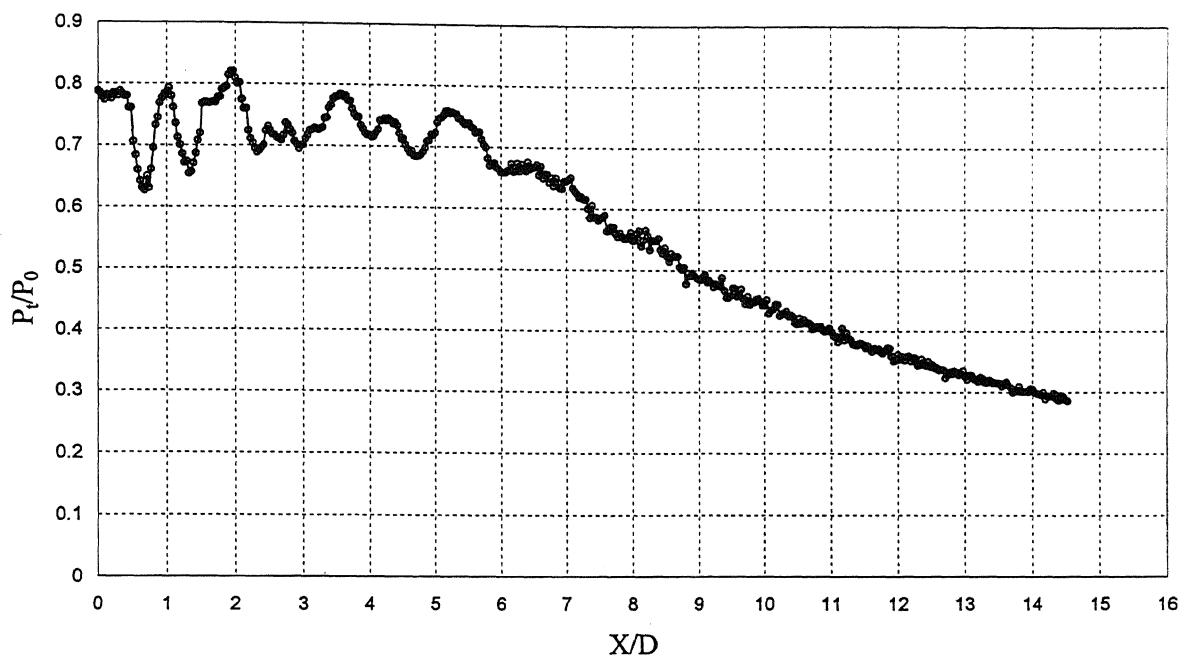
Figure 4.1c CPD of Mach 1.83 jet at NPR 7
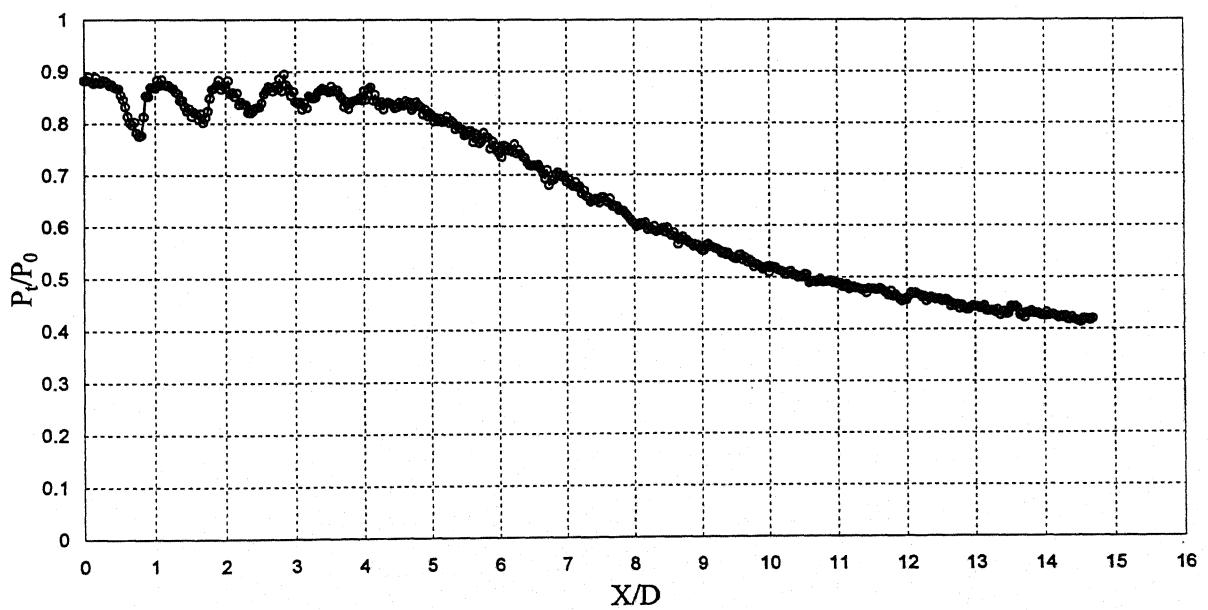
Figure 4.2a CPD of Mach 1.86 jet at NPR 3

38
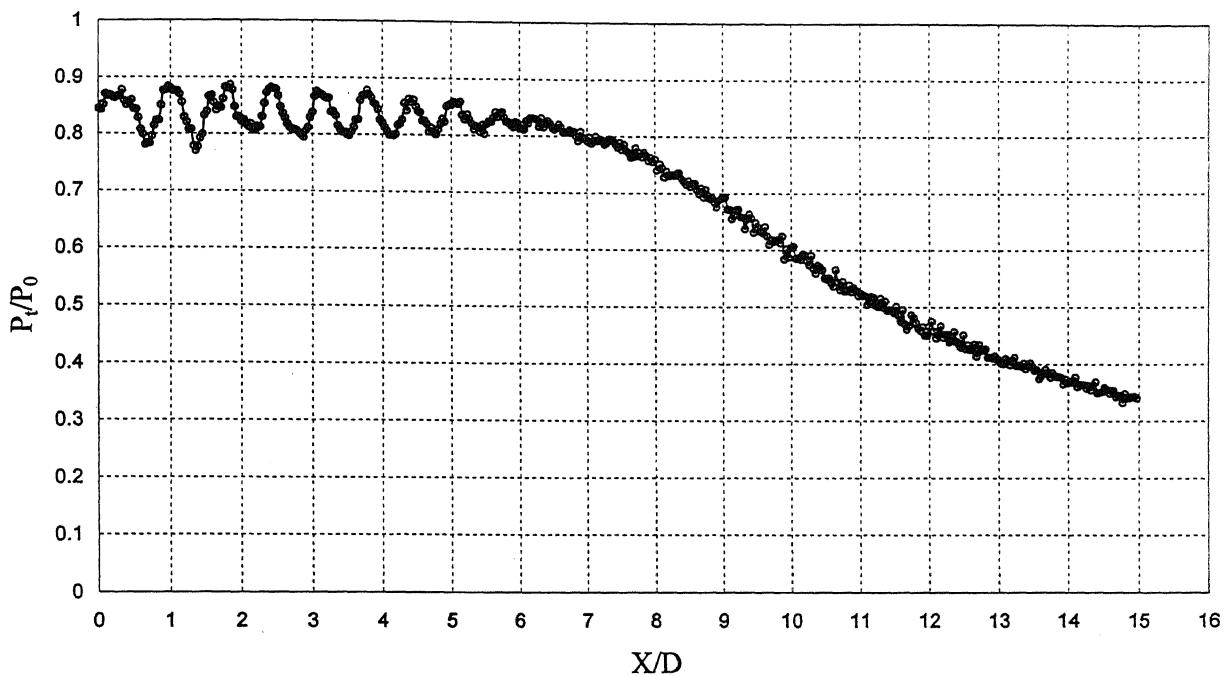
Figure 4.2b CPD of Mach 1.86 jet at NPR 5
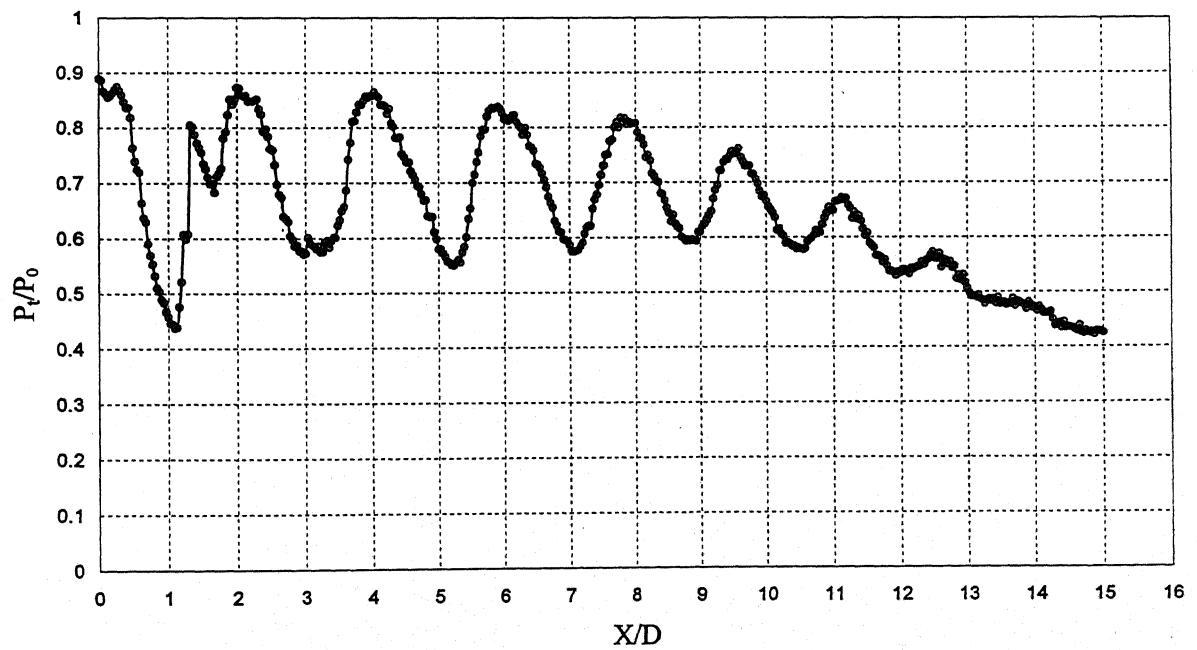
Figure 4.2c CPD of Mach 1.86 jet at NPR 7

39
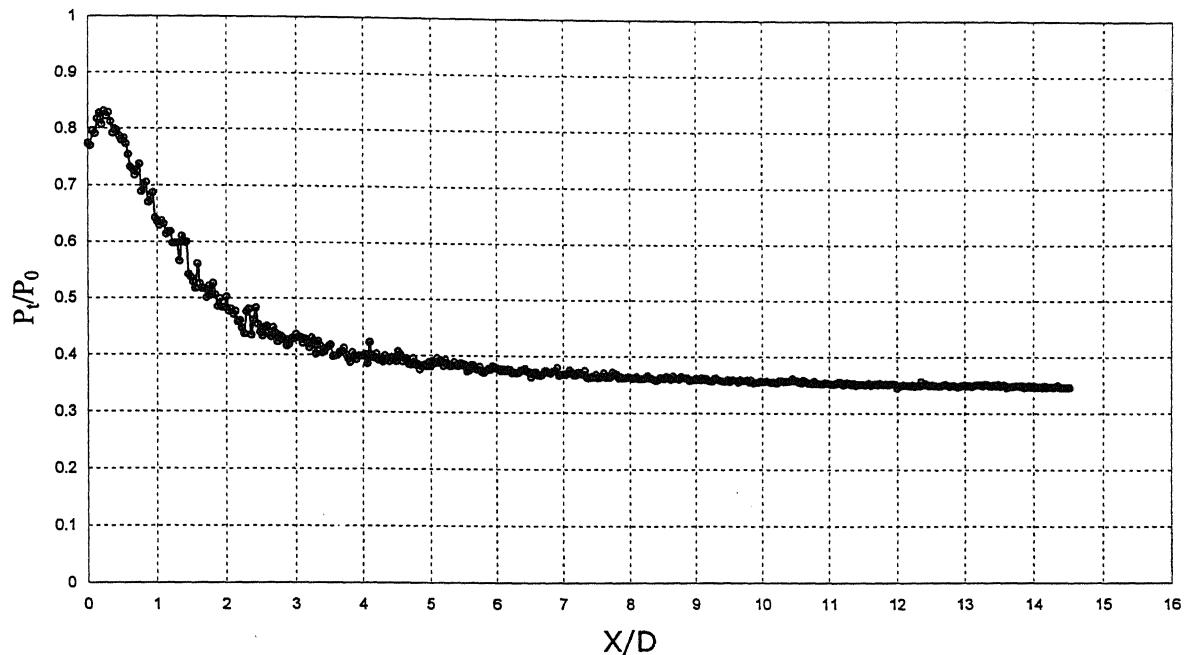
Figure 4.3a CPD of Mach 1.94 jet at NPR 3
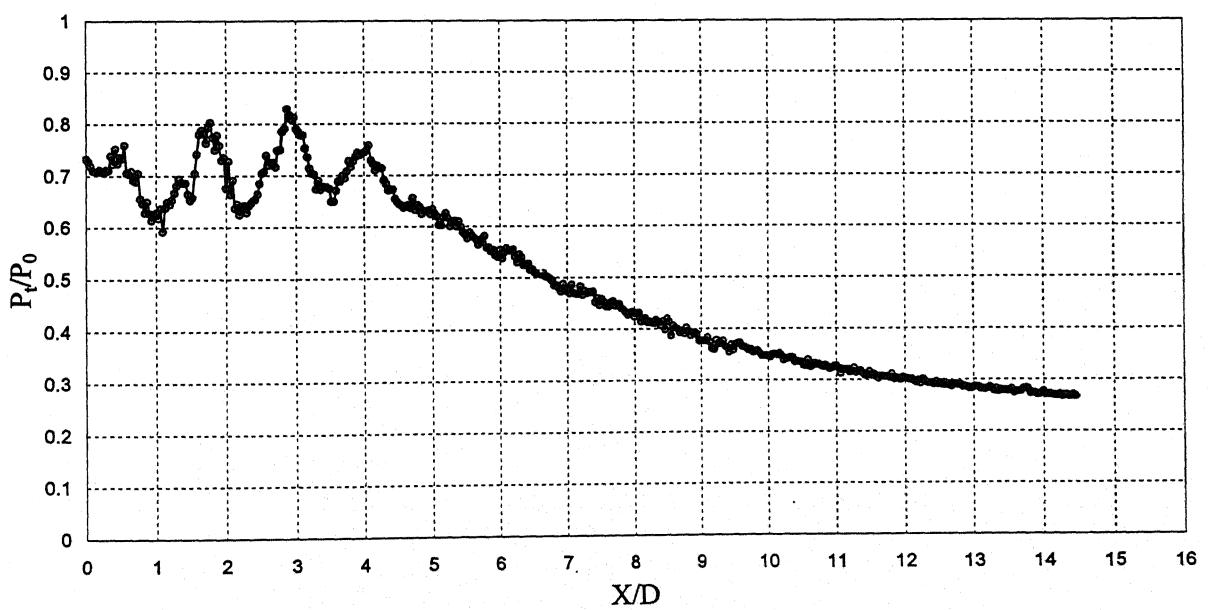
Figure 4.3b CPD of Mach 1.94 jet at NPR 5

40

Figure 4.3c CPD of Mach 1.94 jet at NPR 7

Figure 4.4a CPD of Mach 1.83 jet without control and C-W at 0D, 0.5D (NPR3)
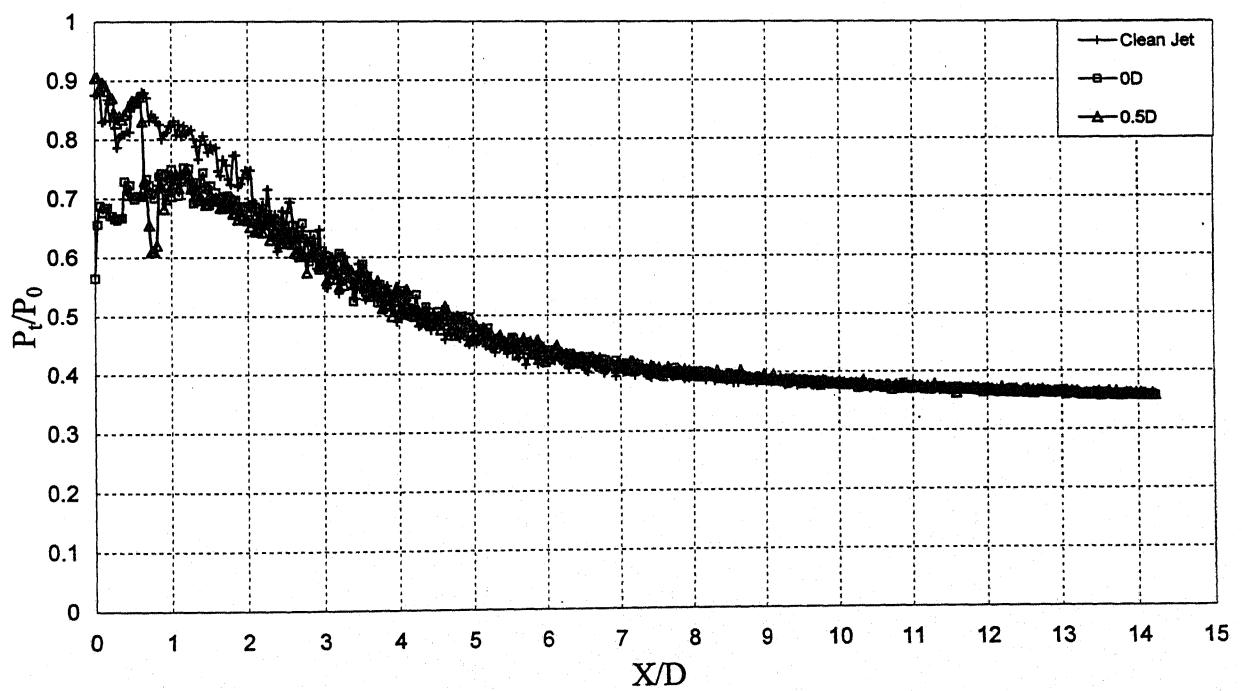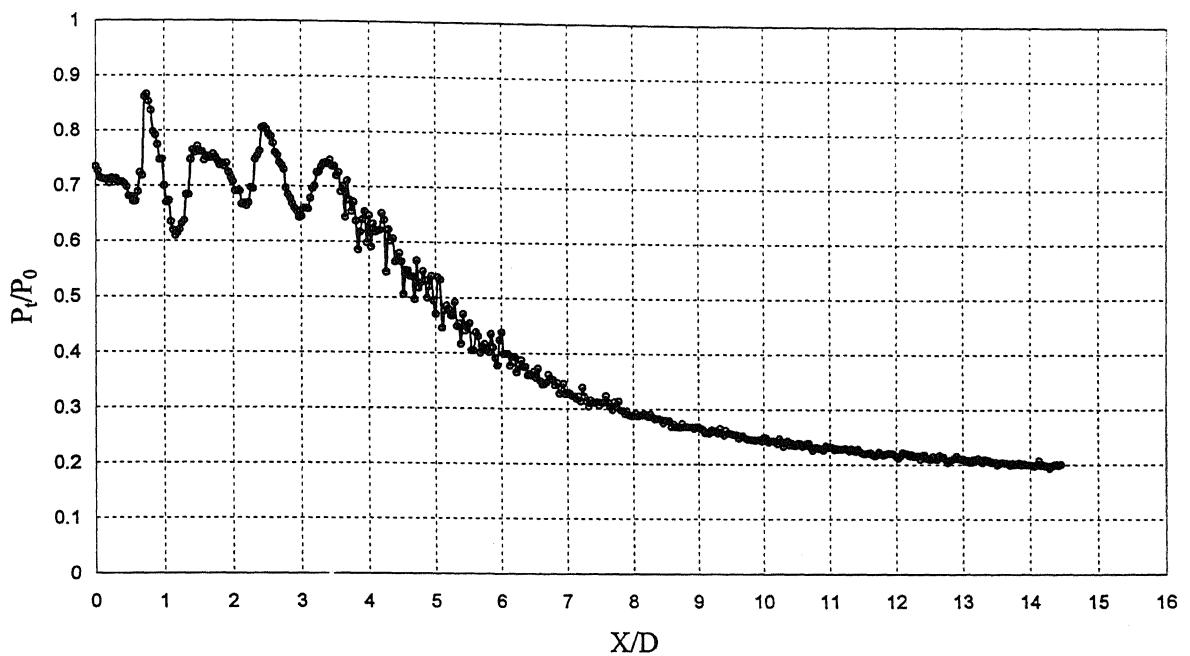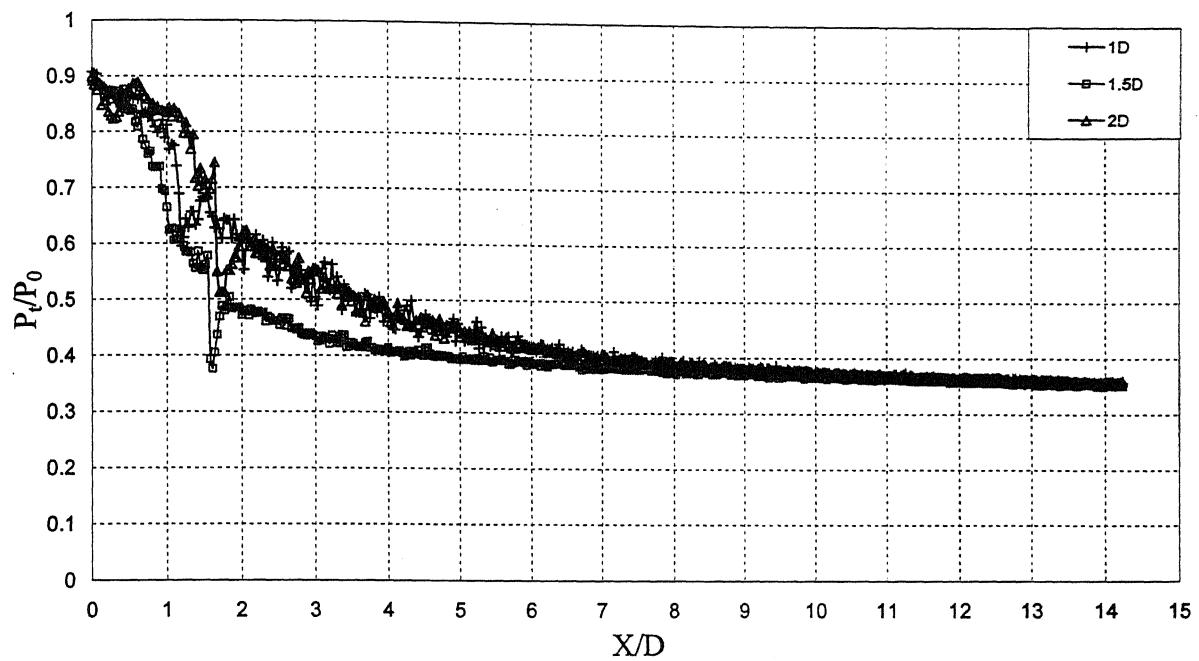
Figure 4.4b CPD of Mach 1.83 jet with C-W at 1D, 1.5D and 2D (NPR3)
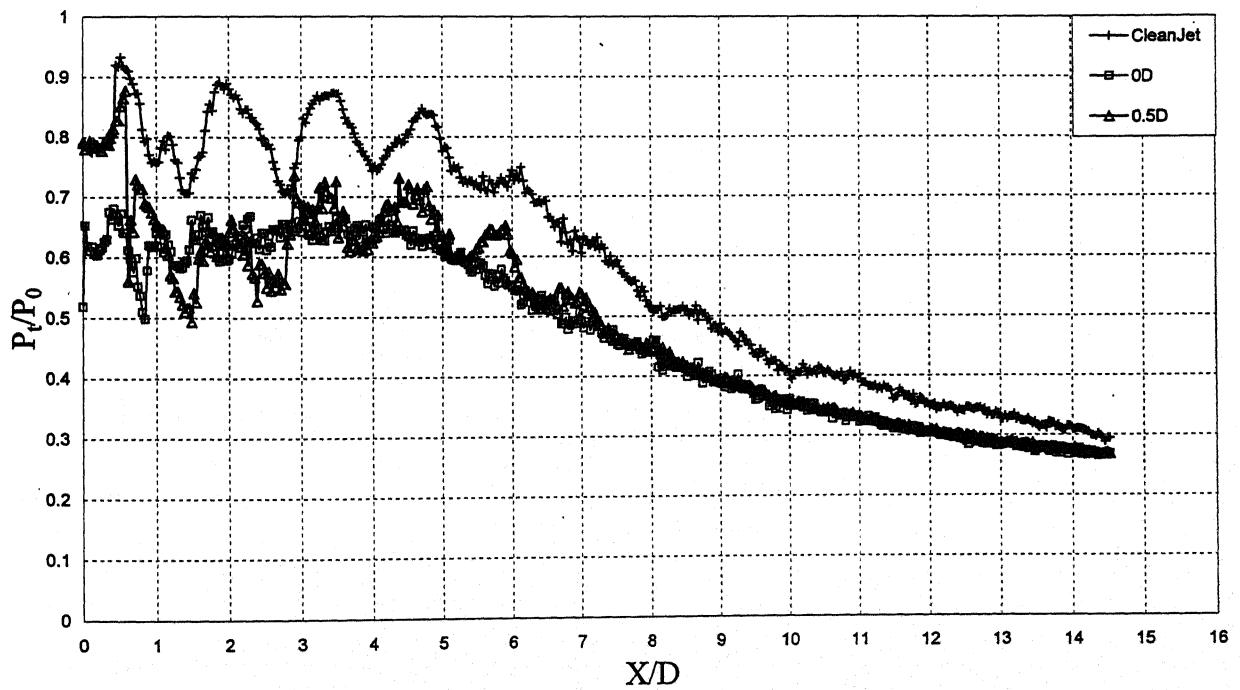
Figure 4.5a CPD of Mach 1.83 jet without control and C-W at 0D, 0.5D (NPR5)

42
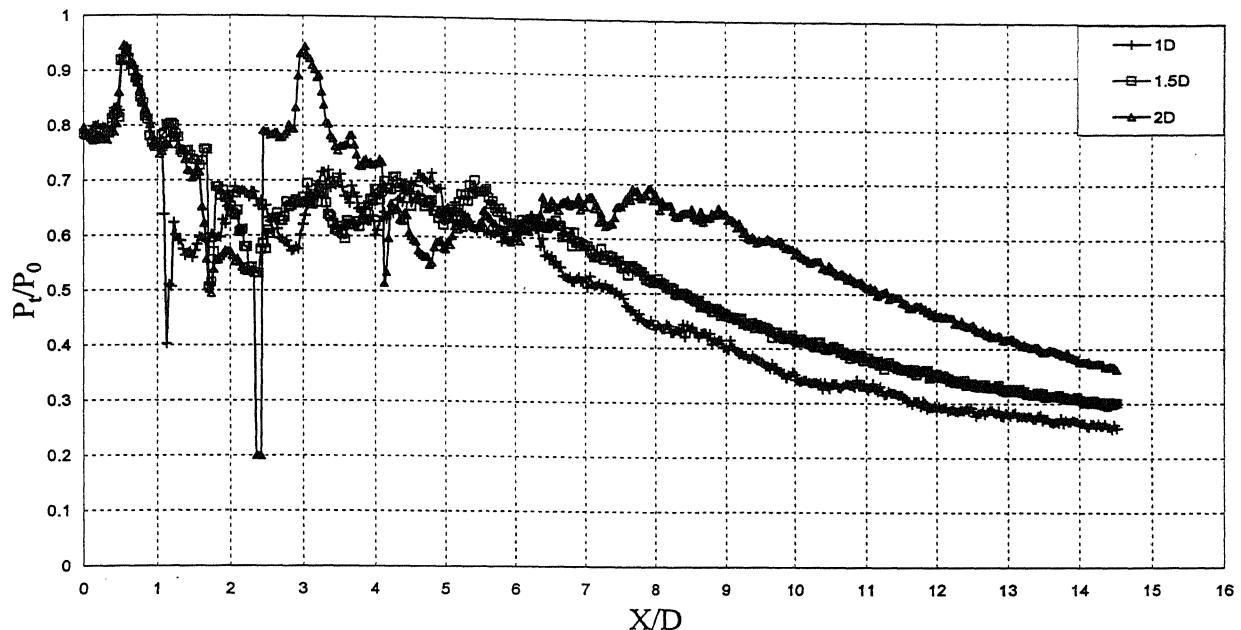
Figure 4.5b CPD of Mach 1.83 jet with C-W at 1.0D, 1.5D and 2D (NPR5)
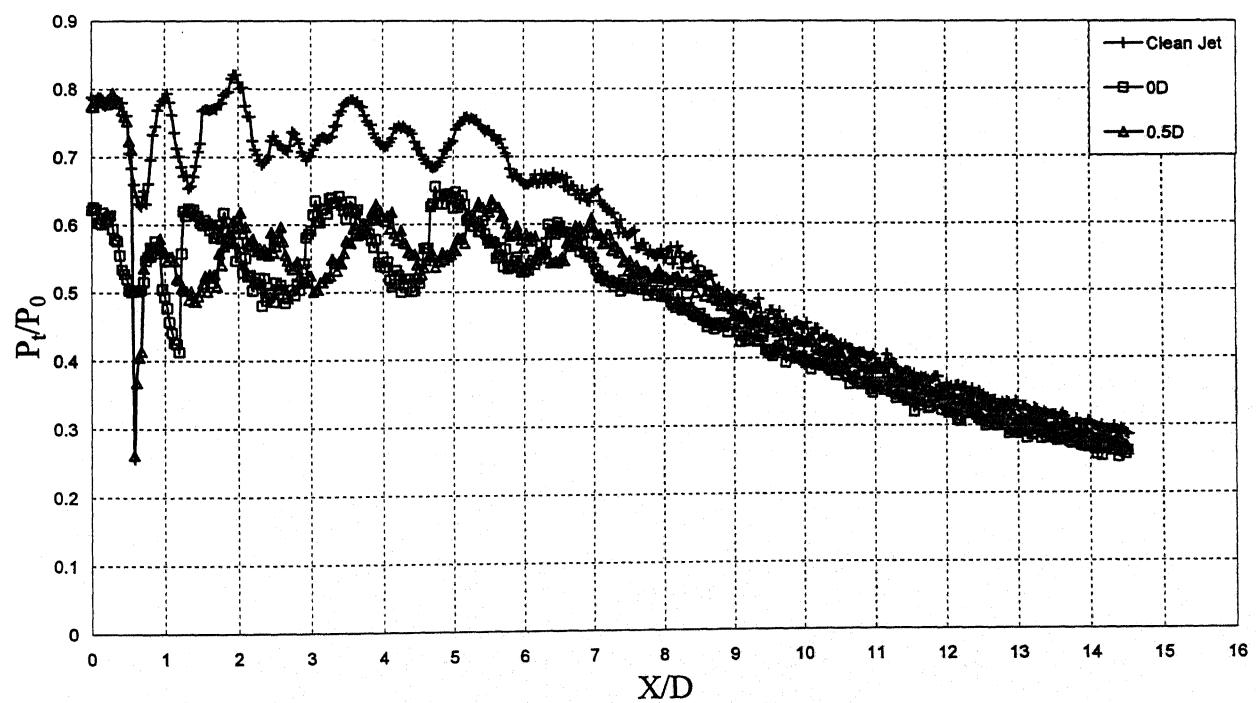
Figure 4.6a CPD of Mach 1.83 jet without control and C-W at 0D, 0.5D (NPR7)

43
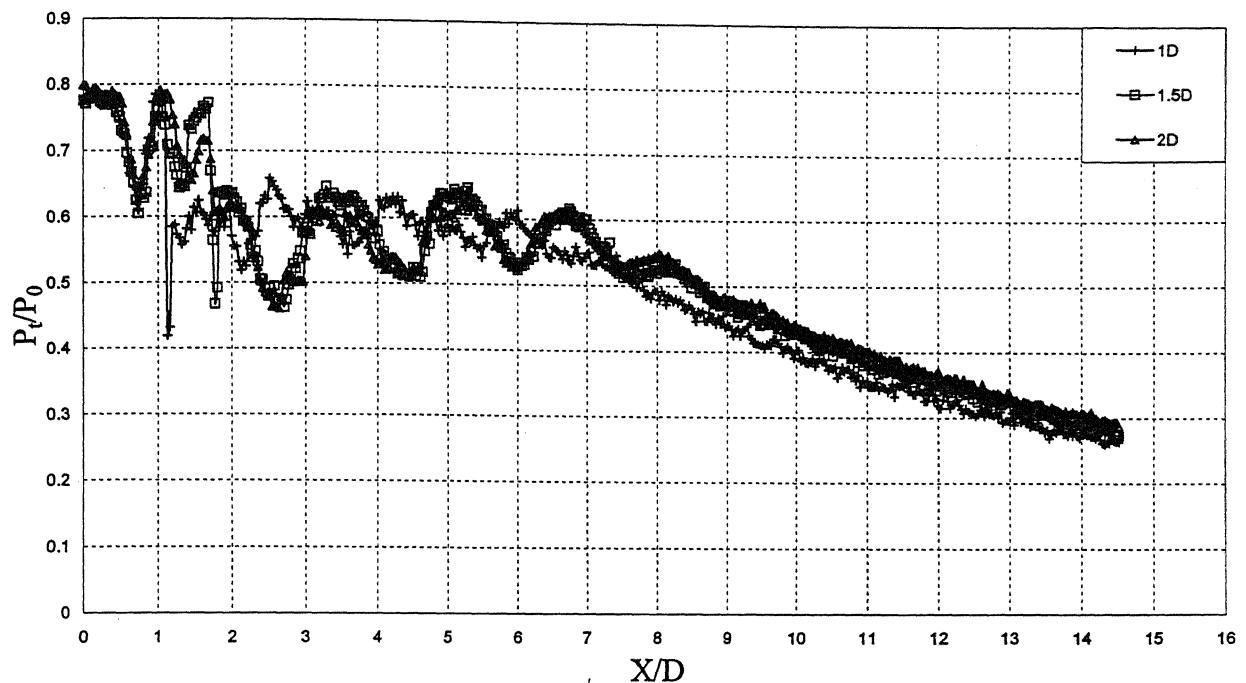
Figure 4.6b CPD of Mach 1.83 jet with C-W at 1.0D, 1.5D and 2D (NPR7)
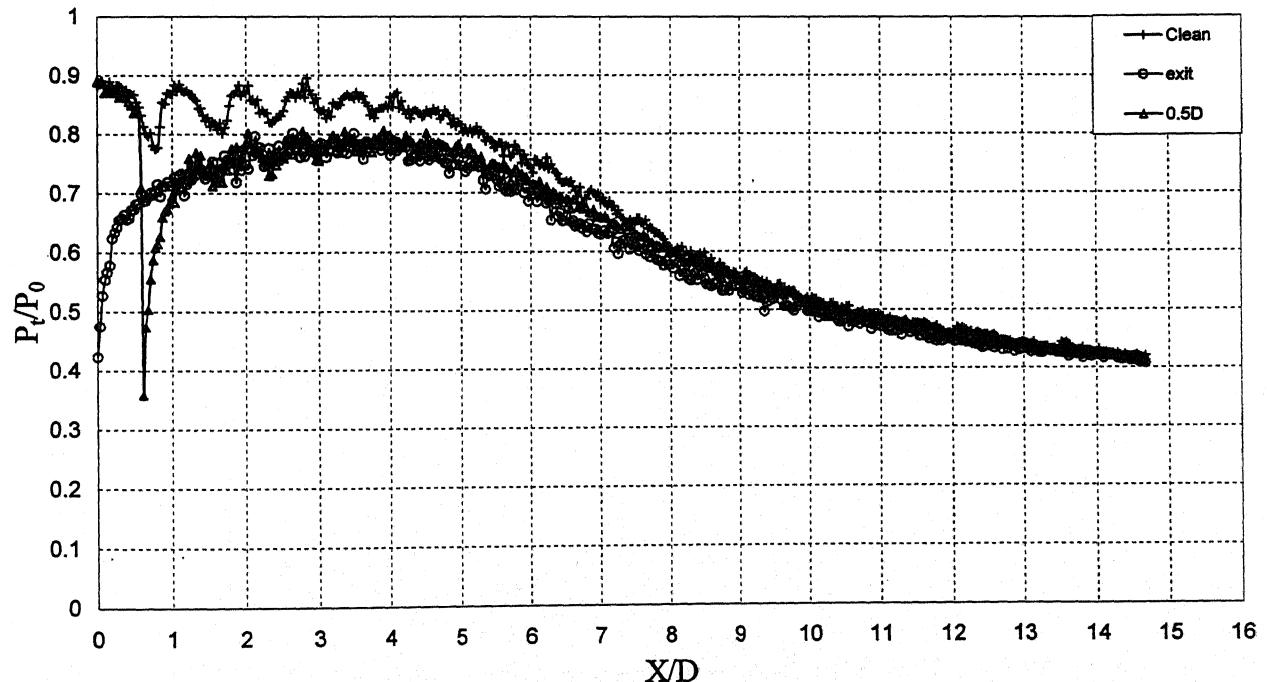
Figure 4.7a CPD of Mach 1.86 jet without control and C-W at 0D, 0.5D (NPR3)
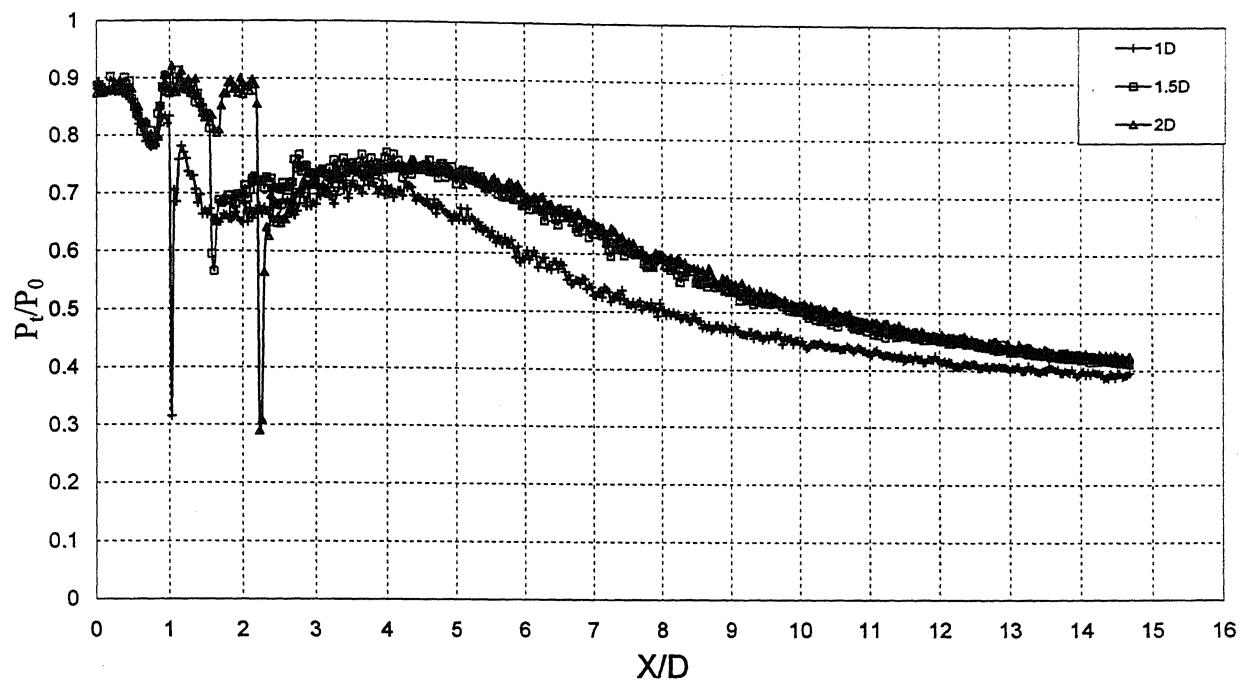
Figure 4.7b CPD of Mach 1.86 jet with C-W at 1D, 1.5D and 2D (NPR3)
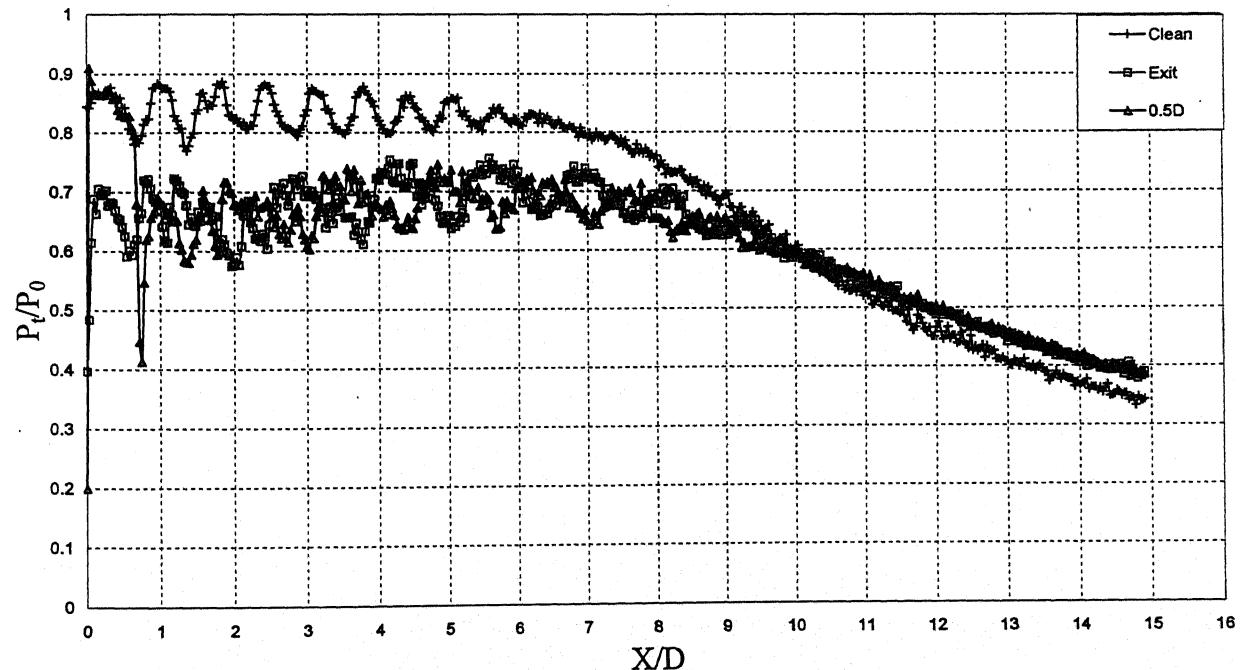
Figure 4.8a CPD of Mach 1.86 jet without control and C-W at 0D, 0.5D (NPR5)

45
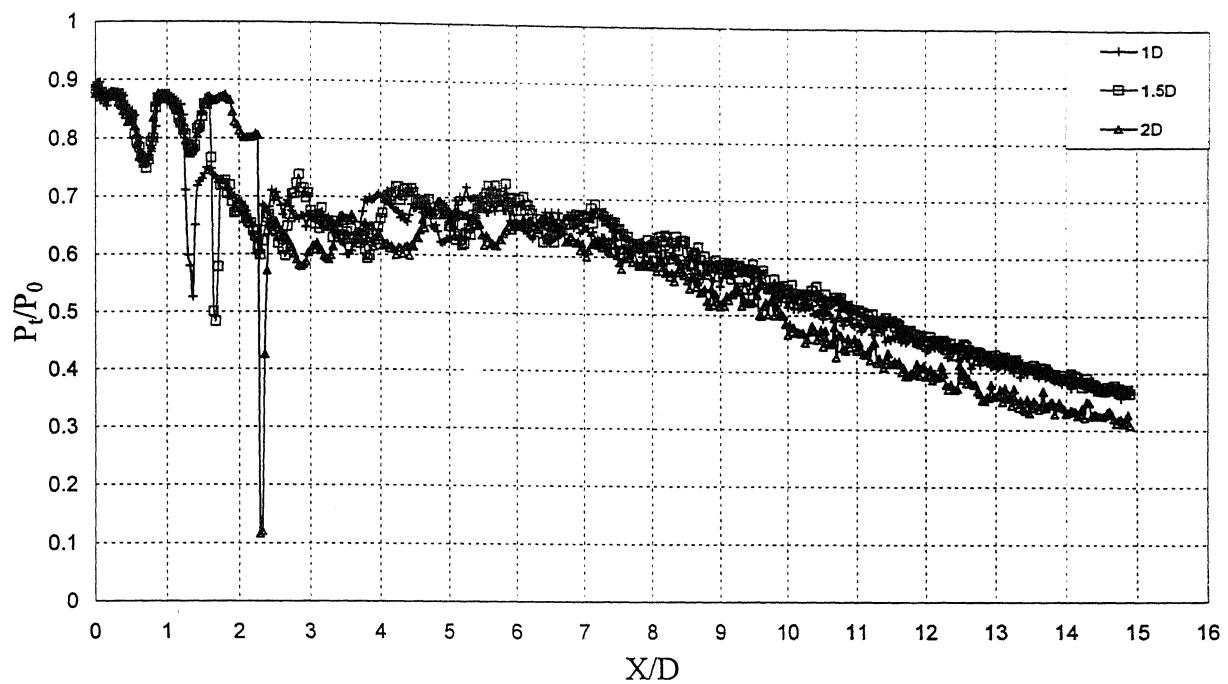
Figure 4.8b CPD of Mach 1.86 jet with C-W at 1.0D, 1.5D and 2D (NPR 5)
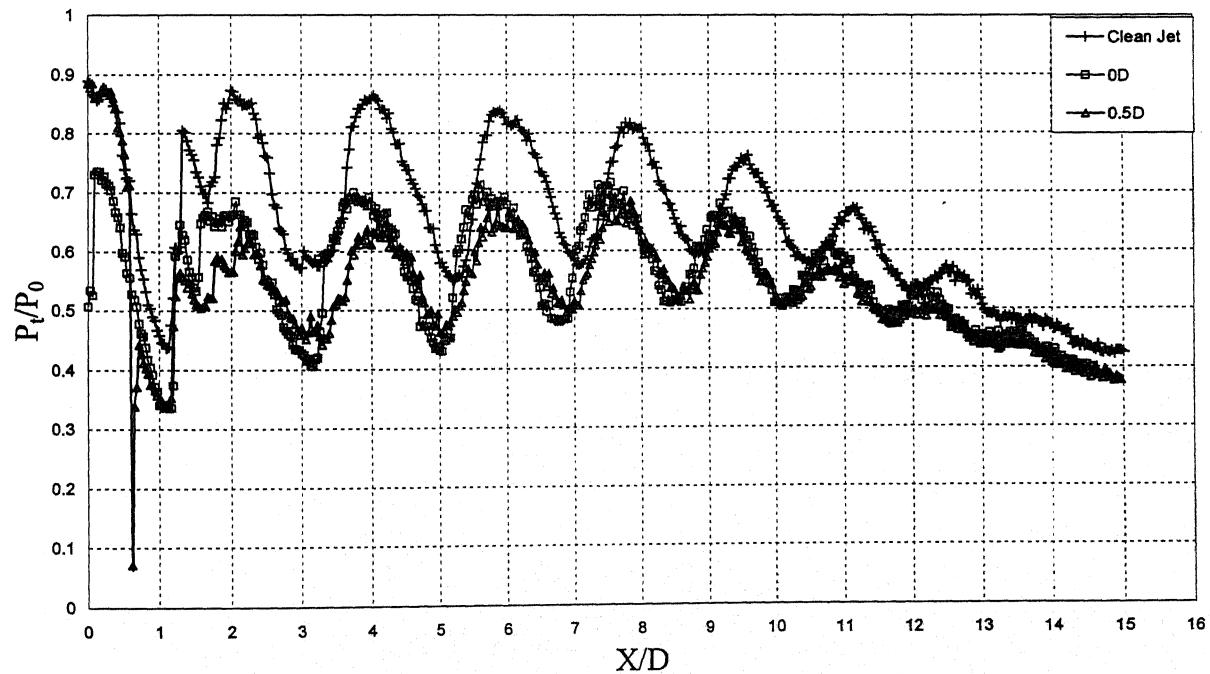
Figure 4.9a CPD of Mach 1.86 jet without control and C-W at 0D, 0.5D (NPR7)
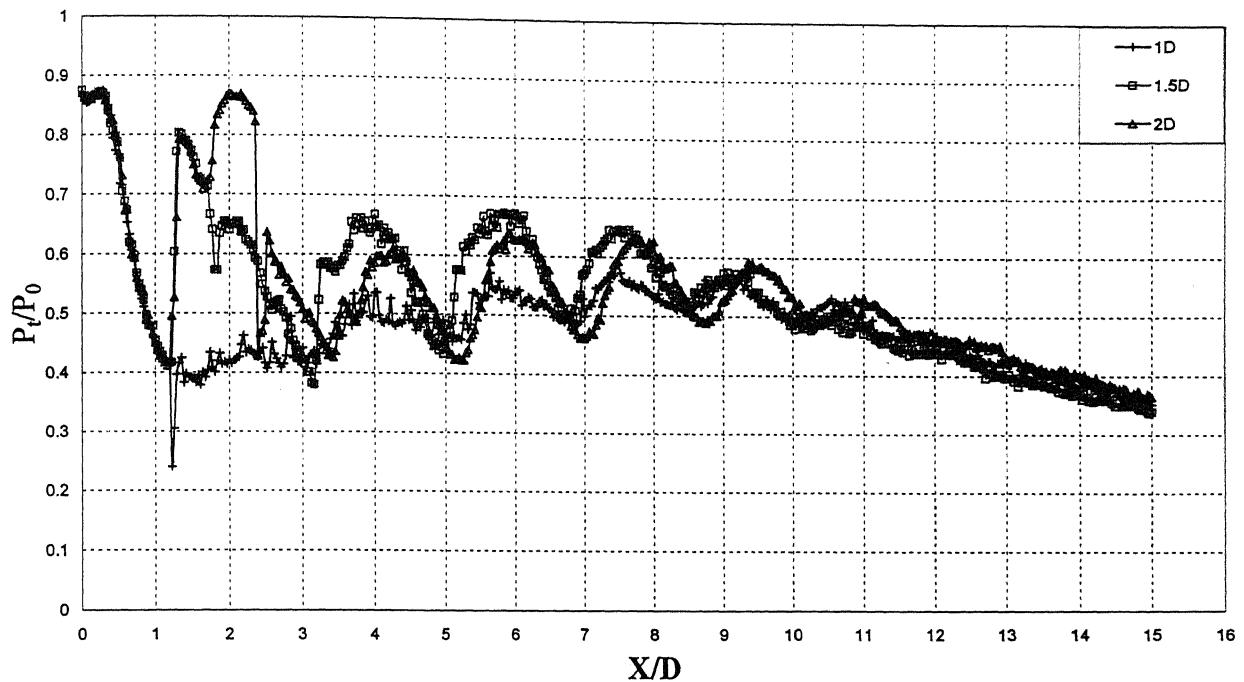
Figure 4.9b CPD of Mach 1.86 jet with C-W at 1.0D, 1.5D and 2D (NPR7)
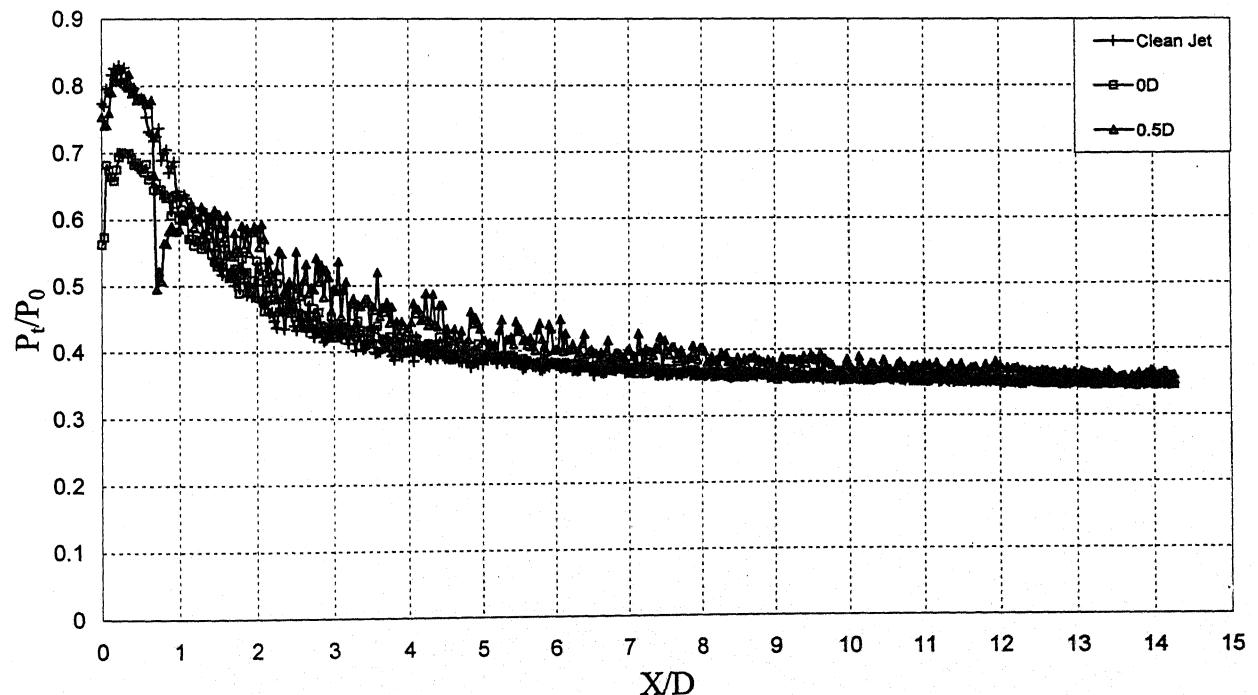
Figure 4.10a CPD of Mach 1.94 jet without control and C-W at 0D, 0.5D (NPR3)
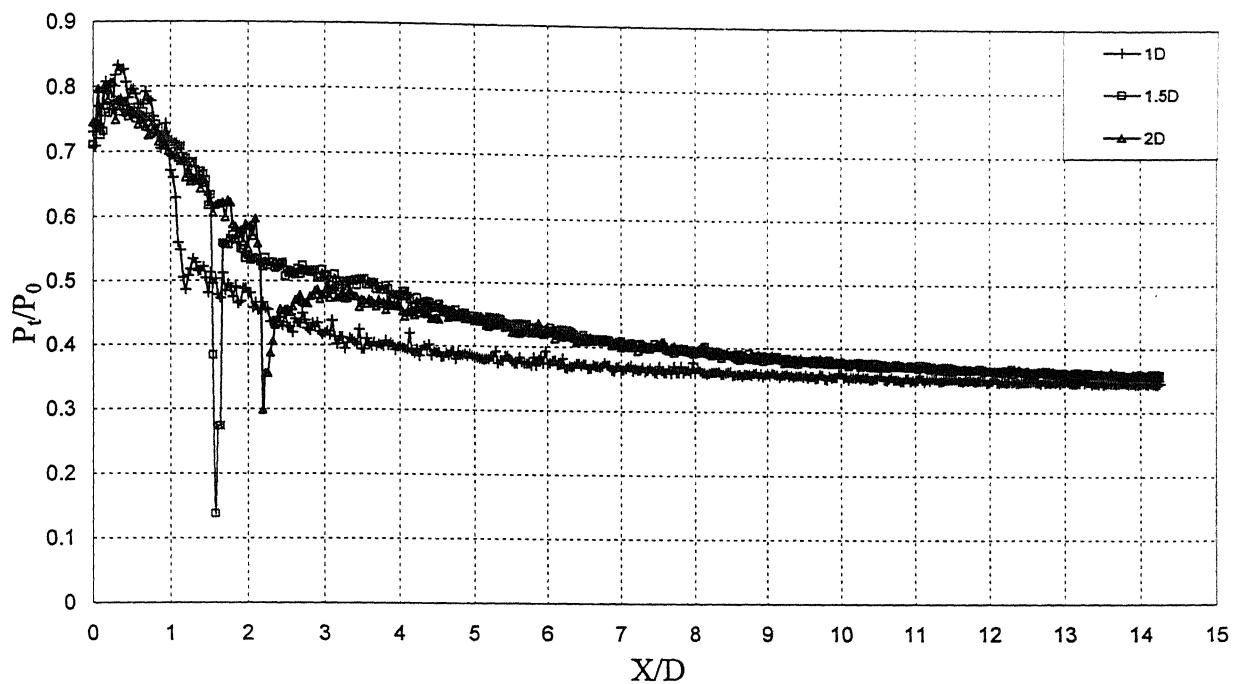
Figure 4.10b CPD of Mach 1.94 jet with C-W at 1D, 1.5D and 2D (NPR3)
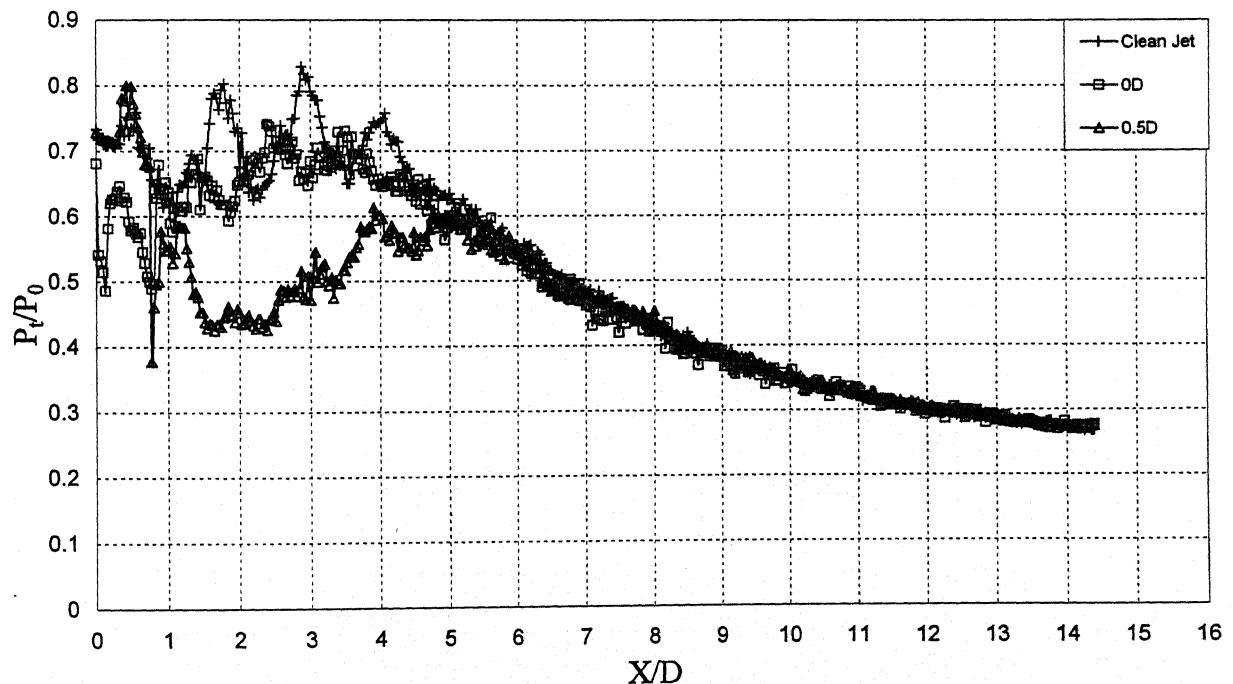
Figure 4.11a CPD of Mach 1.94 jet without control and C-W at 0D, 0.5D (NPR5)

48
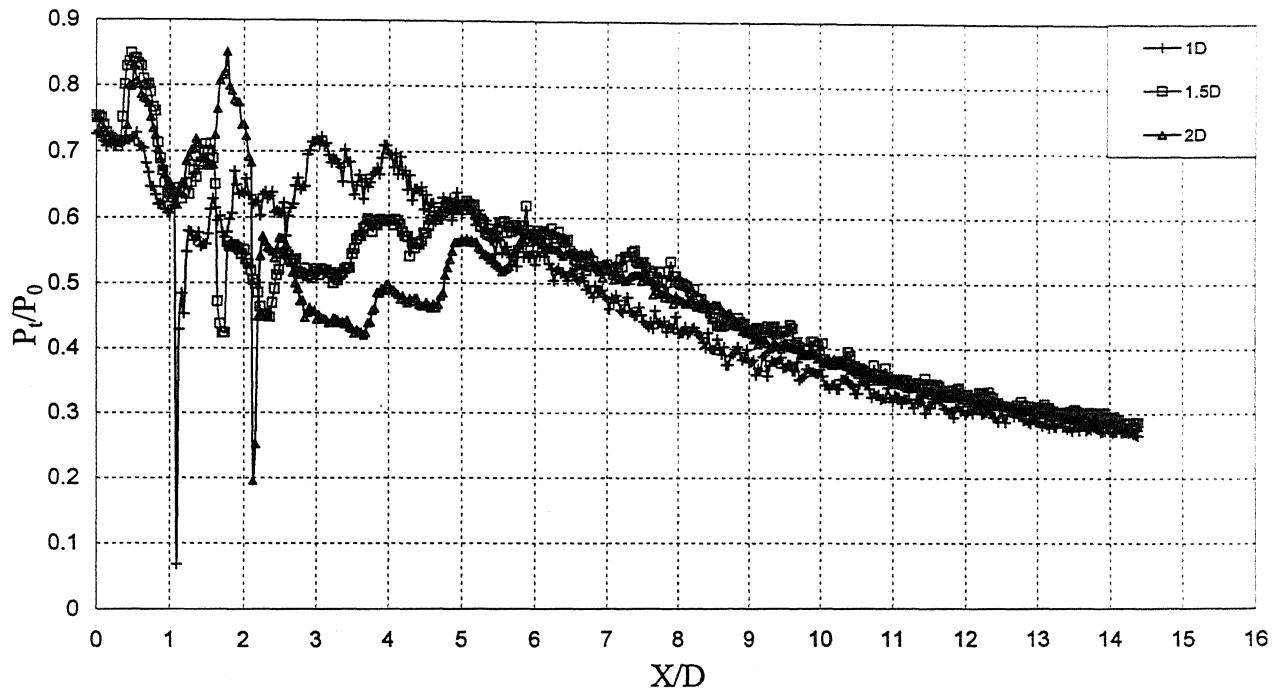
Figure 4.11b CPD of Mach 1.94 jet with C-W at 1.0D, 1.5D and 2D (NPR5)
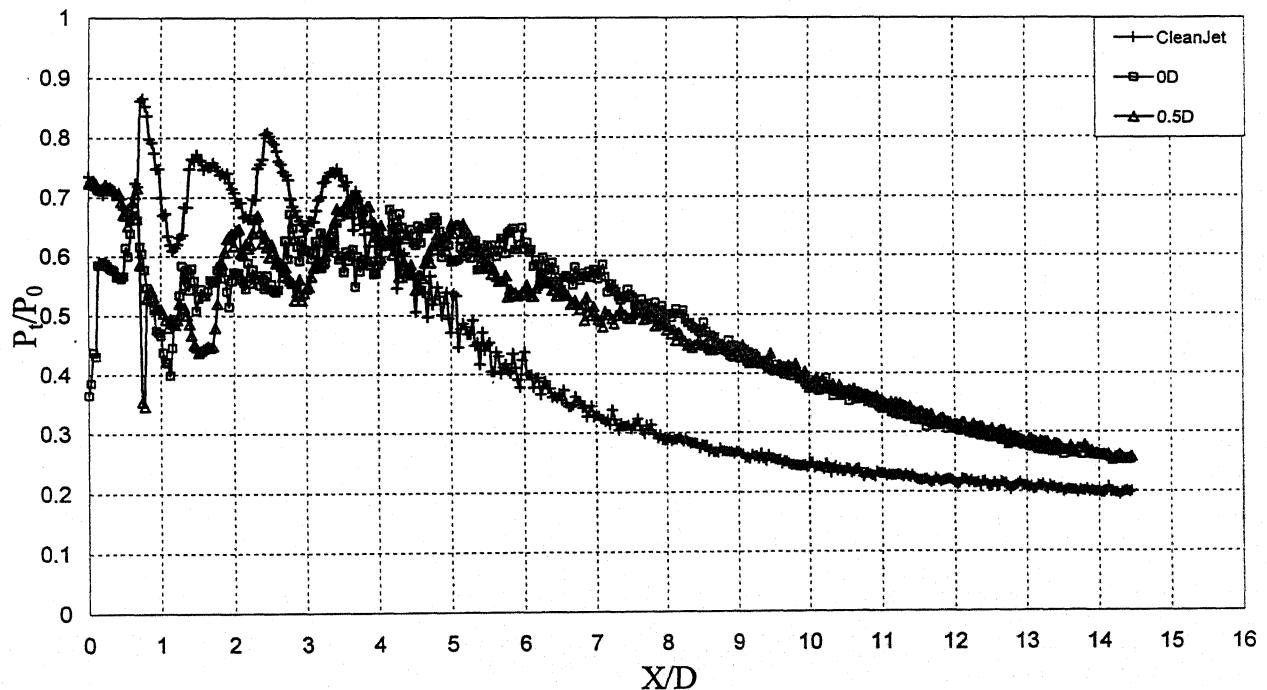
Figure 4.12a CPD of Mach 1.94 jet without control and C-W at 0D, 0.5D (NPR7)
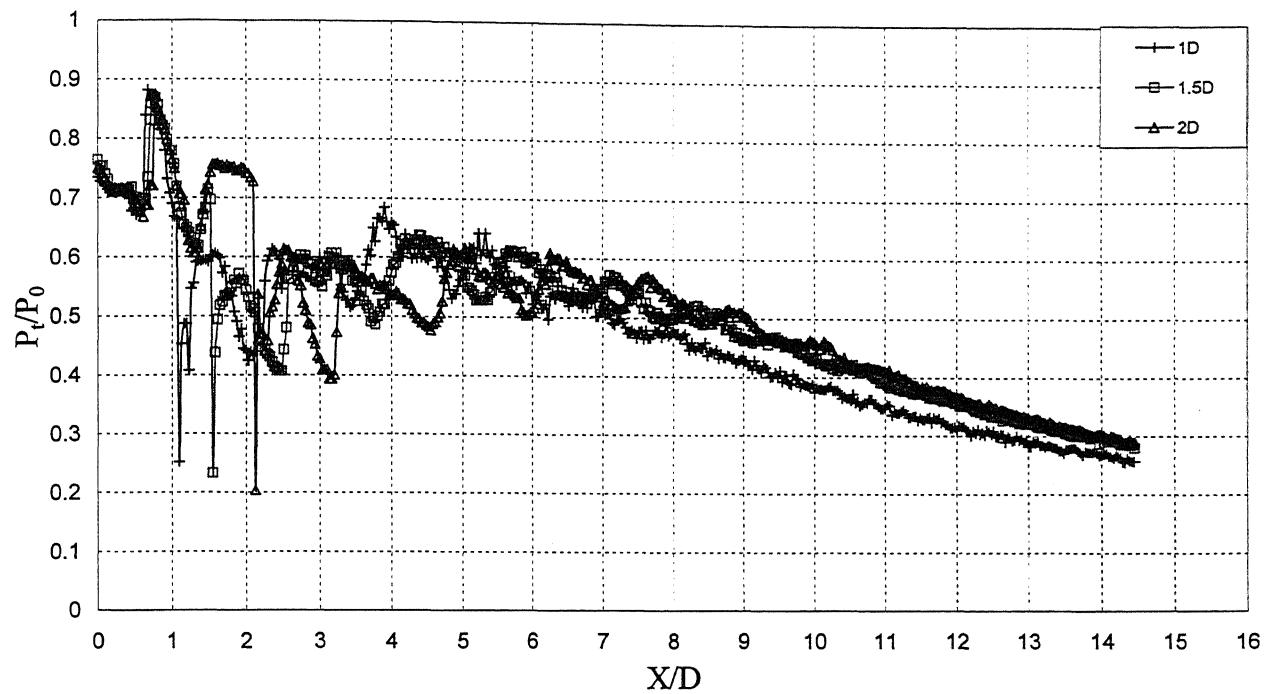
Figure 4.12b CPD of Mach 1.94 jet with C-W at 1.0D, 1.5D and 2D (NPR7)
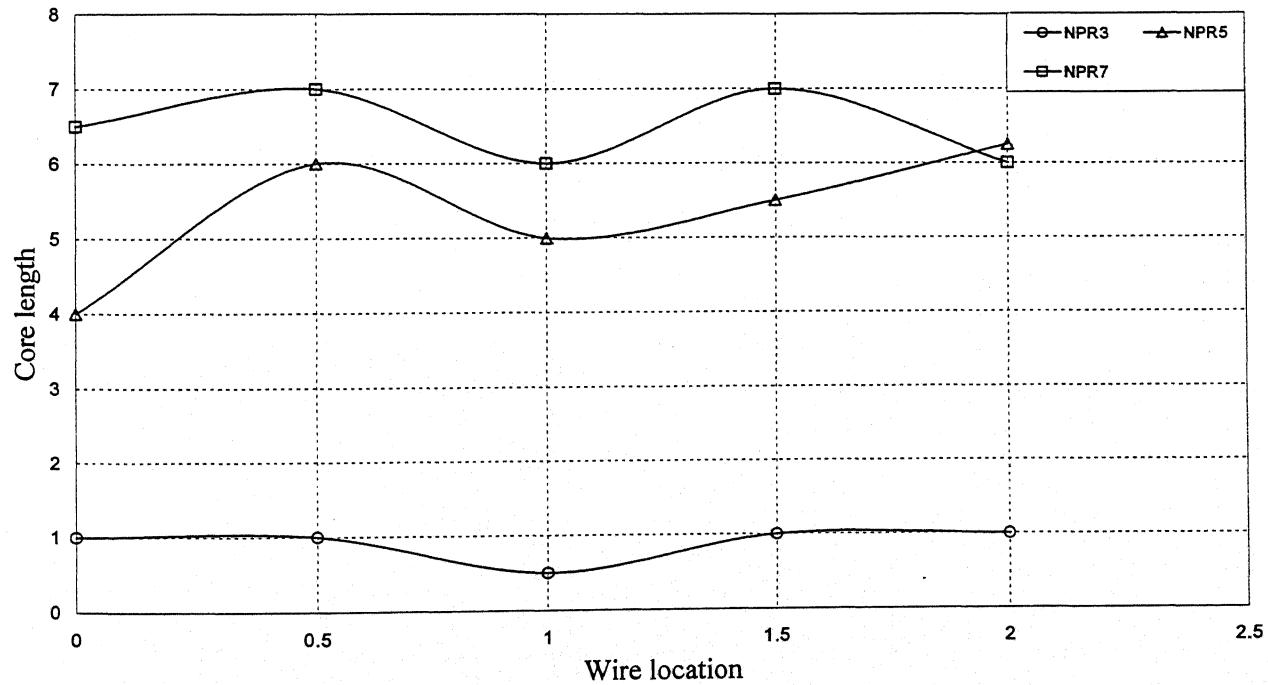
Figure 4.13 Core length variations with C-W location for Mach 1.83 jet
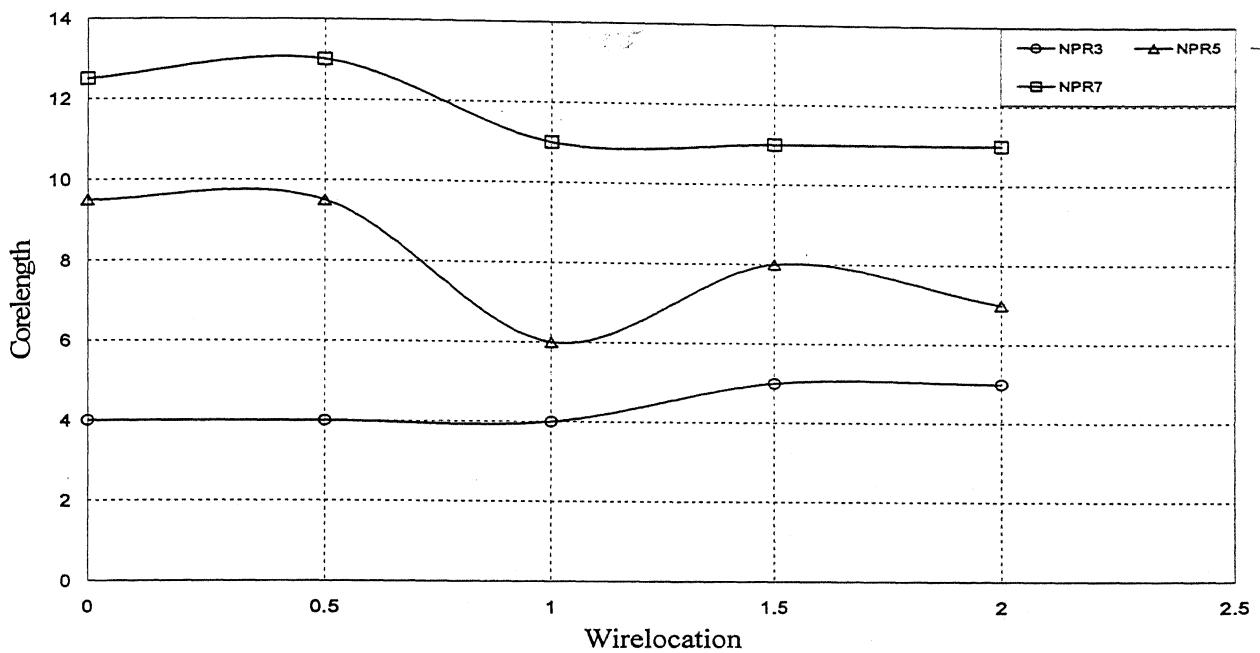
Figure 4.14 Core length variations with C-W location for Mach 1.86 jet
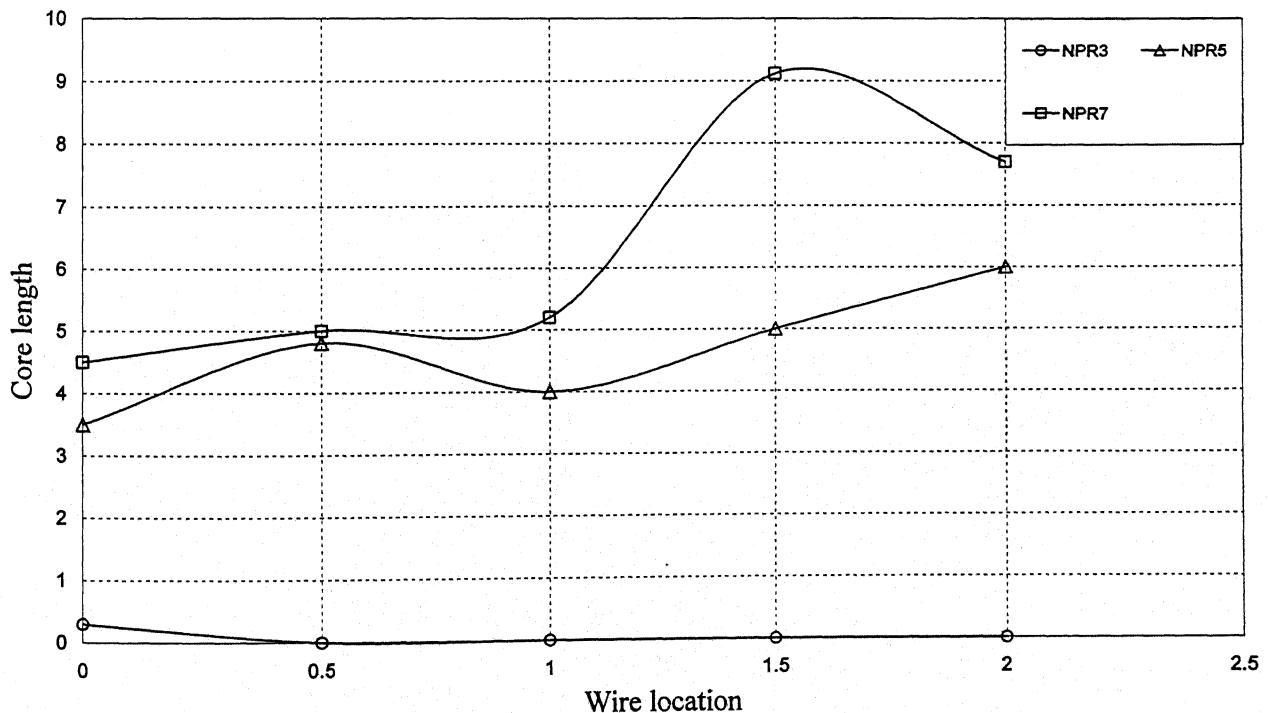
Figure 4.15 Core length variations with C-W location for Mach 1.94 jet

51
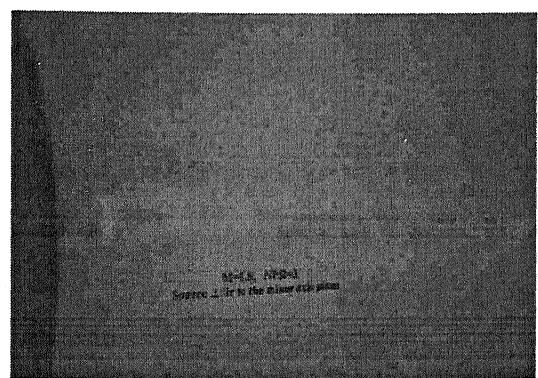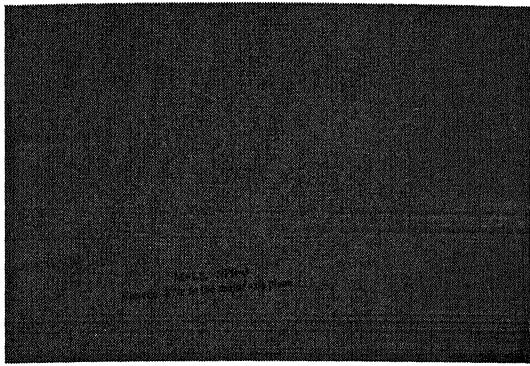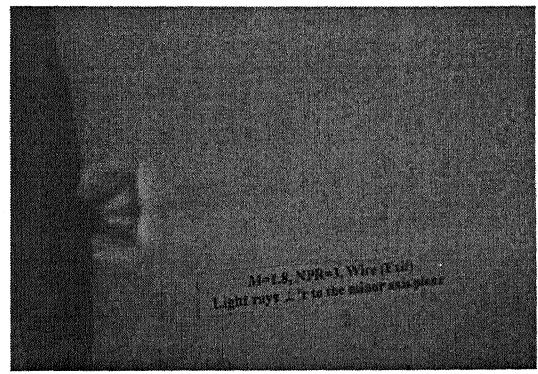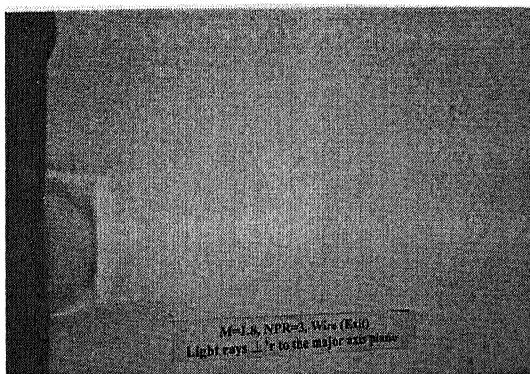
Without C-W
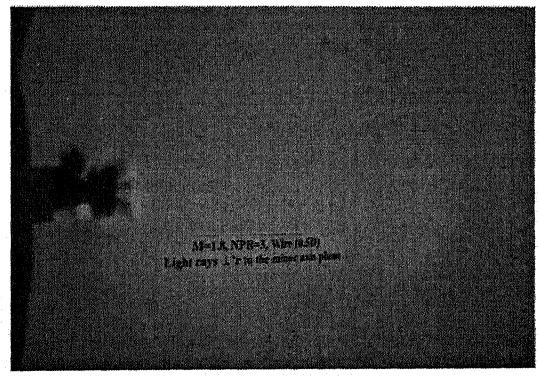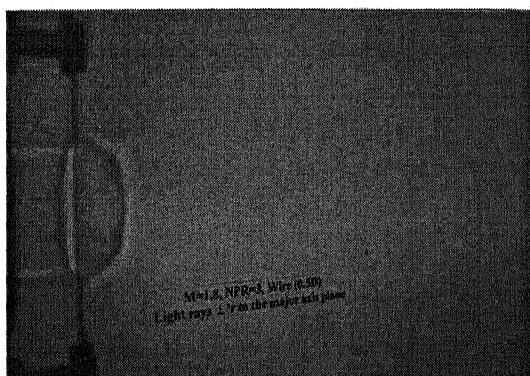
With C-W at X/D = 0

With C-W at X/D = 0.5

Major axis plane   Minor axis plane

Figure 4.16a Waves in Mach 1.83 jet at NPR 3

52
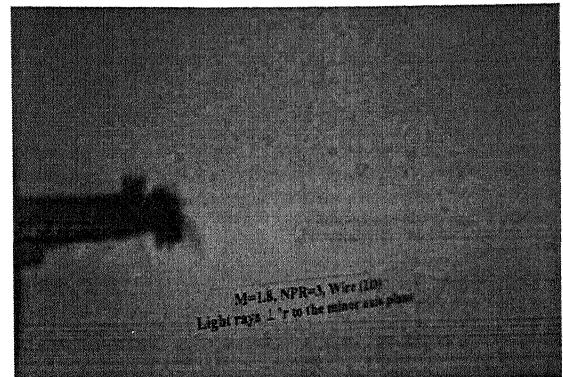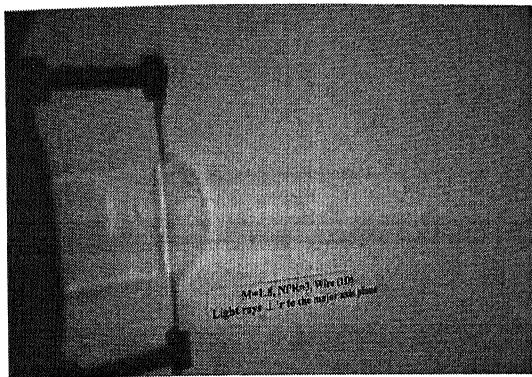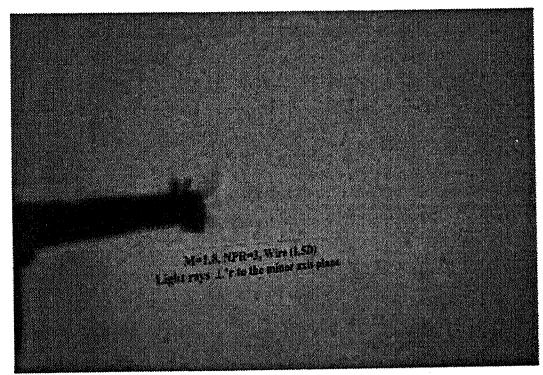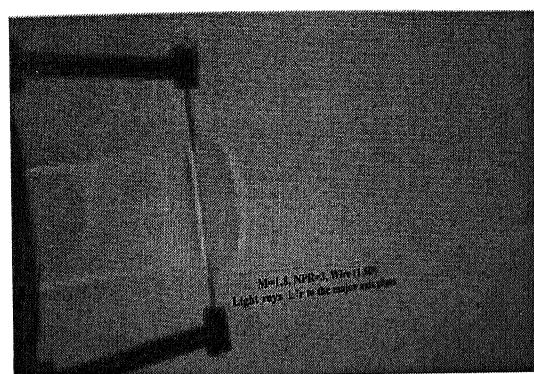
With C-W at X/D = 1.0
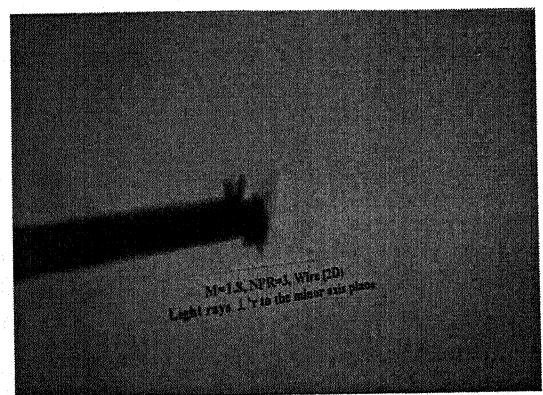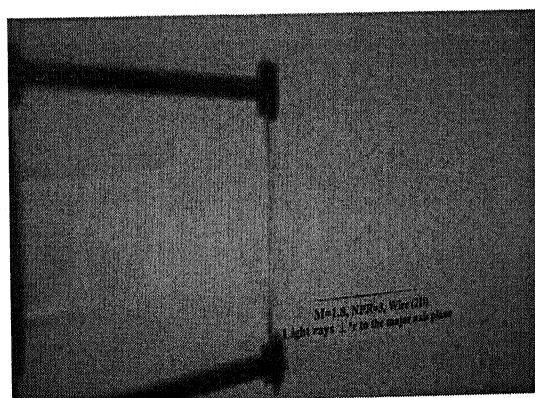

With C-W at X/D = 1.5

With C-W at X/D = 2.0

Major axis plane   Minor axis plane

Figure 4.16b Waves in Mach 1.83 jet at NPR 3

53
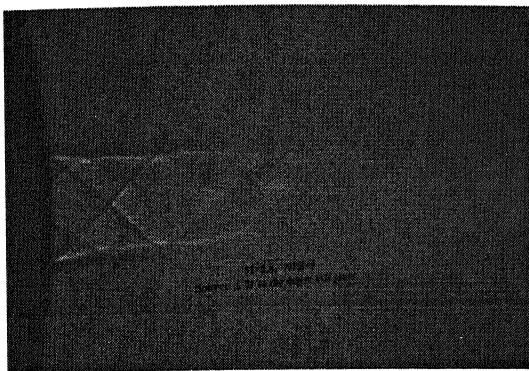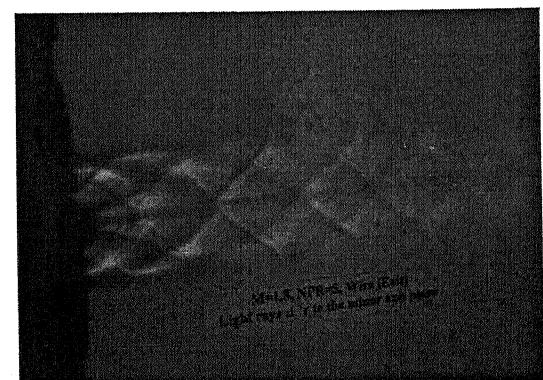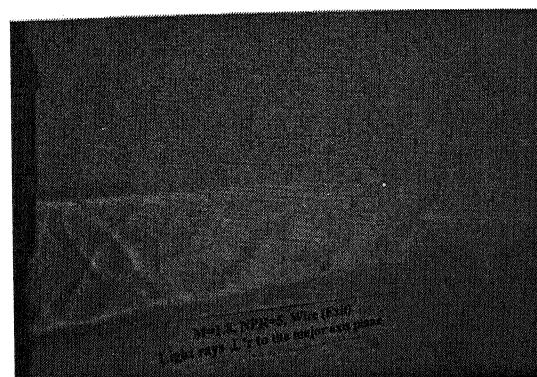
Without C-W

With C-W at X/D = 0

With C-W at X/D = 0.5

Major axis plane   Minor axis plane

Figure 4.17a Waves in Mach 1.83 jet at NPR 5
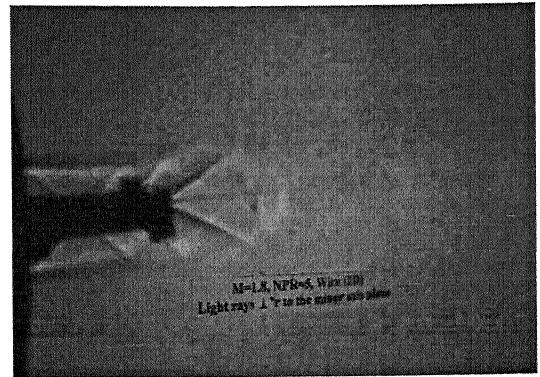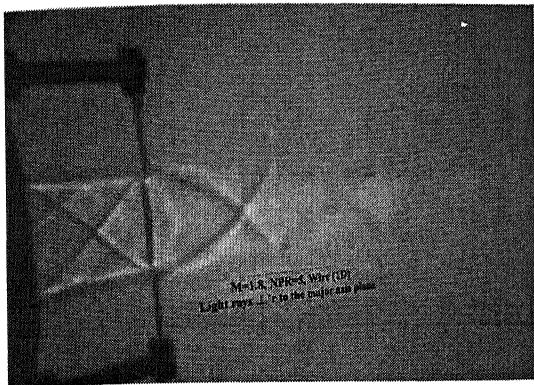
With C-W at X/D = 1.0
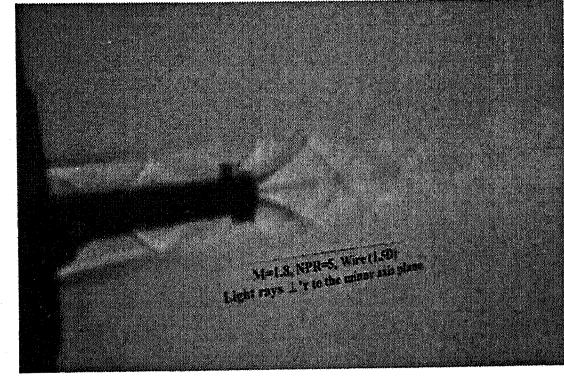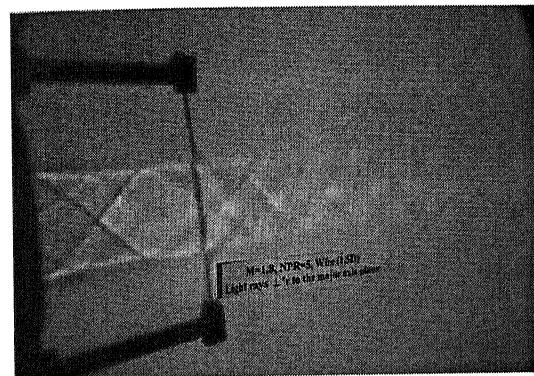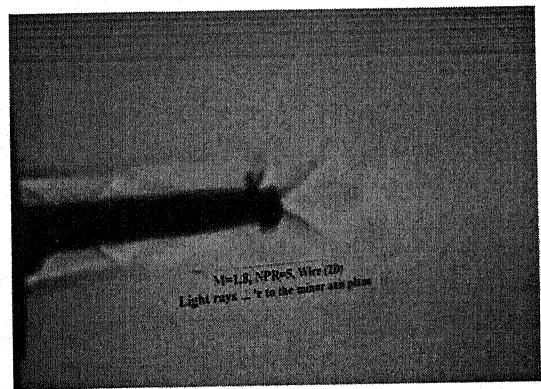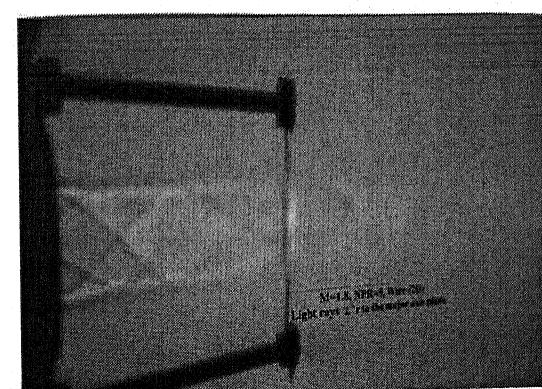
With C-W at X/D = 1.5

With C-W at X/D = 2.0

Major axis plane   Minor axis plane

Figure 4.17b Waves in Mach 1.83 jet at NPR 5
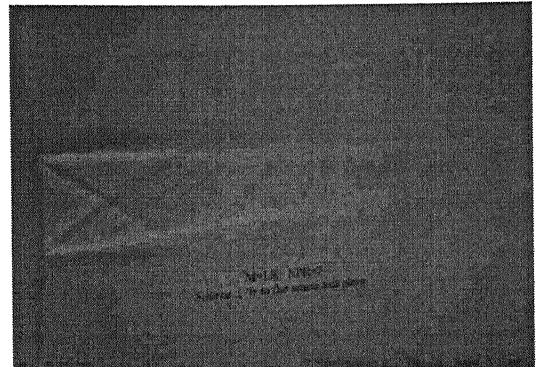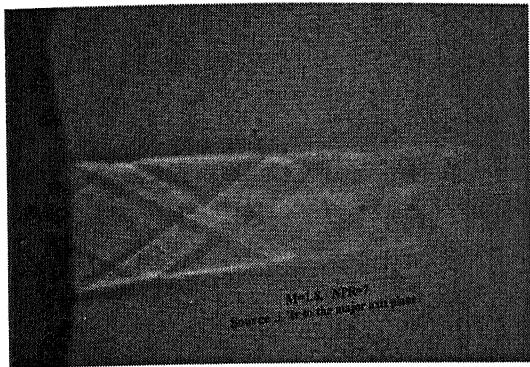
Without C-W
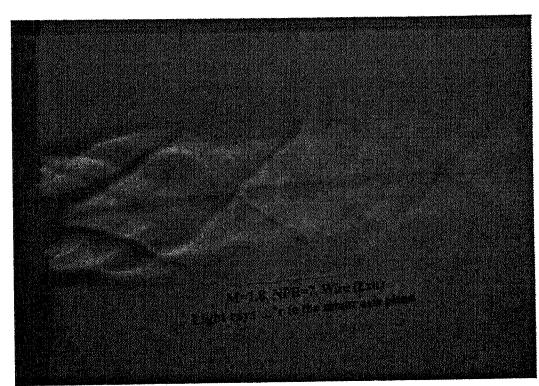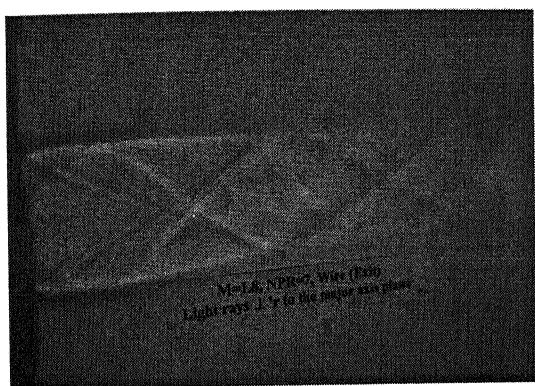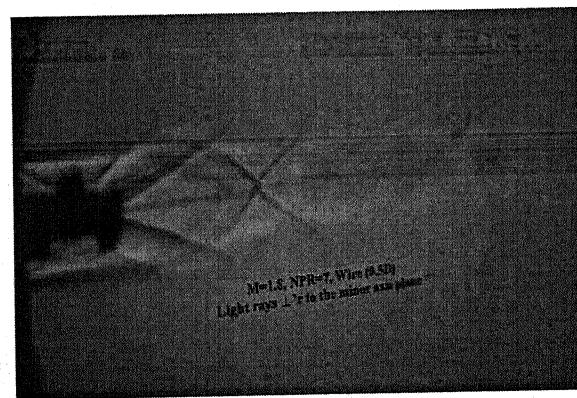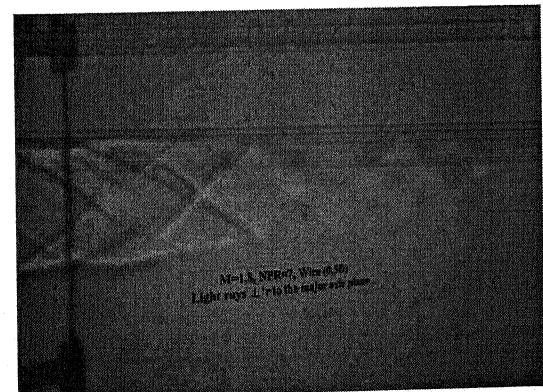
With C-W at X/D = 0

With C-W at X/D = 0.5

Major axis plane   Minor axis plane

Figure 4.18a Waves in Mach 1.83 jet at NPR 7
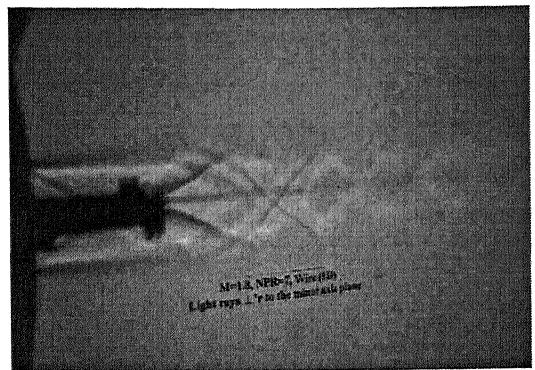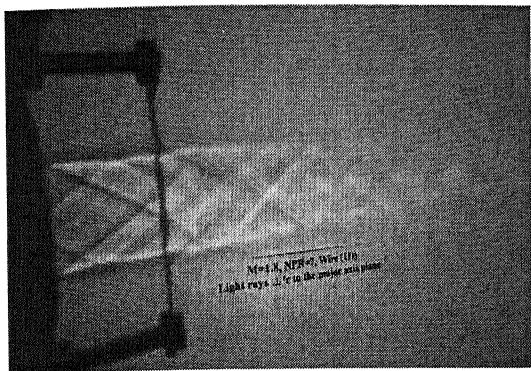
With C-W at X/D = 1.0
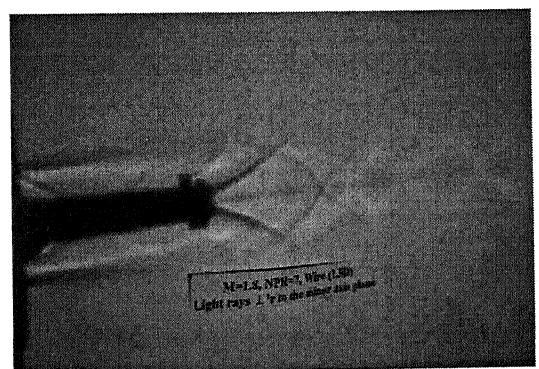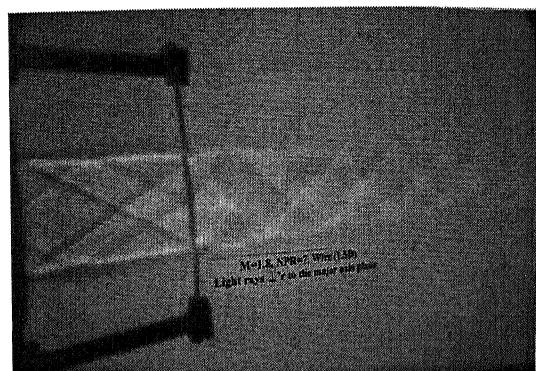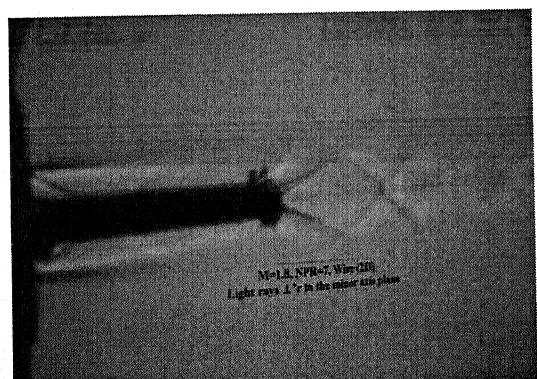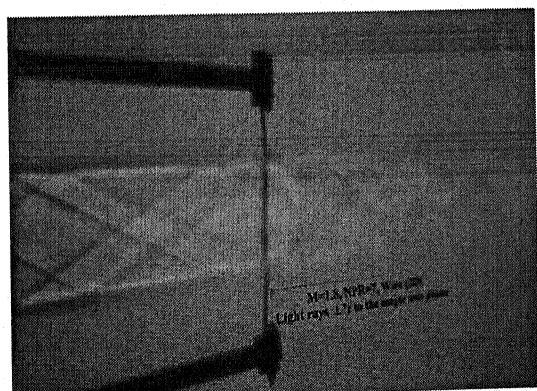
With C-W at X/D = 1.5

With C-W at X/D = 2.0

Major axis plane   Minor axis plane

Figure 4.18b Waves in Mach 1.83 jet at NPR 7
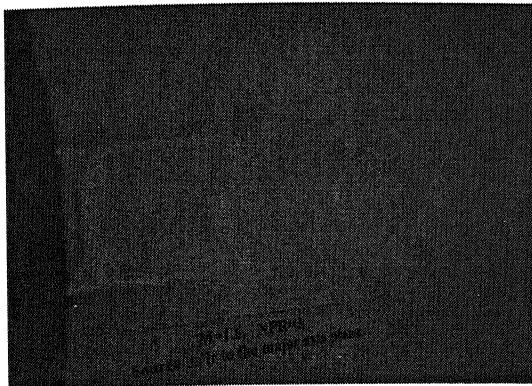
Without wire
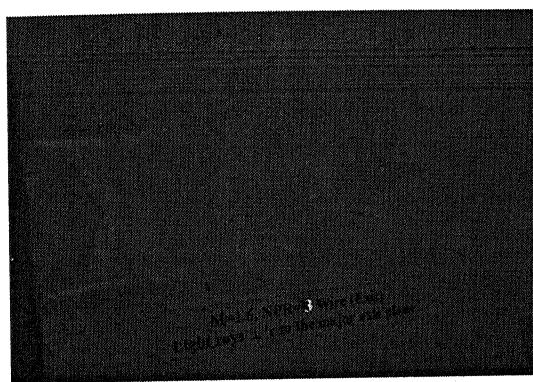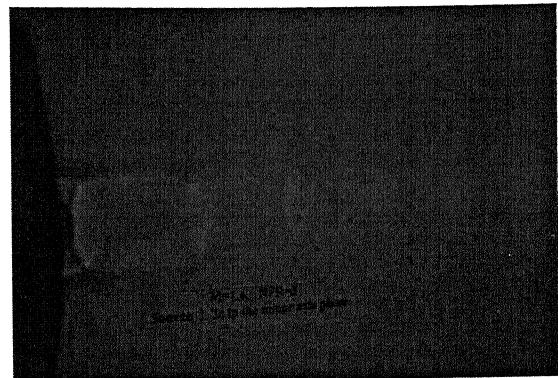
With C-W at X/D = 0
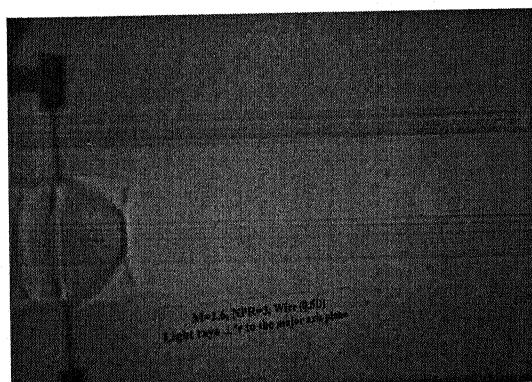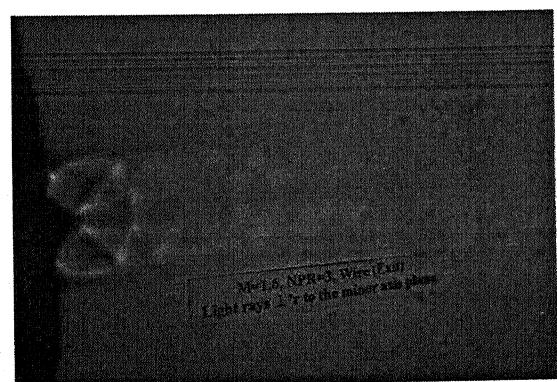
With C-W at X/D = 0.5
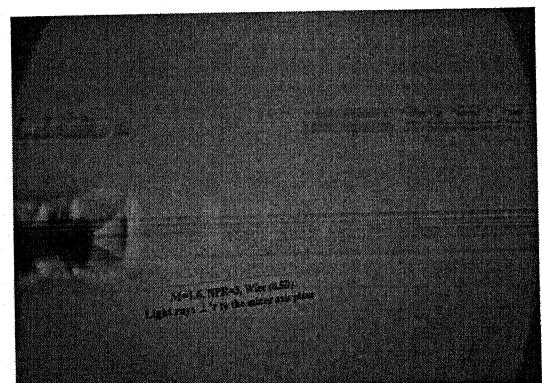
Major axis plane   Minor axis plane

Figure 4.19a Waves in Mach 1.86 jet at NPR 3
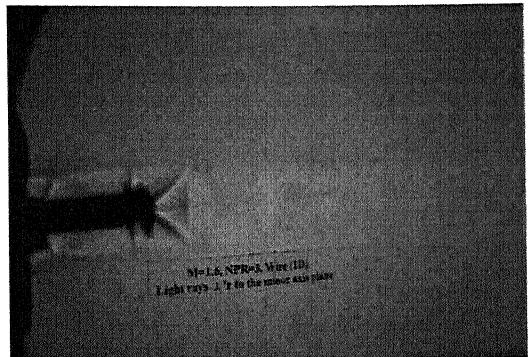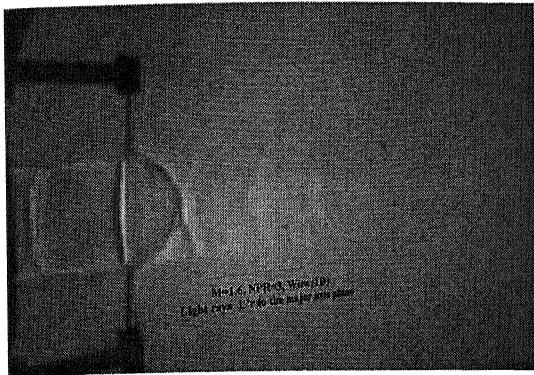
With C-W at X/D = 1.0
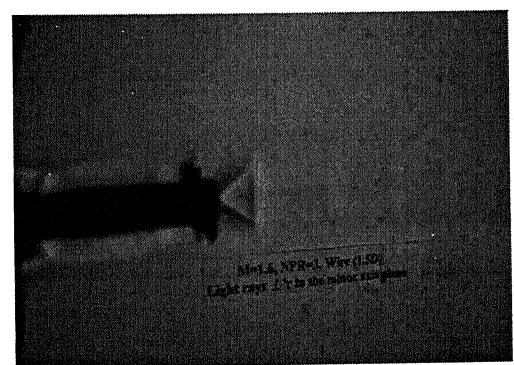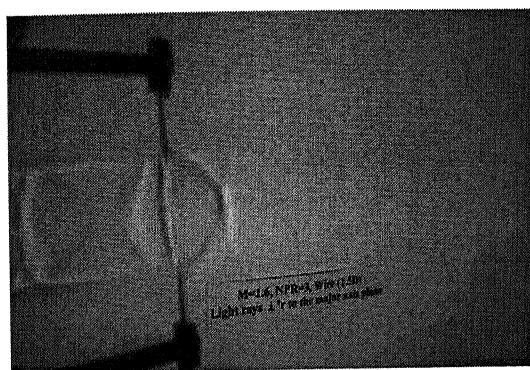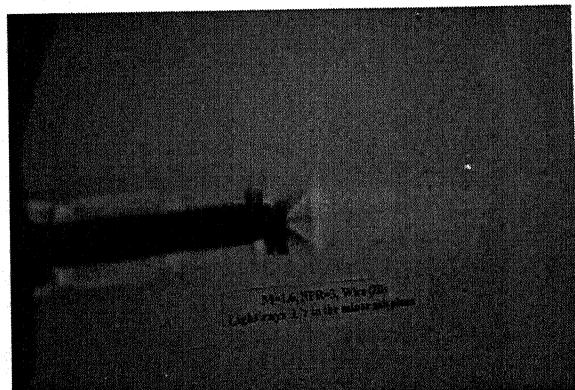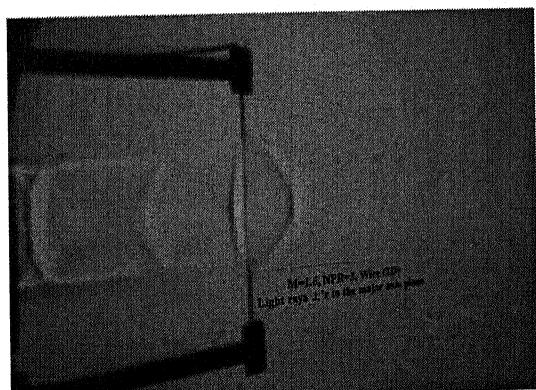
With C-W at X/D = 1.5

With C-W at X/D = 2.0

Major axis plane

Minor axis plane

Figure 4.19b Waves in Mach 1.86 jet at NPR 3

59
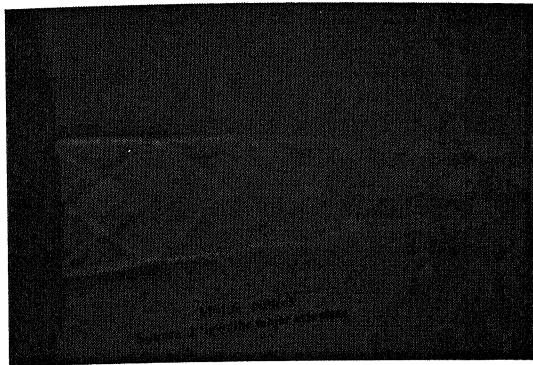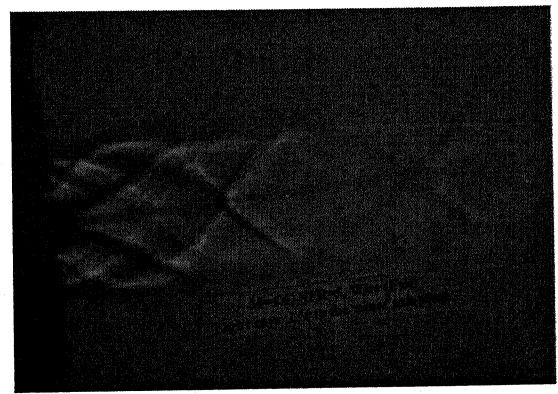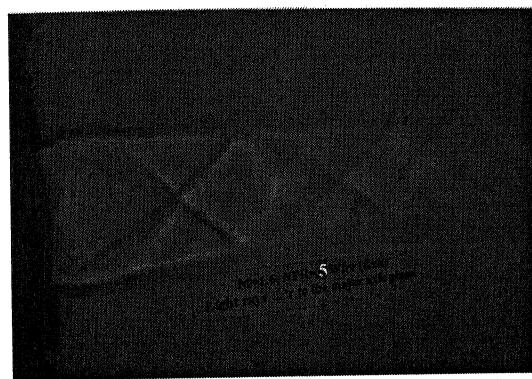
Without C-W

With C-W at X/D = 0

With C-W at X/D = 0.5

Major axis plane   Minor axis plane

Figure 4.20a Waves in Mach 1.86 jet at NPR 5
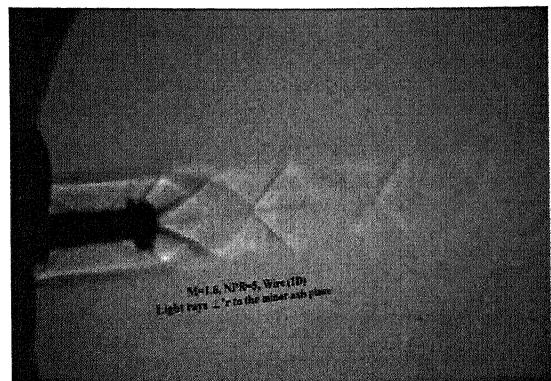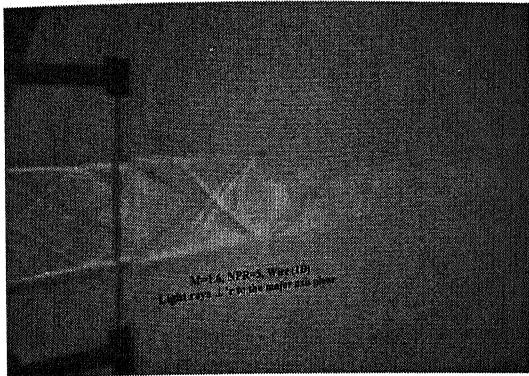
With C-W at X/D = 1.0
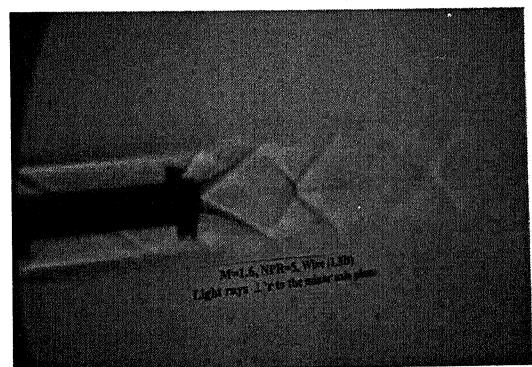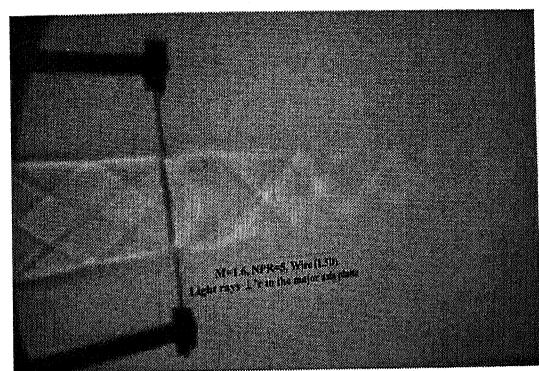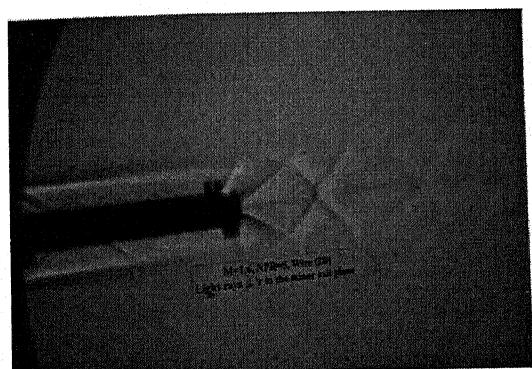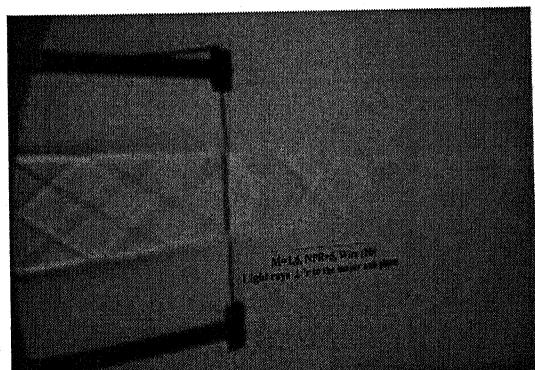
With C-W at X/D = 1.5

With C-W at X/D = 2.0

Major axis plane   Minor axis plane

Figure 4.20b Waves in Mach 1.86 jet at NPR 5

61
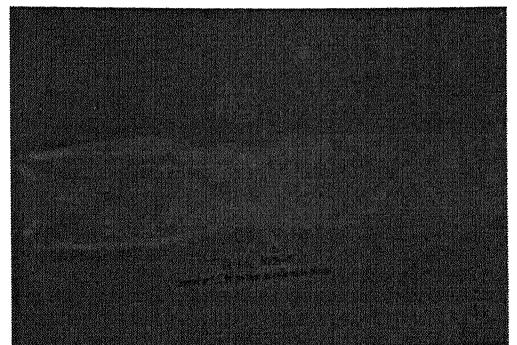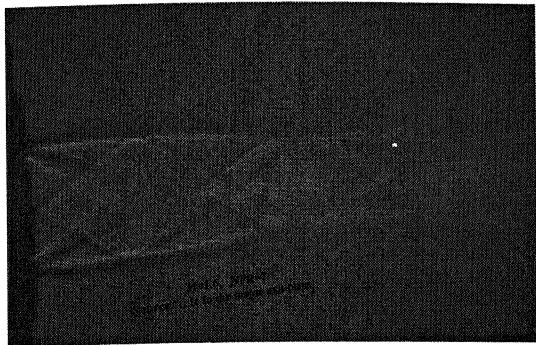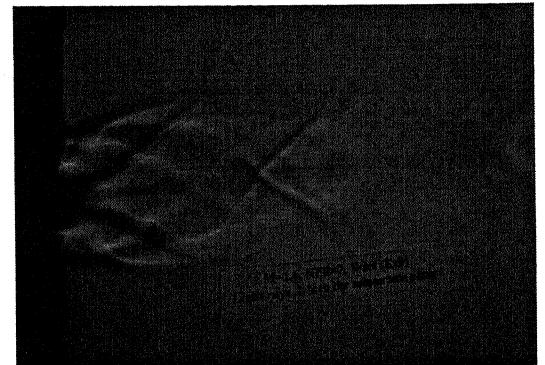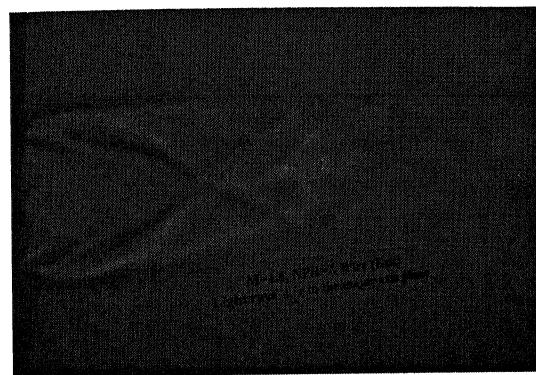
Without C-W
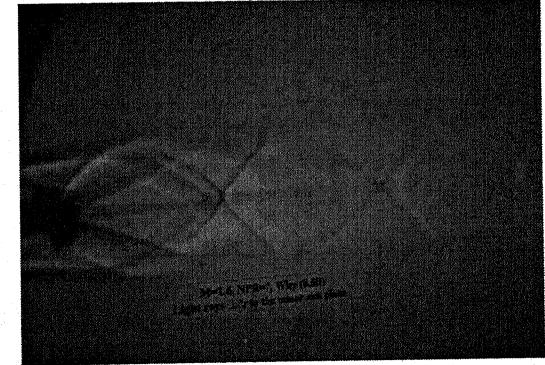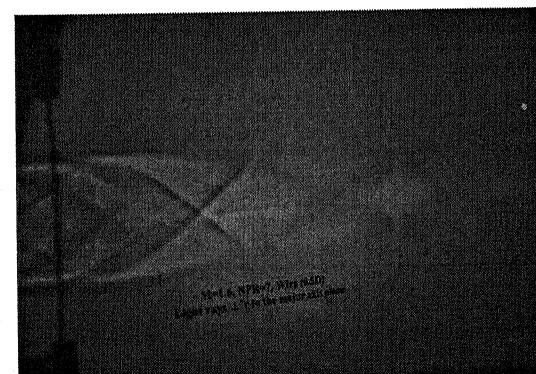
With C-W at X/D = 0

With C-W at X/D = 0.5

Major axis plane   Minor axis plane

Figure 4.21a Waves in Mach 1.86 jet at NPR 7
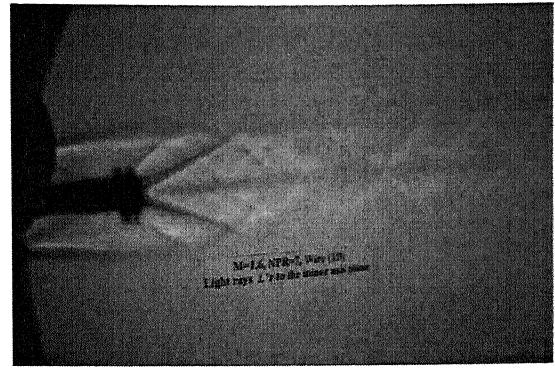
With C-W at X/D = 1.0
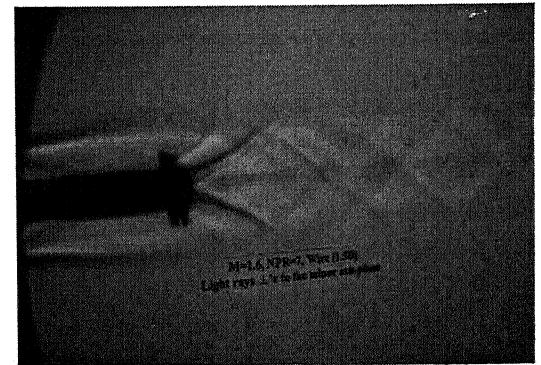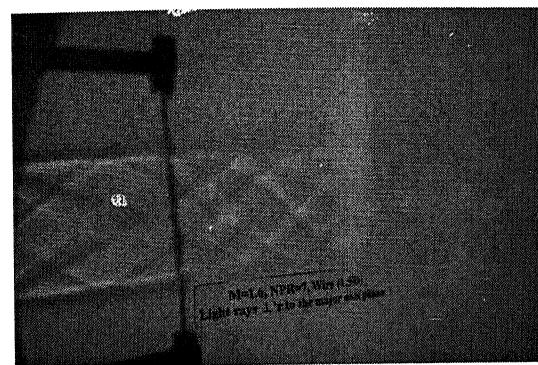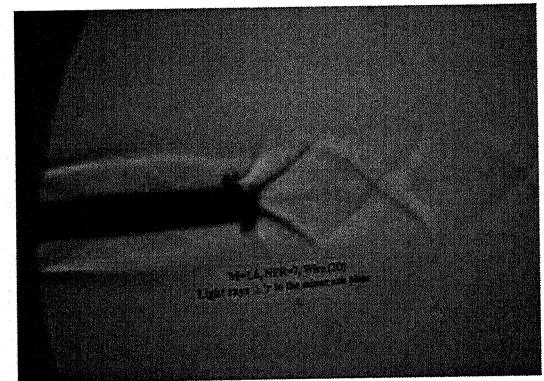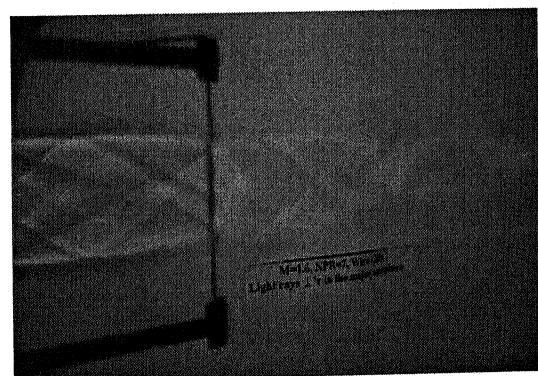
With C-W at X/D = 1.5



With C-W at X/D = 2.0

Major axis plane

Minor axis plane

Figure 4.21b Waves in Mach 1.86 jet at NPR 7

63
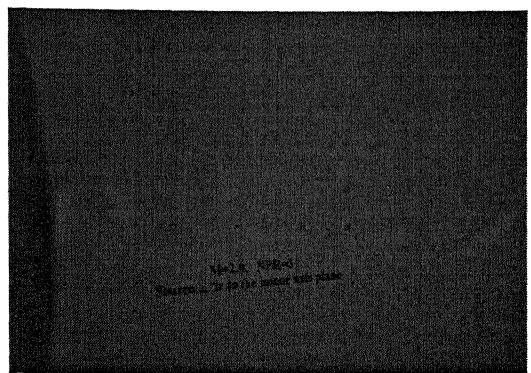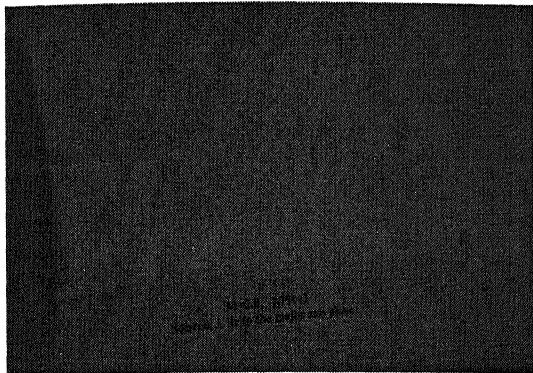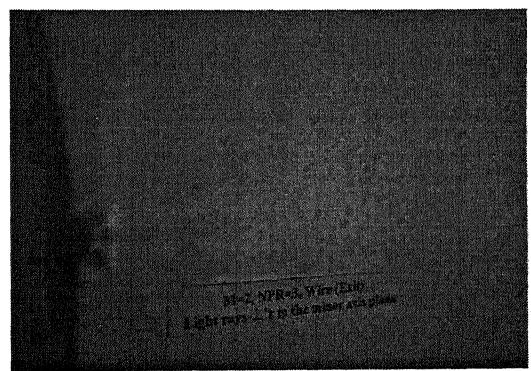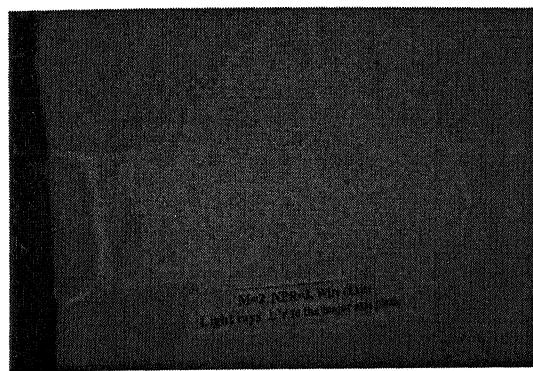
Without C-W
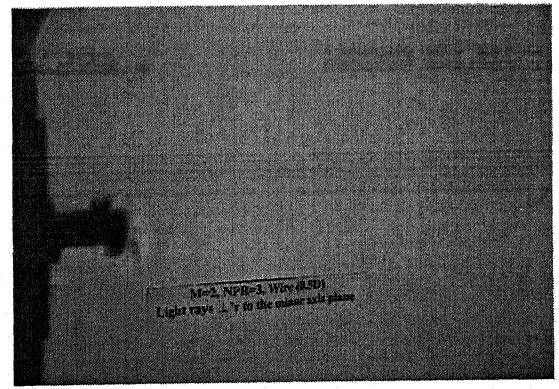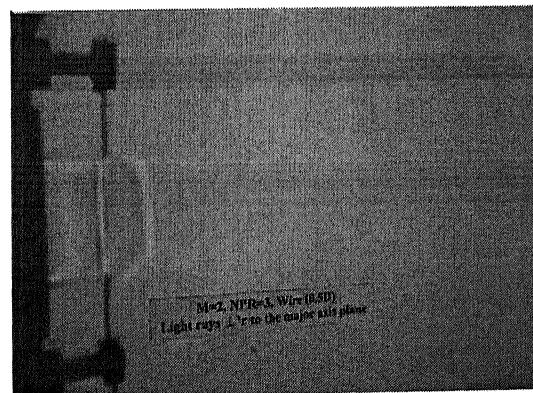
With C-W at X/D = 0


With C-W at X/D = 0.5

Major axis plane   Minor axis plane

Figure 4.22a Waves in Mach 1.94 jet at NPR 3
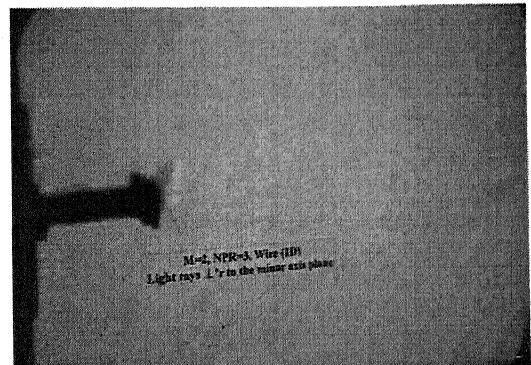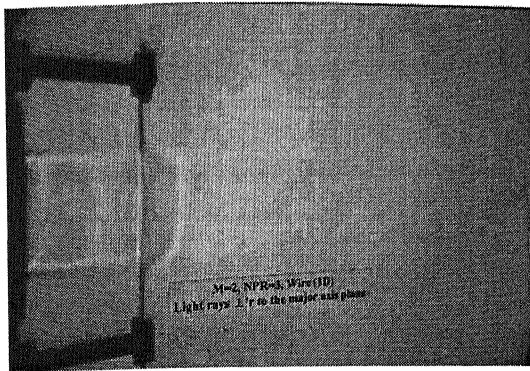
With C-W at X/D = 1.0
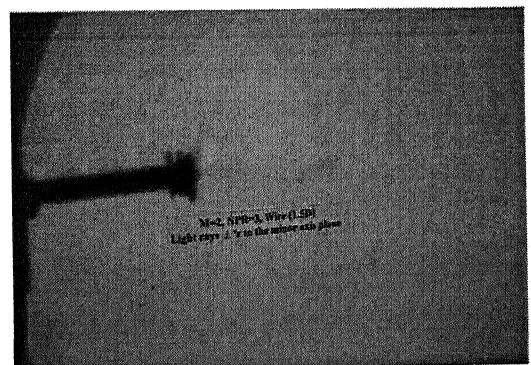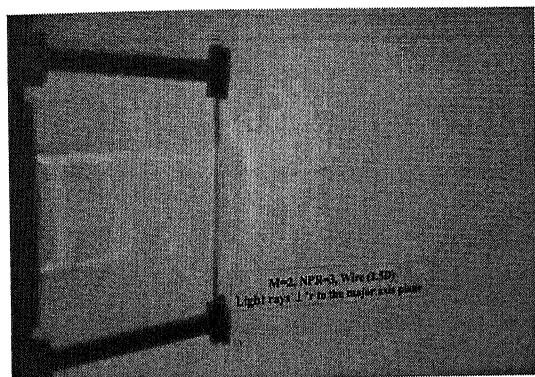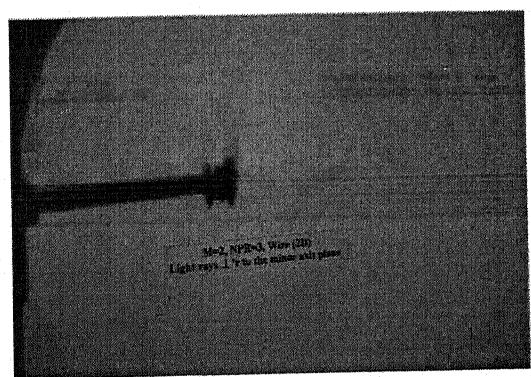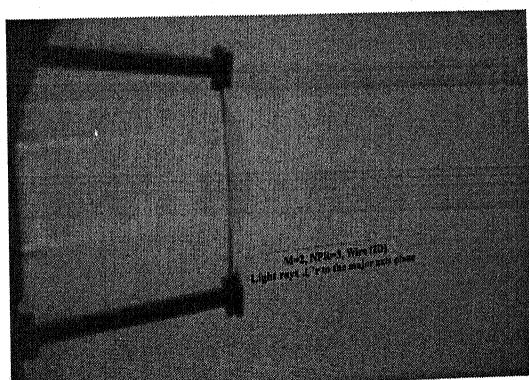
With C-W at X/D = 1.5

With C-W at X/D = 2.0

Major axis plane

Minor axis plane

Figure 4.22b Waves in Mach 1.94 jet at NPR 3

Without C-W
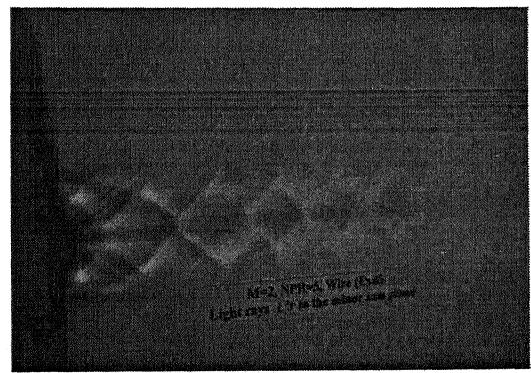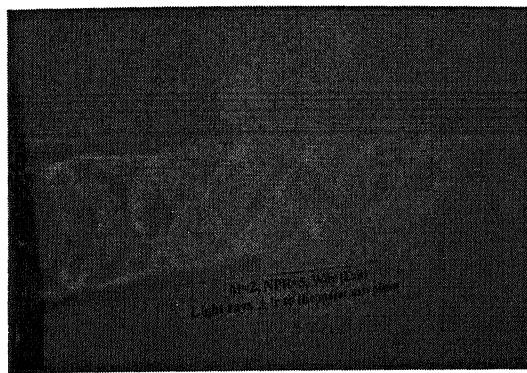
With C-W at X/D = 0
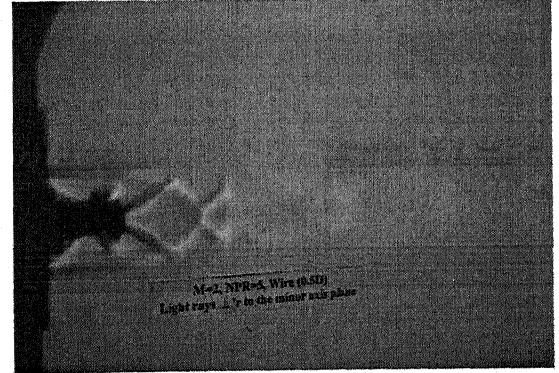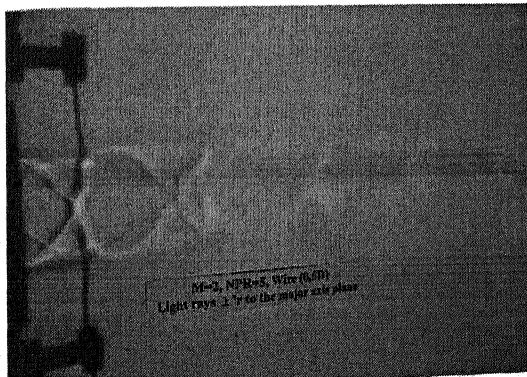

With C-W at X/D = 0.5

Major axis plane   Minor axis plane

Figure 4.23a Waves in Mach 1.94 jet at NPR 5
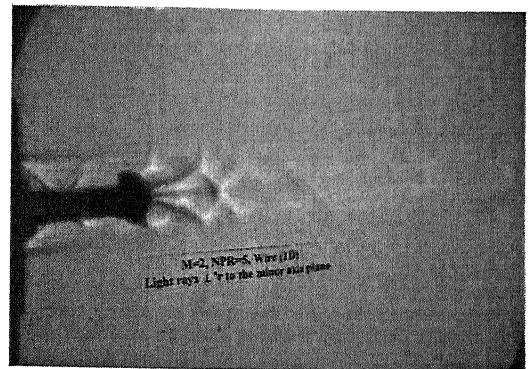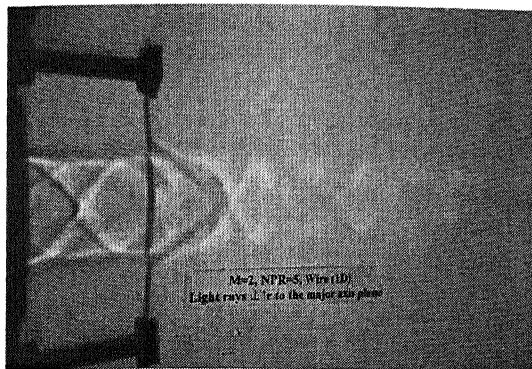
With C-W at X/D = 1.0
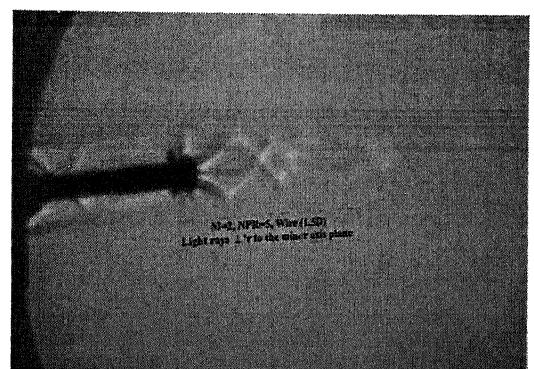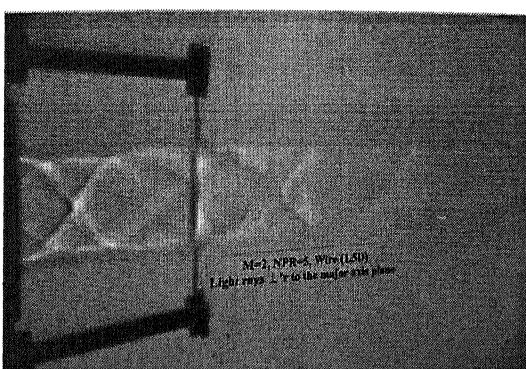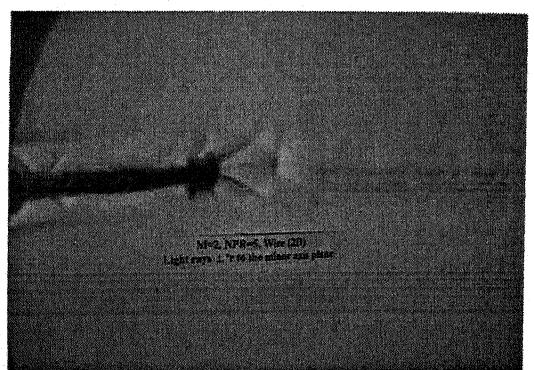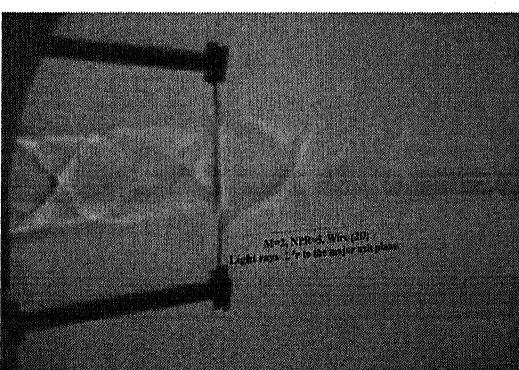
With C-W at X/D = 1.5

With C-W at X/D = 2.0

Major axis plane   Minor axis plane

Figure 4.23b Waves in Mach 1.94 jet at NPR 5
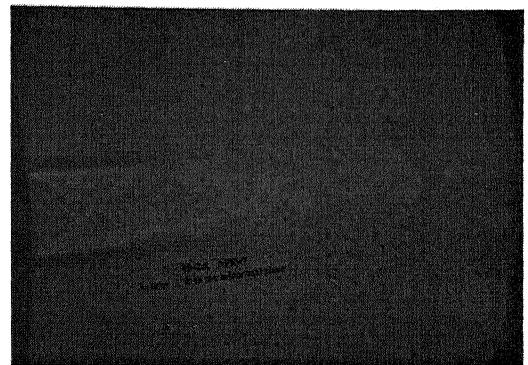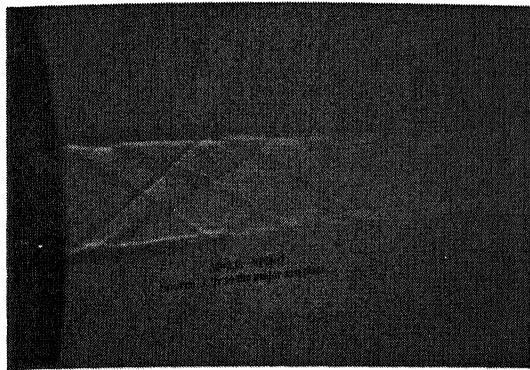
Without C-W
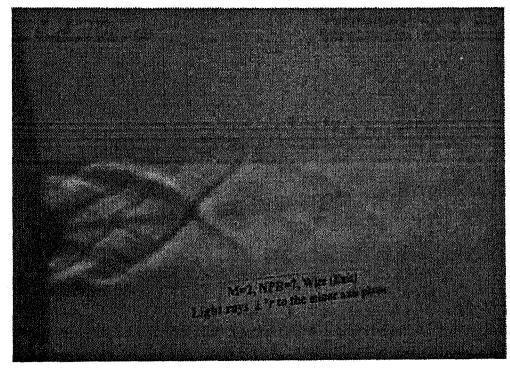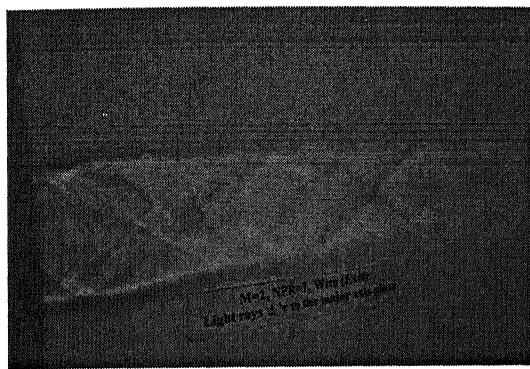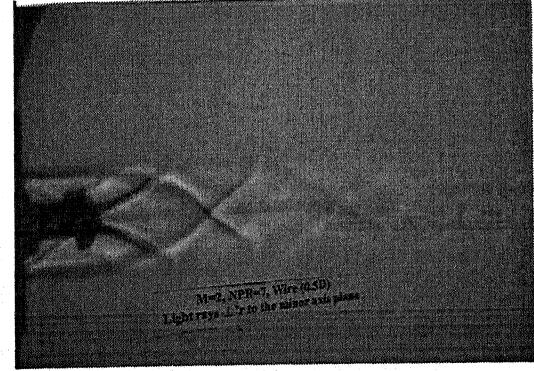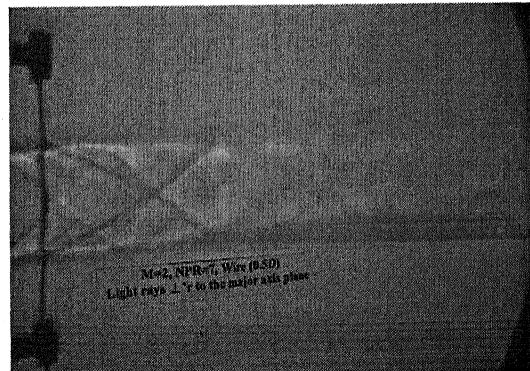
With C-W at X/D = 0

With C-W at X/D = 0.5

Major axis plane   Minor axis plane

Figure 4.24a Waves in Mach 1.94 jet at NPR 7
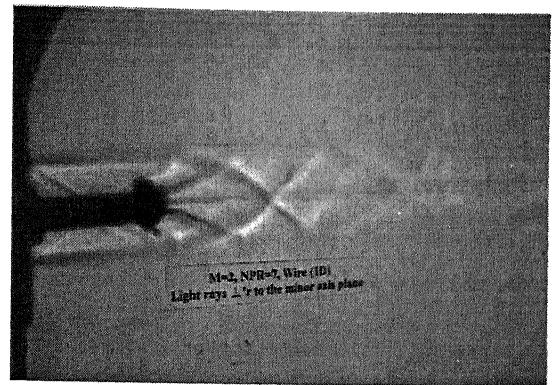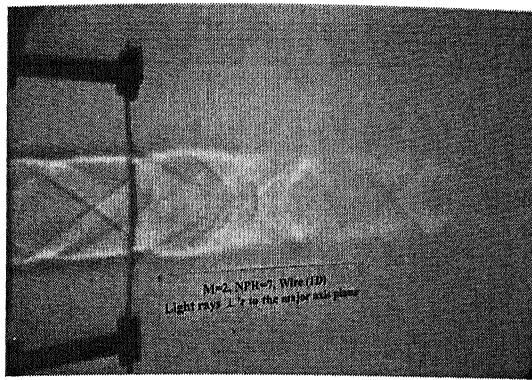
With C-W at X/D = 1.0
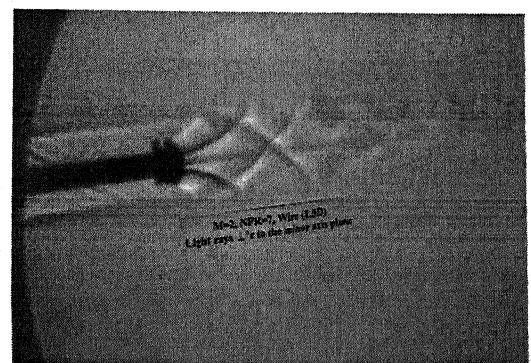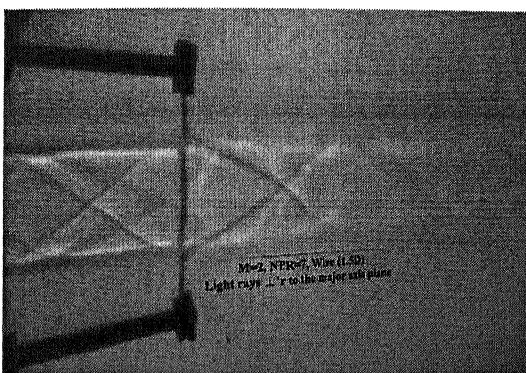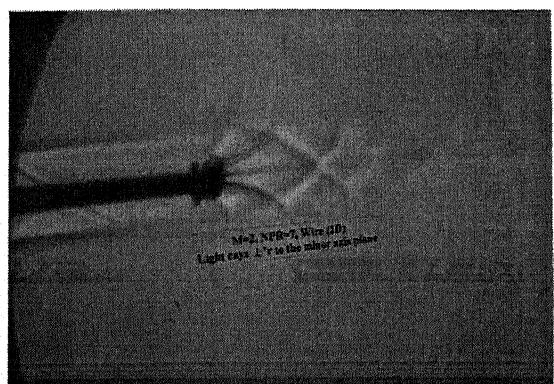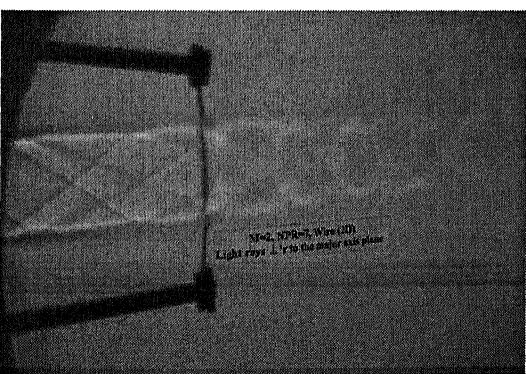
With C-W at X/D = 1.5

With C-W at X/D = 2.0

Major axis plane   Minor axis plane

Figure 4.24b Waves in Mach 1.94 jet at NPR 7

M1.8,NPR3,x/d=1.
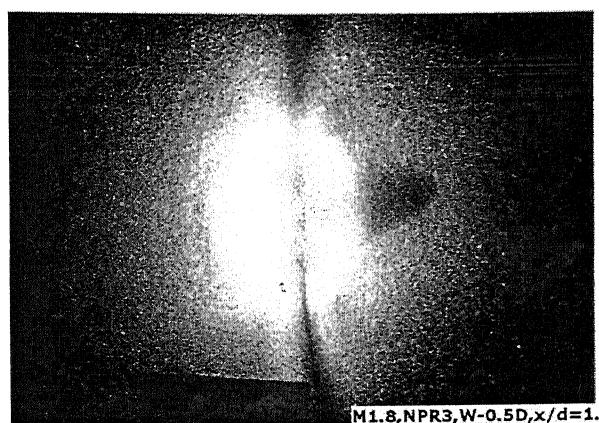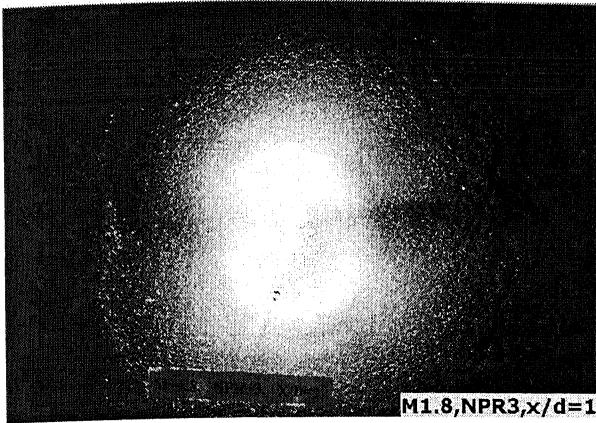
M1.8,NPR3,W-0.5D,x/d=1.

Figure 4.25 Surface visualization of Mach 1.83 jet at NPR 3 (X/D=1)

M1.8,NPR3,x/d=2.

M1.8,NPR3,w-0.5d,x/d=2

M1.8,NPR3,W-1D,x/d=2.
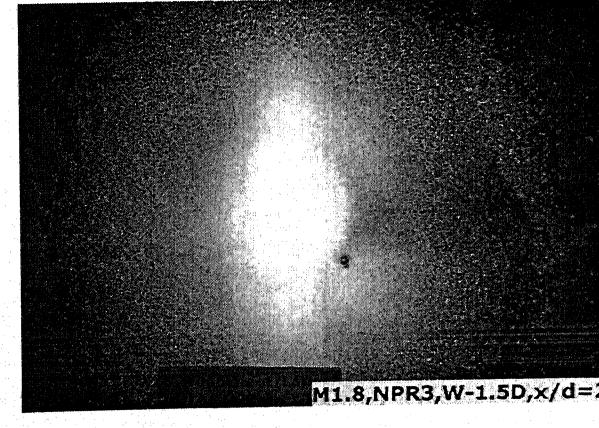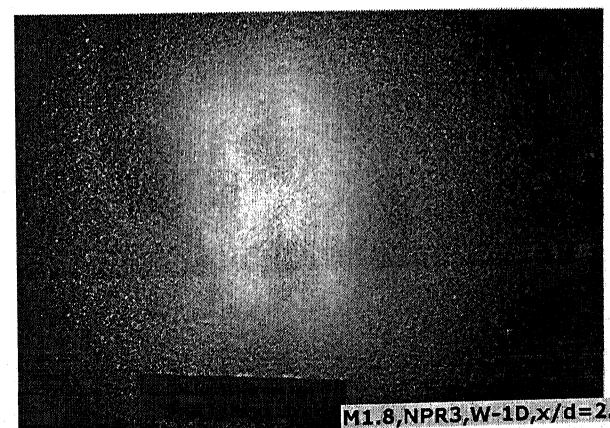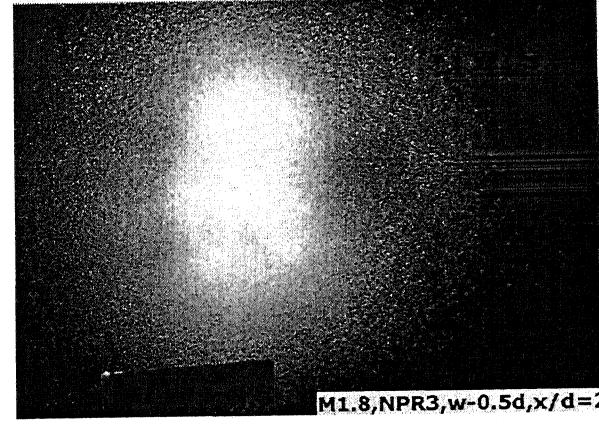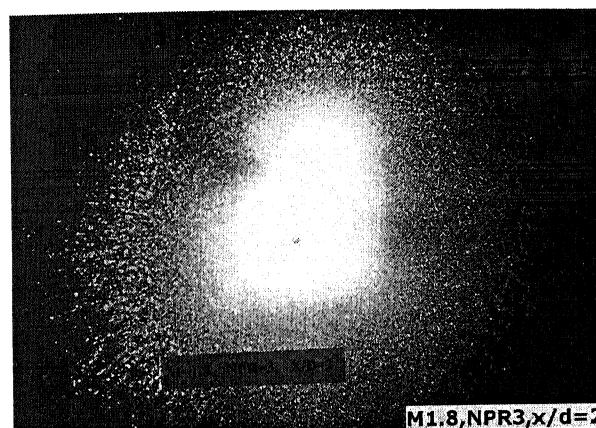
M1.8,NPR3,W-1.5D,x/d=2.

Figure 4.26 Surface visualization of Mach 1.83 jet at NPR 3 (X/D=2)
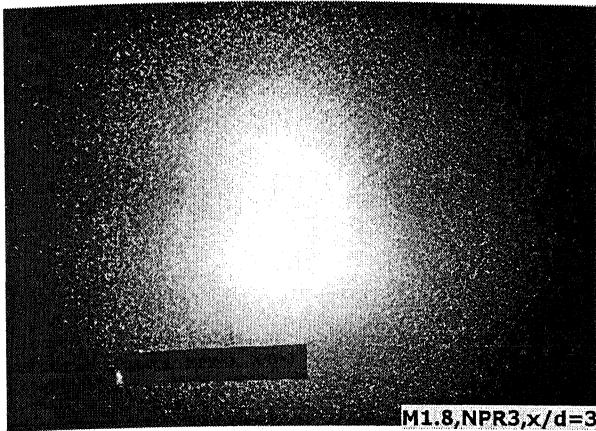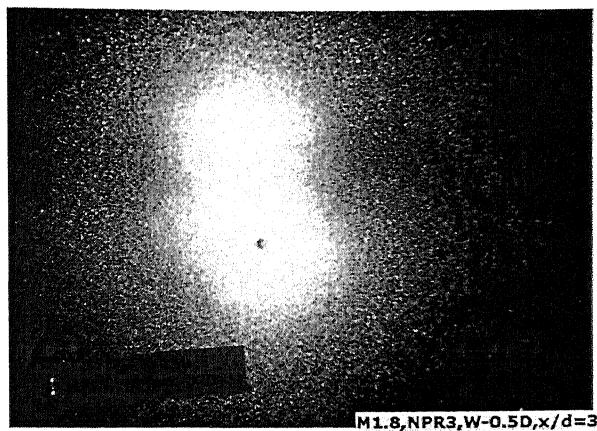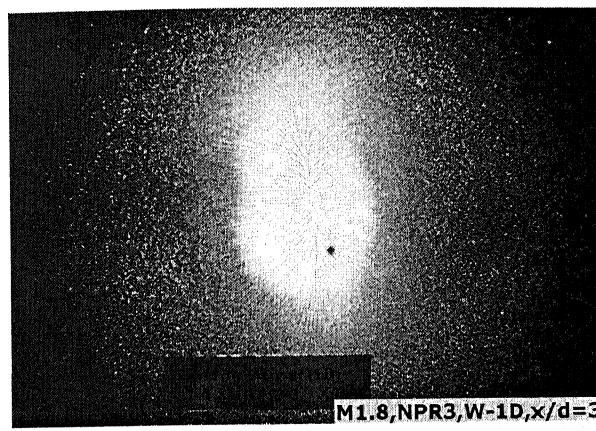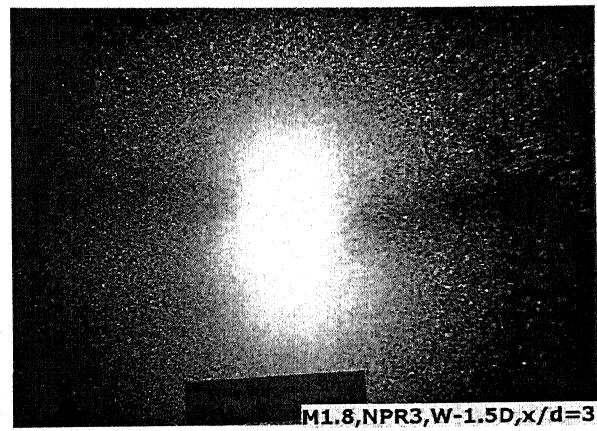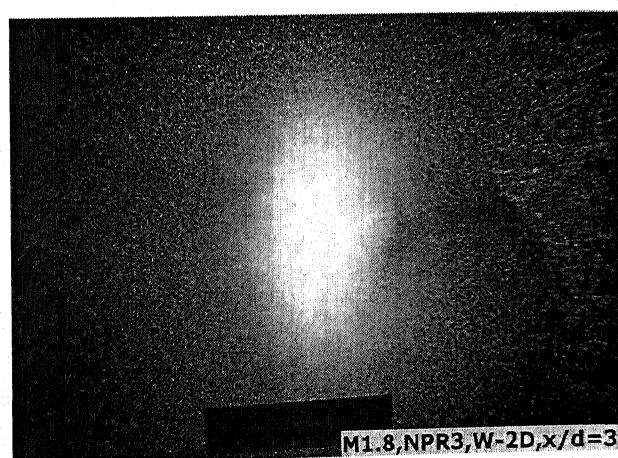
Figure 4.27 Surface visualization of Mach 1.83 jet at NPR 3 (X/D=3)

M1.6,NPR3,x/d=1.
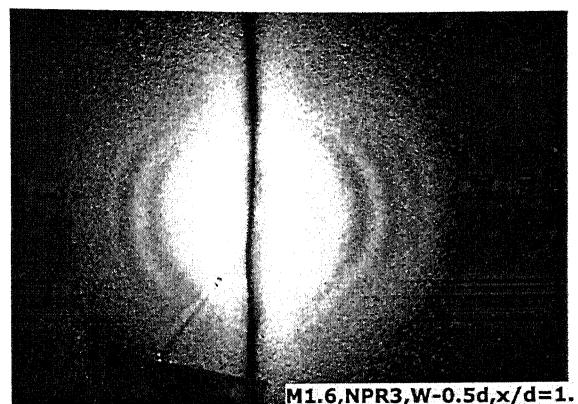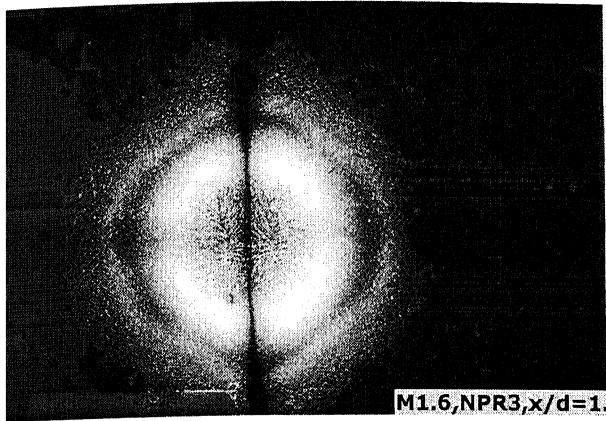
M1.6,NPR3,W-0.5d,x/d=1.

Figure 4.28 Surface visualization of Mach 1.86 jet at NPR 3 (X/D=1)

M1.6,NPR3,x/d=2.

M1.6,NPR3,W-0.5d,x/d=2.

M1.6,NPR3,W-1d,x/d=2.
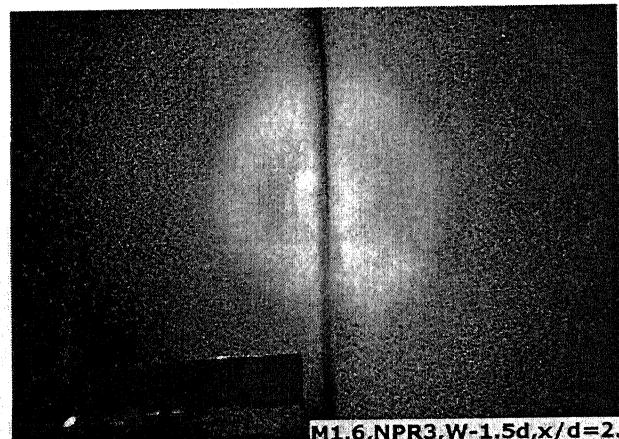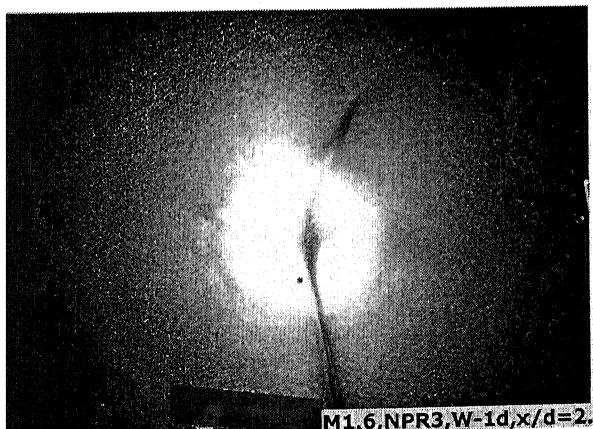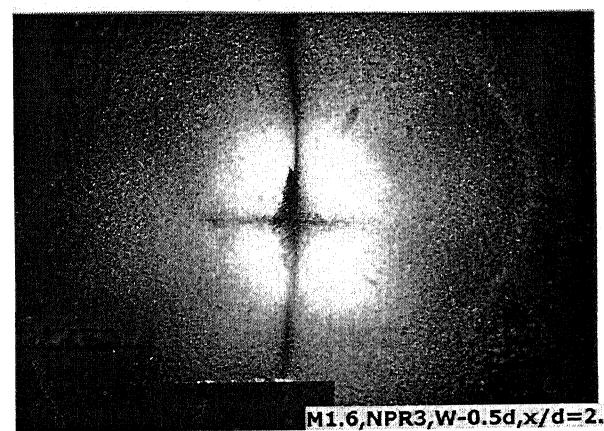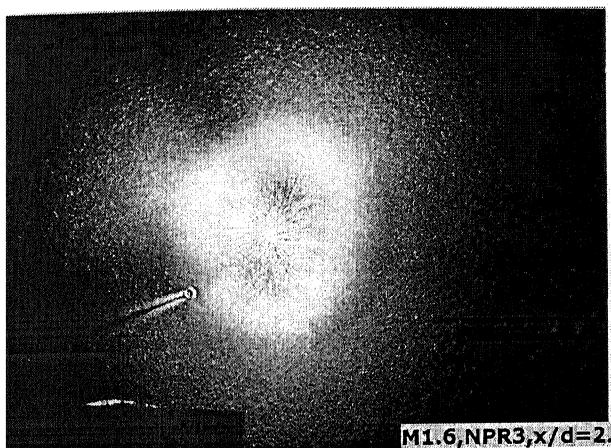
M1.6,NPR3,W-1.5d,x/d=2.

Figure 4.29 Surface visualization of Mach 1.86 jet at NPR 3 (X/D=2)
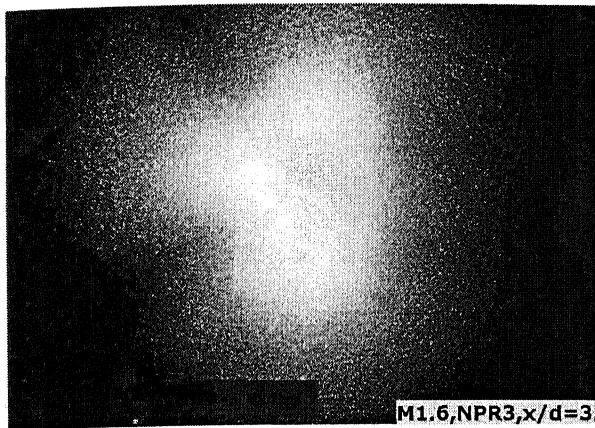
M1.6,NPR3,x/d=3.
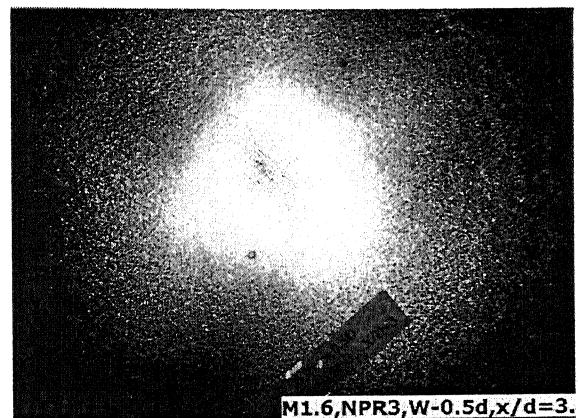
M1.6,NPR3,W-0.5d,x/d=3.
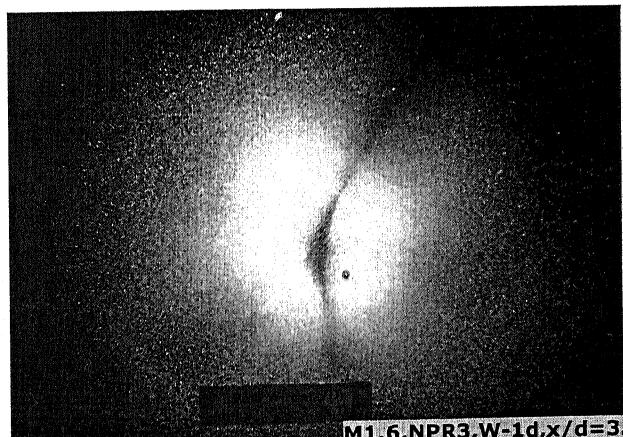
M1.6,NPR3,W-1d,x/d=3.
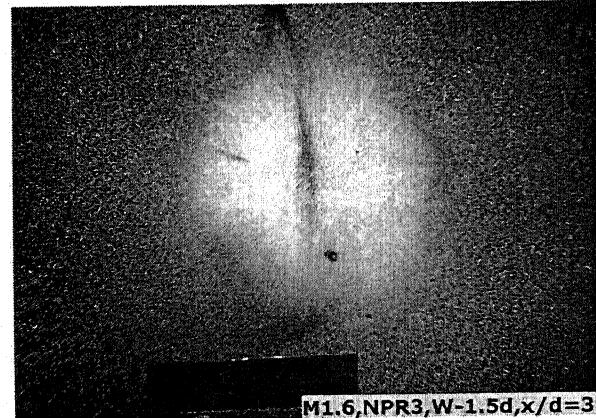
M1.6,NPR3,W-1.5d,x/d=3.

Figure 4.30 Surface visualization of Mach 1.86 jet at NPR 3 (X/D=3)
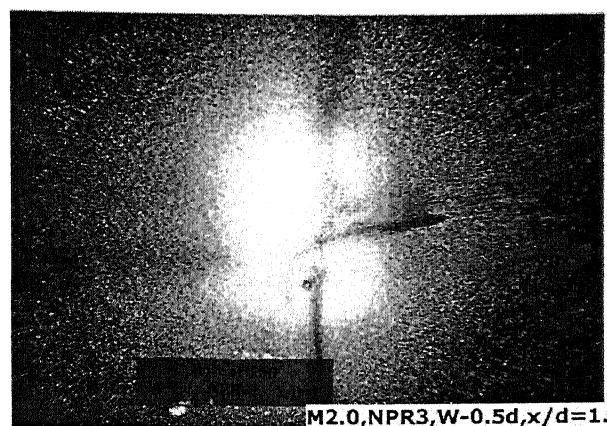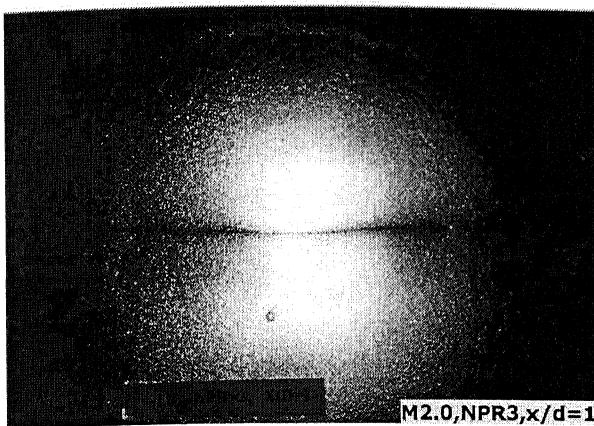
Figure 4.31 Surface visualization of Mach 1.94 jet at NPR 3 (X/D=1)
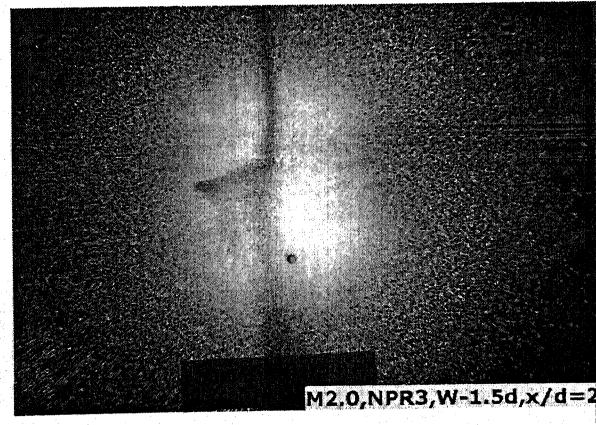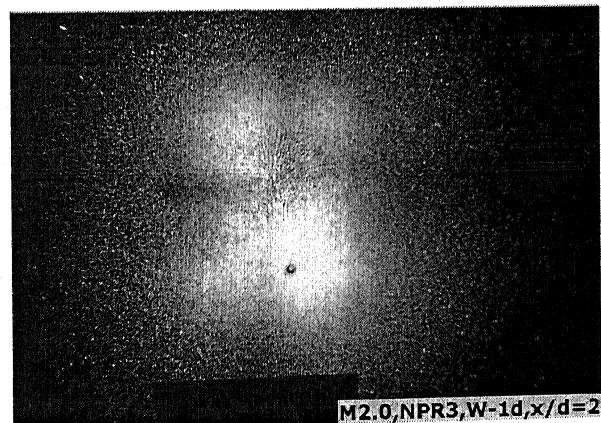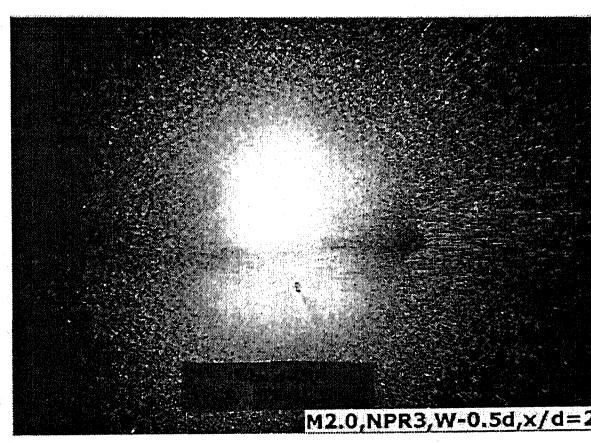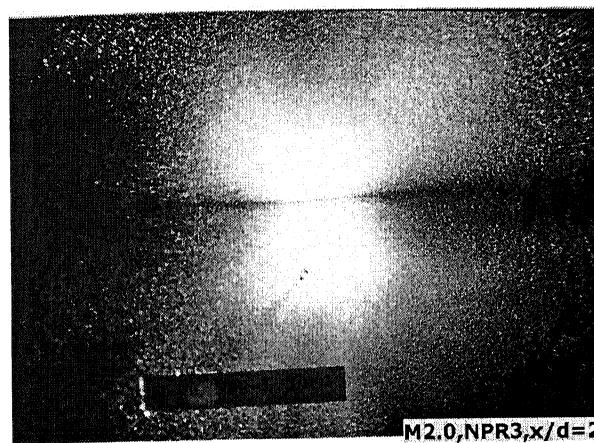
Figure 4.32 Surface visualization of Mach 1.94 jet at NPR 3 (X/D=2)

M2.0,NPR3,x/d=3.

M2.0,NPR3,W-0.5d,x/d=3.

M2.0,NPR3,W-1d,x/d=3.

M2.0,NPR3,W-1.5d,x/d=3.

M2.0,NPR3,W-2d,x/d=3.
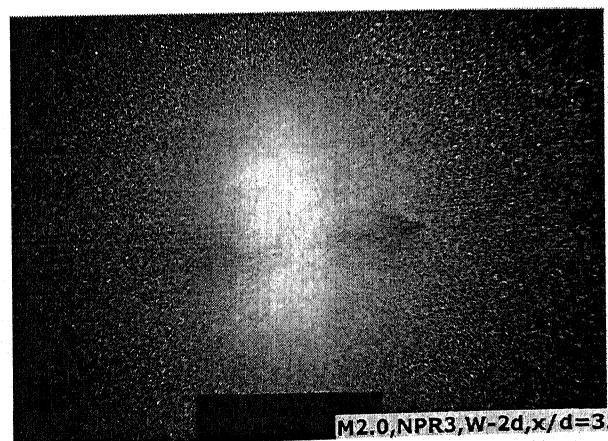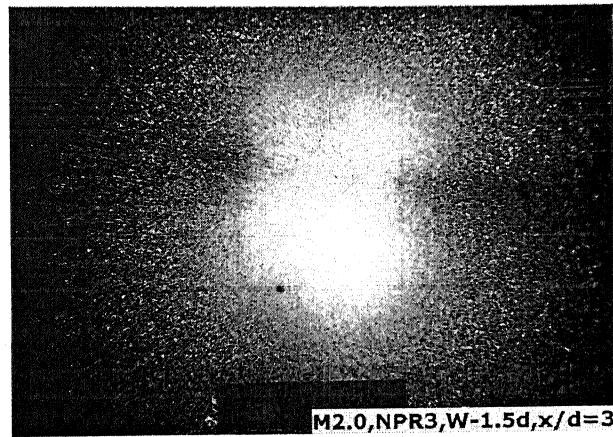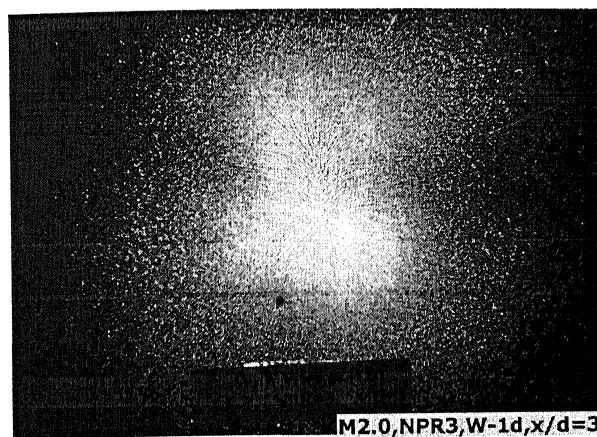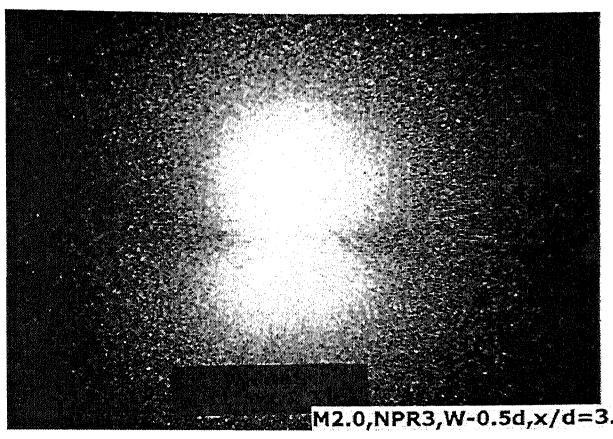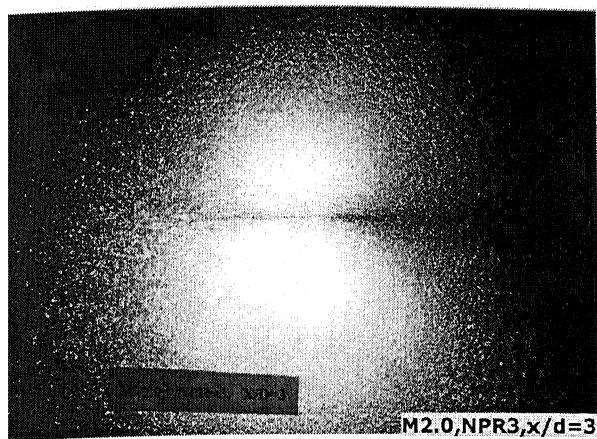
Figure 4.33 Surface visualization of Mach 1.94 jet at NPR 3 (X/D=3)
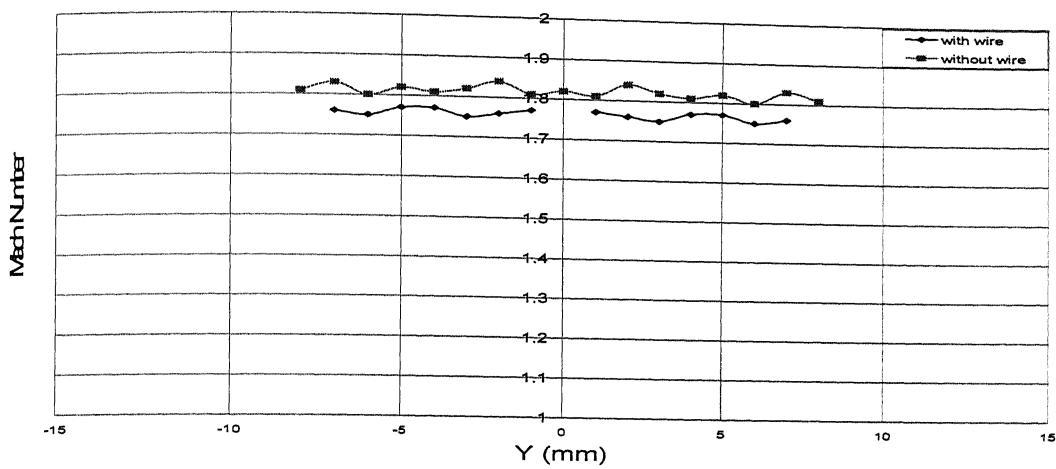
NPR 3
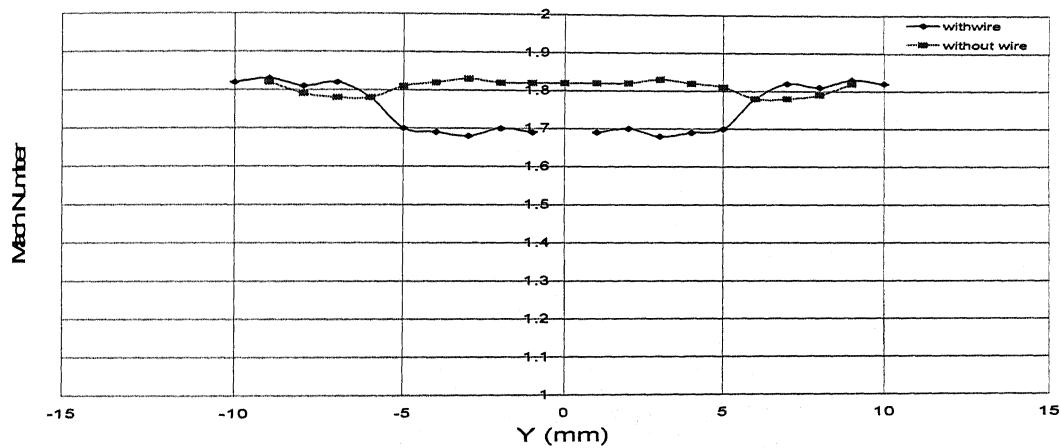
NPR 5
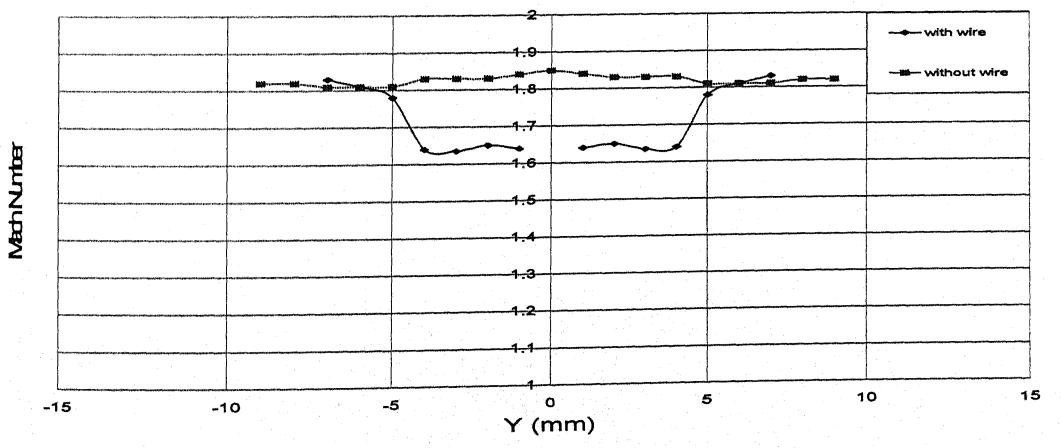
NPR 7

Figure 4.34 Mach number distributions at the exit of M 1.83 jet with and without control
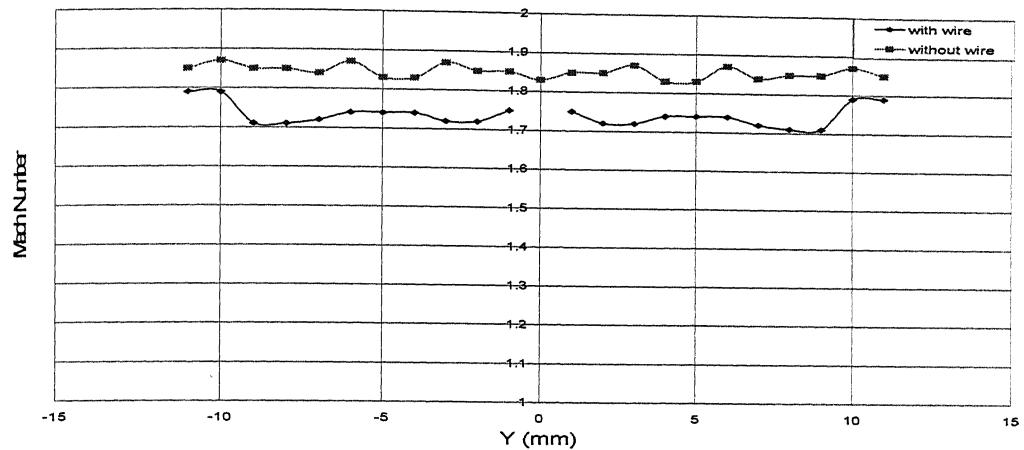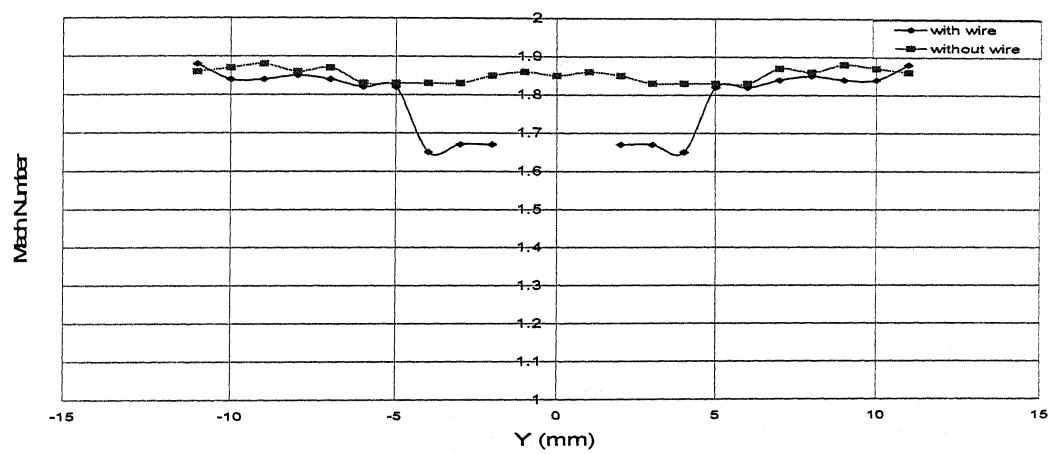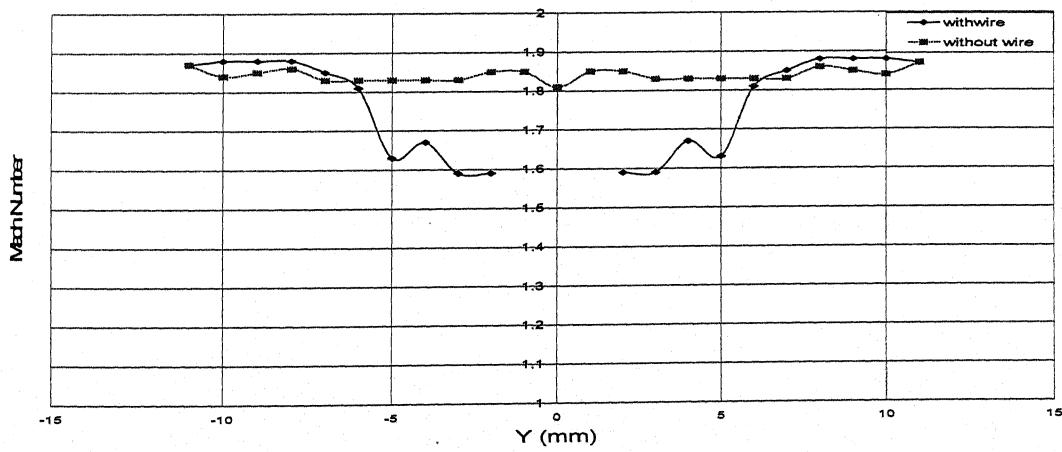
NPR 3

NPR 5

NPR 7

Figure 4.35 Mach number distributions at the exit of M 1.86 jet with and without control
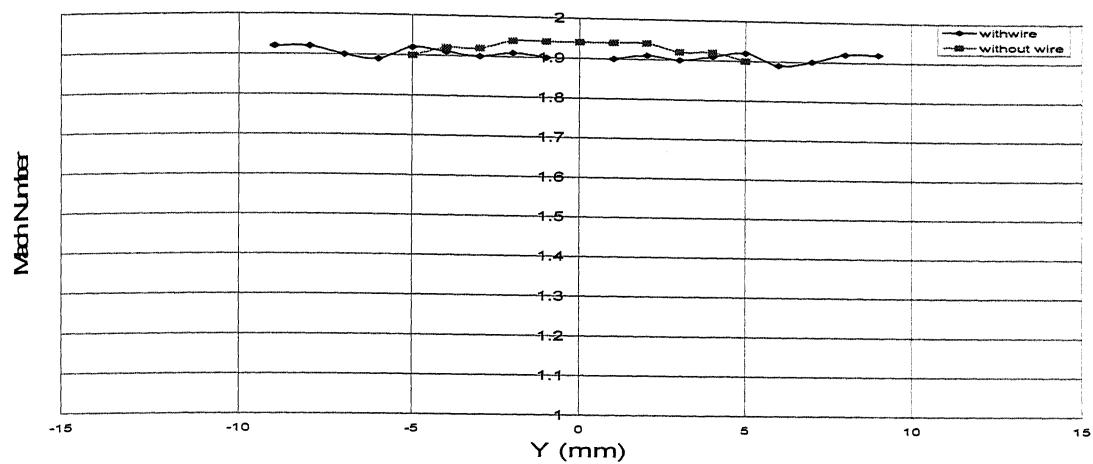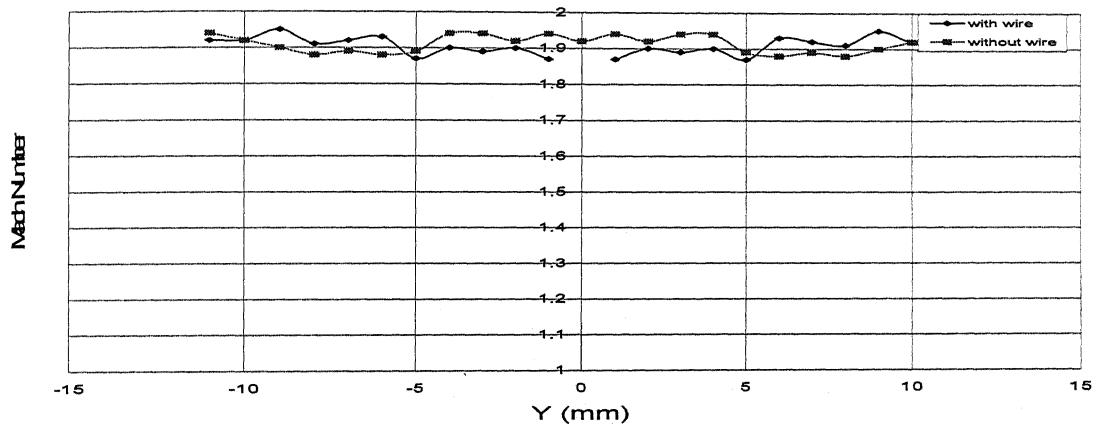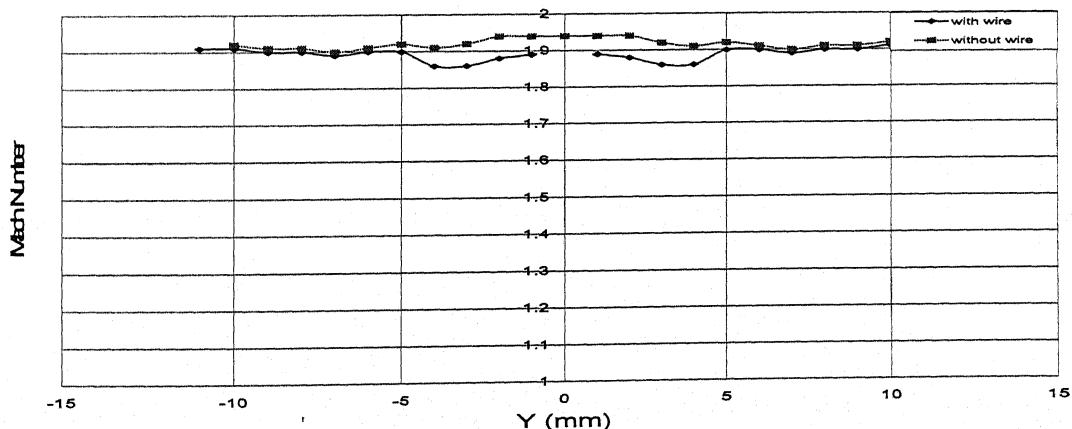
NPR 3

NPR 5

NPR 7

Figure 4.36 Mach number distributions at the exit of M 1.94 jet with and without control

	NPR 3	NPR 5	NPR 7
Mach 1.83	4.17	4.26	4.54
Mach 1.86	4.42	4.32	4.59
Mach 1.94	3.89	4.52	3.76

Table 4.1 Percentage thrust loss of Mach 1.83, 1.86 and 1.94 nozzles

Chapter 5

Conclusions

From the results of the experimental investigation on jets with shifted cross-wire, it is found that the shifted cross-wire is effective in promoting the jet mixing. The intersting feature of the control is that downstream of the wire, the entire jet activity is taking place at a much reduced Pitot pressure level compared to its uncontrolled counter parts. The detached shock envelope around the wire at the nozzle exit is found to be distrub the nozzle exit flow, rendering the flow Mach number to decrease over almost the entire area for NPR 3. But with increase of NPR the distrubed area comes down with much reduced Mach number.

Even though the wire distrubs large portion of the exit area, the thrust loss due to this pertrubation is almost proportional to the percentage area blocked by the wire presence. In addition to enhanced mixing the presence of wire influences the shock cells too favourably. For the present range of parameters a maximum core length reduction of 30.76% was achieved for Mach 1.86 jet at NPR 7, with wire at $X/D = 1$. Further, wire at $X/D = 1$ appears to be optimum location for the cross-wire resulting in maximum mixing enhancement.

5.1   Future scope of work

- The cross-wire tested in the present investigation is circular, Since it is meant for vortex generation, a flat wire may proved to be better than a circular one.

- Similar studies with high Mach number will be of wider application.

- Similar studies with high temparature jets will be of use.

- Mass entrainment studies will give a better insight into the spread caused by the wire.

- The effectiveness of cross-wire location has to be done thoroughly at the end of first Mach disc location for various Mach numbers.

- The effectiveness of cross-wire can be studied for subsonic jets.

References

[1] Abrmovich G.N. *Theory of Turbulent Jets.* M.I.T. Press, Massachusetts U.S.A., 1963.

[2] Pai S. *Fluid Dynamics of Jets* Von Nostrand, New York.

[3] Rajaratnam N. *Turbulent Jets* Elsevier Sci. Publishing. Co., New York., 1976

[4] Gutmark E.J. and Grinstein F.F. Flow control with noncircular jets. *Journal of Fluid Mechanics,* Vol. 31, pp. 234–272, 1999.

[5] Murugan K.N. Superiority of elliptic jets. *Master's thesis,* Department of Aerospace Engineering, Indian Institute of Technology Kanpur, India, Dec'2002.

[6] Guntmark E, et al. Noncircular jets in combustion systems. *Journal of Experiments in Fluids,* Vol. 7, pp. 248–258.

[7] Hussain F. and Hussain H.S. Elliptic jet part1: Characteristics of unexited and exited jets. *Journal of Fluid Mechanics,* pp. 208–257, 1991.

[8] Sfroza M.P. Steiger M.H and Trentacoste N. Studies in three dimensional viscous jets. *AIAA Journal,* Vol. 4, pp. 800–806, 1966.

[9] Gutmark E.J. Vortex induction and mass entrainment in a small aspect ratio elliptic jets. *Journal of Fluid Mechanics,* Vol. 179, pp. 393–405, 1987.

[10] Zaman K.B.M.Q. Spreading characteristics of compressible jets from nozzles of various geometries. *Journal of Fluid Mechanics,* Vol. 383, pp. 197–228, 1999.

[11] Bradbury E.J.S. and Khadem A.H. The distortion of jets by tabs. *Journal of Fluid Mechanics,* Vol. 70, pp. 801–813, 1975.

[12] Samimy Zaman K.B.M.Q. and Reeder M.F. Effect of tabs on the flow and noise field of an axisymmetric jet. *AIAA Journal,* Vol. 31, pp. 609–619, 1993.

[13] Navinkumar singh and Rathakrishnan E. Sonic jet control with tabs. *Journal of Turbo and Jet engines*, Vol. 19, pp. 107–118, 2002.

[14] Sreejith R.B. and Rathakrishnan E. Cross-wire as passive device for supersonic jet control. *Joint Propulsion Conference*, Indianapolis, July 7–10, 2002.

[15] Rathakrishnan E. *Gas Dynamics*, Prentice Hall of India, 1995.

[16] Rathakrishnan E. *Instrumentation, Measurements and Experiments in Fluids*, Book to be published

[17] Rathakrishnan E. *Fluid Mechanics* Book to be published.

[18] Rathakrishnan E. *Fundamentals of Engineering Thermodynamics*,Prentice Hall of India, 1995.

[19] Tam C.K.W Supersonic jet noise. *Annual Review of Fluid Mechanics*, Vol. 27, pp. 17–43, 1995.

[20] http://www.allstar.fiu.edu/aero/rocket3.html

Appendix A

Virtual Instrumentation Based Pressure Aquistion System

Pressure measurement in the supersonic field is one of the challenging tasks, it can not be measured directly by any means but it can be very easily measured by an indirect means through a Pitot probe. It is emphasized by many experimentalists and researchers in the high speed arena that Pitot pressure measurement is the best. The pressure obtained from the Pitot can be read by many means like manometers, Bourdon gauge etc. In high speed flows , pressure measurement is the one of the difficult tasks, as the pressure values are continuously oscillating in nature (especially in open flows) and also it is necessary to read the pressure at faster rate which is only possible with electronic sensing devices, and an automated data acquisition system which eliminates the human prone errors completely.

At aerodynamics lab IIT Kanpur the jet testing facility is equipped with 16 port pressure scanner (PSI 9010) with a range of 2.5kpa to 5200kpa. The main feature of this system is that it can average 256 readings by the time of scanning and gives the averaged value with in fraction of seconds, and also the data acquisition is done by LAB view based application software which is developed in such a fashion that it can acquire the data by mouse clicking and saves the data in a text file which will be processed and analyzed further. The complete pressure measurements system consists of pressure scanner, and a VI based software to acquire the pressure from different parts.

System description

Figure. A.1 shows the implementation of the Virtual Instrumentation based pressure measurement system. As shown in the Fig. A.1 The system mainly consists of the

following components

- System hardware.

- Host computer loaded with application software to acquire pressure.

Description of instrument

The system 9010 intelligent pressure scanner is a pressure measuring device intended for use in test and production environments. It consists of 16 channels and is working in differential mode. It has an asynchronous RS 422/485 host communication interface. It also includes a standard RS-232 diagnostic interface that may also be used as host interface. The optomux style command set is used to send commands and receives response from all ports. It may be configured to communicate in the multidrop network communication always at selected baud rate using the optomux protocol. The multidrop communication always operates with no parity, 8 bit data bits and 1 stop bit. The default baud rate is 9600. Changes to baud rate can be made using special procedure via the DIP switch used to select the node address during initialization at power up. During this special baud rate selection procedure, the Number of averages used during the data acquisition is also selected.

The application software developed using the Lab VIEW (shown in figure 3.3) links the host computer to the pressure scanner via RS 232 communication. The application software performs all the required functions like initialize, reset, rezero calibration and read pressure. The detailed description of these functions is given as follows.

Initialize

The initialize VI of the application software is intended to initialize the module address and check the power restart has occur or not, and also it displays the response of the scanner on the monitor of the host computer.

Reset

Reset VI is intended to instruct the scanner to reset and set all internal control variables to their default reset state.

Rezero calibration

This VI is intended to perform the calibration of the scanner with reference to the standard atmospheric pressure, finds the calibration coefficients (recalibrated offset coefficients) and stores them in nonvolatile transducer memory.

Read pressure

Figure A.3 shows the front panel of the read pressure VI. This VI performs the major task in the entire application software that is to acquired pressure. In this VI, it is provided with a flexible advanced file handling system so that all the acquire data will be saved in the form of text file along with the date time and the details of the channel numbers from which data has been acquired. It also displays the measured pressure value currently on the monitor of the host computer. The main attraction of this VI is that we can display the measured pressure in different units as per users choice like Pascal, inches of mercury and atmospheres etc., logic behind this program is shown in Fig. A.3.
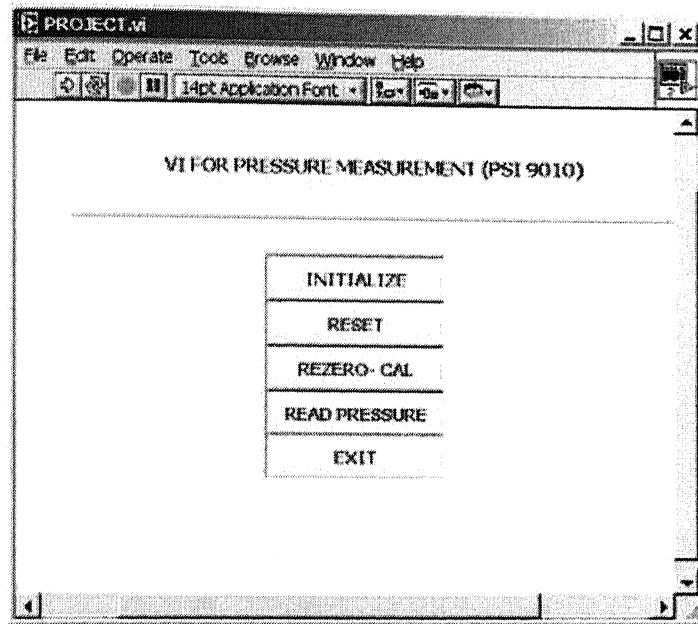
Figure A.1 VI main program front panel
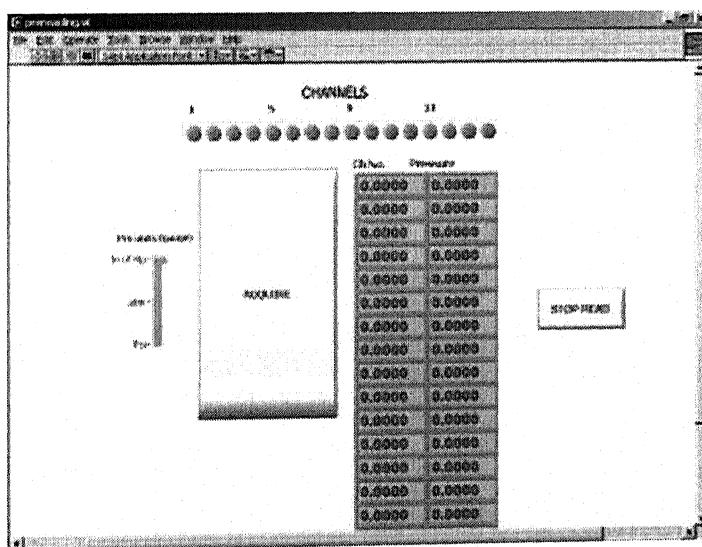
Figure A.2 Read function front panel
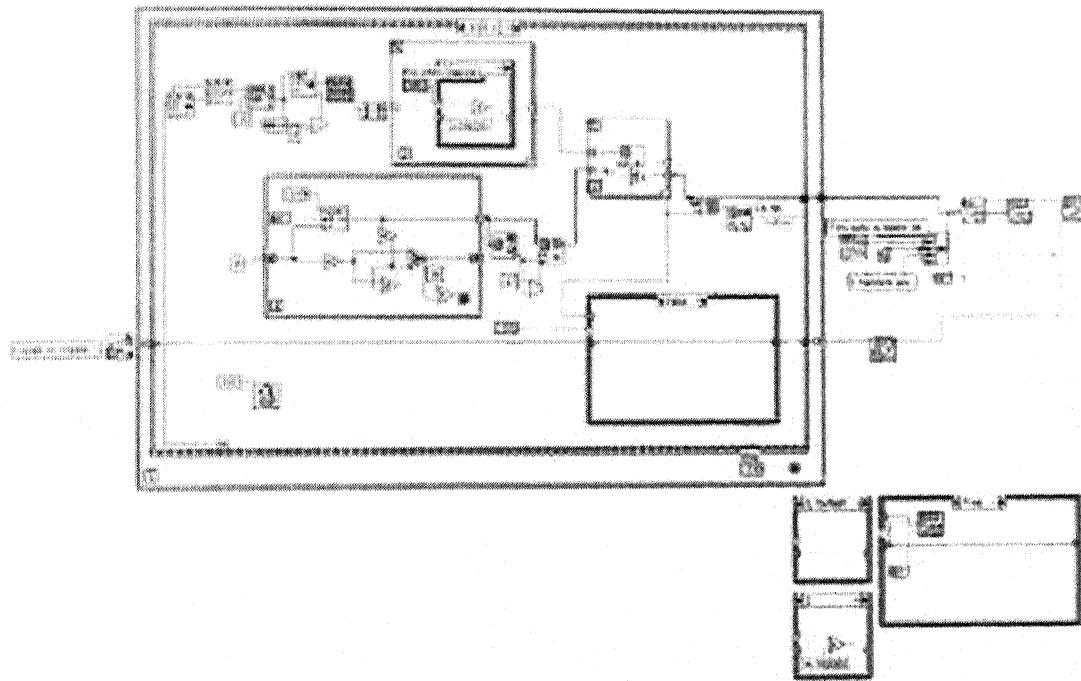
Figure A.3 Block diagram of the program

Appendix B

Thrust Loss Estimation

Passive control of jet has a severe setback as mentioned in the chapter 4. That is, the control results in blockage of a precious exit area of the nozzle, which inturn results in a distrubed Mach number distrubution at the nozzle exit plane. The reduced velocity zone near the control is because of the shock envelope all around the cross-wire. Reason for thrust loss associated with the cross-wire is clearly explained in chapter 4. Here a detailed analysis of the thrust loss assosiated with the cross-wire as a passive control has been carried out by making the Pitot pressure measurements of controlled and uncontrolled jets at the exit planes of the nozzle. The distrubed Mach number distrubtion is shown in Figs. 4.34–4.56. The estimated thrust loss associated with Mach 1.86, 1.83 and 1.94 nozzles of the present investigation is tabulated in Table 4.1. The procedure employed to compute the thrust loss is given here for Mach 1.86 nozzle.

On calibration the nozzle of design Mach number 1.6 is found to deliver Mach 1.86 jet. Exit area of the nozzle is divided into different Mach number zones form Mach number distribution plots.Thrust calculations are made accordingly.

Mach 1.86 jet

NPR 3

The loss of momentum thrust for Mach 1.86 jet is as follows. For the without cross-wire, the thrust is

$$\text{Thrust} = \dot{m}V_j = (\rho_e A_e V_e)\, V_e$$

Where the subscript 'e' refers to nozzle exit state.

At NPR 3, the stagnation conditions were

$$P_0 \; = \; 3\,\mathrm{Pa}, \;\; T_0 = 300\,\mathrm{K}$$

$$= \; 3 \times 97325$$

$$= \; 291975\,\mathrm{Pa}$$

From isentropic table for $M_e = 1.86$

$$\frac{\rho_e}{\rho_0} = 0.2686, \quad \frac{T_e}{T_0} = 0.5910$$

Therefore

$$\rho_e \; = \; 0.2686 \times \frac{P_0}{RT_0}$$

$$= \; 0.2686 \times \frac{291975}{287 \times 300}$$

$$= \; 0.911\,\mathrm{kg}/m^3$$

$$T_e \; = \; 0.5910 \times 300 = 177.3\,\mathrm{K}$$

The speed of sound $a_e = \sqrt{1.4 \times 287 \times 177.3} = 266.9\,\mathrm{m/s}$

The exit velocity $V_e = M_e a_e = 1.86 \times 266.9 = 496.43\,\mathrm{m/s}$

Thus, the thrust

$$T \; = \; \rho_e A_e V_e^2 = 0.911 \times 750 \times 10^{-6} \times (496.43)^2$$

$$= \; \boxed{168.40\,\mathrm{N}}$$

Controlled jet

From the Mach number distribution of the controlled jet at the exit of the nozzle. It is found that the Mach 1.86 jet is almost delivering a Mach 1.72 jet uniformly at the exit of the nozzle.

The speed of sound $a_e = \sqrt{1.4 \times 287 \times 177.3} = 266.9\,\text{m/s}$

The exit velocity $V_e = M_e a_e = 1.72 \times 266.9 = 459.068\,\text{m/s}$

Thus, the thrust

$$T = \rho_e A_e V_e^2 = 1.0607 \times 720 \times 10^{-6} \times (459.068)^2$$

$$= \boxed{160.95\,\text{N}}$$

The loss of thrust in Percentage

$$\frac{(168.4 - 160.95)}{168.4} = 4.42.$$

NPR 5

At NPR 5, the stagnation conditions are

$$P_0 = 5\,\text{Pa}, \quad T_0 = 300\,\text{K}$$

$$= 5 \times 97325$$

$$= 4859875\,\text{Pa}$$

From isentropic table for $M_e = 1.86$

$$\frac{\rho_e}{\rho_0} = 0.2686, \quad \frac{T_e}{T_0} = 0.5910$$

Therefore

$$\rho_e = 0.2686 \times \frac{P_0}{RT_0}$$

$$= 0.2686 \times \frac{4859875}{287 \times 300}$$

$$= 1.5180 \, kg/m^3$$

$$T_e = 0.5910 \times 300 = 177.3 \, K$$

The speed of sound $a_e = \sqrt{1.4 \times 287 \times 177.3} = 266.9 \, m/s$

The exit velocity $V_e = M_e a_e = 1.86 \times 266.9 = 496.43 \, m/s$

Thus, the thrust

$$T = \rho_e A_e V_e^2 = 1.5180 \times 750 \times 10^{-6} \times (496.43)^2$$

$$= \boxed{280.14 \, N}$$

Controlled jet

For this NPR the exit Mach number is altered into two differnt Mach number zones namely, A and B because of the presence of cross-wire at the exit. The zone near the wire occupies an area of 4.5×30 on either side of the cross-wire with a reduced Mach number of 1.66. Zone B occupies the remaining area with a Mach number of 1.86. Therefore, total trust of the controlled jet is the sum of thrust because of Mach 1.66 jet over 9×30 exit area and the thrust because of M 1.86 jet over 15×30 exit area.Therefore, Total thrust of controlled jet is the sum of Thrust in zone A and Zone B.

Thrust in zone A (Mach 1.66 region)

From isentropic table for $M_e = 1.66$

$$\frac{\rho_e}{\rho_0} = 0.3337$$

Therefore

$$\rho_e = 0.3337 \times \frac{P_0}{RT_0}$$

$$= 0.3337 \times \frac{4859875}{287 \times 300}$$

$$= 1.886 \, \text{kg}/m^3$$

The speed of sound $\quad a_e = \sqrt{1.4 \times 287 \times 177.3} = 266.9 \, \text{m/s}$

The exit velocity $\quad V_e = M_e a_e = 1.66 \times 266.9 = 443.054 \, \text{m/s}$

Thus, the thrust in zone A is

$$T_A = \rho_e A_e V_e^2 = 1.886 \times 270 \times 10^{-6} \times (443.054)^2$$

$$= \boxed{99.96 \, \text{N}}$$

Thrust in zone B (Mach 1.86 region)

From isentropic table for $M_e = 1.86$

$$\frac{\rho_e}{\rho_0} = 0.2686$$

Therefore

$$\rho_e = 0.2686 \times \frac{P_0}{RT_0}$$

$$= 0.2686 \times \frac{4859875}{287 \times 300}$$

$$= 1.518 \, \text{kg}/m^3$$

The speed of sound $a_e = \sqrt{1.4 \times 287 \times 177.3} = 266.9\,\text{m/s}$

The exit velocity $V_e = M_e a_e = 1.86 \times 266.9 = 496.43\,\text{m/s}$

Thus, the thrust in zone A is

$$T_A = \rho_e A_e V_e^2 = 1.518 \times 450 \times 10^{-6} \times (496.43)^2$$

$$= \boxed{174.94\,\text{N}}$$

Total Thrust = 268.04 N

The loss of thrust in Percentage

$$\frac{(280.14 - 268.04)}{280.14} = 4.32.$$

NPR 7

At NPR 7 the stagnation conditions are

$$P_0 = 7\,\text{Pa}, \quad T_0 = 300\,\text{K}$$

$$= 7 \times 97325$$

$$= 681275\,\text{Pa}$$

From isentropic table for $M_e = 1.86$

$$\frac{\rho_e}{\rho_0} = 0.2686, \quad \frac{T_e}{T_0} = 0.5910$$

Therefore

$$\rho_e = 0.2686 \times \frac{P_0}{RT_0}$$

$$= 0.2686 \times \frac{681275}{287 \times 300}$$

$$= 2.125 \, \text{kg}/m^3$$

$$T_e = 0.5910 \times 300 = 177.3 \, \text{K}$$

The speed of sound $\quad a_e = \sqrt{1.4 \times 287 \times 177.3} = 266.9 \, \text{m/s}$

The exit velocity $\quad V_e = M_e a_e = 1.86 \times 266.9 = 496.43 \, \text{m/s}$

Thus, the thrust

$$T = \rho_e A_e V_e^2 = 2.125 \times 750 \times 10^{-6} \times (496.43)^2$$

$$= \boxed{392.87 \, \text{N}}$$

Controlled jet

For this NPR the exit Mach number is altered into two differnt Mach number zones namely, A and B because of the presence of cross-wire at the exit. The zone near the wire occupies an area of 4.5 × 30 on either side of the cross-wire with a reduced Mach number of 1.62. Zone B occupies the remaining area with a Mach number of 1.86. Therefore, total trust of the controlled jet is the sum of thrust because of Mach 1.66 jet over 9 × 30 exit area and the thrust because of M 1.86 jet over 15 × 30 exit area. Therefore, Total thrust of controlled jet is the sum of Thrust in zone A and Zone B.

Thrust in zone A (Mach 1.62 region)

From isentropic table for $M_e = 1.62$

$$\frac{\rho_e}{\rho_0} = 0.3483$$

Therefore

$$\rho_e = 0.3483 \times \frac{P_0}{RT_0}$$

$$= 0.3483 \times \frac{681275}{287 \times 300}$$

$$= 2.756 \, \text{kg}/m^3$$

The speed of sound $a_e = \sqrt{1.4 \times 287 \times 177.3} = 266.9 \, \text{m/s}$

The exit velocity $V_e = M_e a_e = 1.62 \times 266.9 = 432.378 \, \text{m/s}$

Thus, the thrust in zone A is

$$T_A = \rho_e A_e V_e^2 = 2.756 \times 270 \times 10^{-6} \times (443.054)^2$$

$$= \boxed{139.12 \, \text{N}}$$

Thrust in zone B (Mach 1.86 region)

From isentropic table for $M_e = 1.86$

$$\frac{\rho_e}{\rho_0} = 0.2686$$

Therefore

$$\rho_e = 0.2686 \times \frac{P_0}{RT_0}$$

$$= 0.2686 \times \frac{681275}{287 \times 300}$$

$$= 2.125 \, \text{kg}/m^3$$

The speed of sound $a_e = \sqrt{1.4 \times 287 \times 177.3} = 266.9 \, \text{m/s}$

The exit velocity $V_e = M_e a_e = 1.86 \times 266.9 = 496.43 \, \text{m/s}$

Thus, the thrust in zone A is

$$T_A = \rho_e A_e V_e^2 = 2.125 \times 450 \times 10^{-6} \times (496.43)^2$$

$$= \boxed{235.72 \, \text{N}}$$

Total Thrust = 374.84 N

The loss of thrust in Percentage

$$\frac{(392.87 - 374.84)}{392.87} = 4.59.$$

A 148450